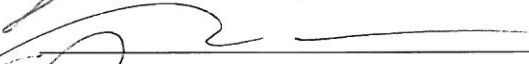
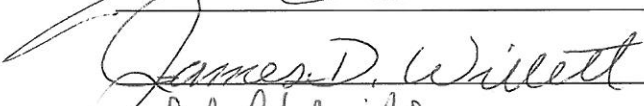
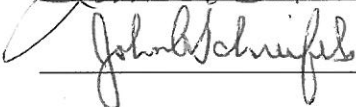


VARIATION IN INTERPERSONAL RESPONSE TO STATIN DRUGS IN
HYPERCHOLESTEROLEMIA.

by

Hameed A Khan
A Thesis
Submitted to the
Graduate Faculty
of
George Mason University
in Partial Fulfillment of
The Requirements for the Degree
of
Master of Science
Chemistry

Committee:

| | |
|---|--|
|  | Dr. Robin D. Couch, Thesis Director |
|  | Dr. Barney Bishop, Committee Member |
|  | Dr. James D. Willett, Committee Member |
|  | Dr. John Schreifels, Department Chairperson |
|  | Dr. Timothy L. Born, Associate Dean for Student and Academic Affairs, College of Science |
|  | Dr. Vikas Chandhoke, Dean, College of Science |
| Date:  | Fall Semester 2012 George Mason University Fairfax, VA |

Variation in Interpersonal Response to Statin Drugs in Hypercholesterolemia.

A thesis submitted in partial fulfillment of the requirements for the degree of Master of Science at George Mason University.

By

Hameed A Khan
Bachelor of Science
George Mason University, 2007

Director: Robin D. Couch, Associate Professor
Department of Chemistry and Biochemistry

Fall Semester 2012
George Mason University
Fairfax, VA

2012 Hameed A. Khan
All Rights Reserved ©

DEDICATION

I am dedicating this work to my father Dr. Mohammad Sher Ali Khan (dec), who is my ideal in all walks of my life.

ACKNOWLEDGEMENTS

I am heartily thankful to my project director, Dr. Robin D. Couch, whose encouragement, guidance and support from the initial to the final level enabled me to develop an understanding of the subject.

Dr. Bishop and Dr. James D. Willett, for their patience, guidance, expertise and particularly for their valuable time and energy they devoted in refining this manuscript.

Arthur Tsang, Justin Davis, Karl Navarro, Allyson Dailey, Chinchu Johny, Steven Roberts, and Tiffani Willis for assisting me in protein purification, analytes library preparation, protein electrophoresis, spectrophotometry and autoclaving.

Dr Weigdong for his LC-MS-MS analysis and protein identification.

Dr. J. Fred Banks at Quest Diagnostics Nichols Institute, Chantilly, VA for his expertise in the interpretation of LC-MS data for unknown compound identification.

What I have achieved could not have been possible without the help of my wife, three daughters and a son. I also acknowledge the support I received from my entire family that includes my parents, my siblings, my in-laws and the outstanding support I received from the Danish family.

Above all, I thank the Almighty God for giving me the passion to pursue knowledge, the steadfastness to proceed towards my vision, and the ability to make sound judgments. It is only through His generosity and compassion, that wisdom is gained.

TABLE OF CONTENTS

| | Page |
|--|------|
| LIST OF TABLES..... | vii |
| LIST OF FIGURES..... | viii |
| ABSTRACT | x |
| I. INTRODUCTION | 1 |
| The Physiology and Pathophysiology of Cholesterol..... | 1 |
| Cholesterol Structure..... | 1 |
| Cholesterol Synthesis..... | 2 |
| The Fate of Cholesterol | 5 |
| Cholesterol Synthesis Regulation..... | 12 |
| The search for Inhibitors | 14 |
| Statins Related Toxicity | 17 |
| Interpersonal Variation in Statin Response..... | 18 |
| HMGCR Structure and Classification | 20 |
| Oligomerization | 26 |
| Catalysis | 38 |
| II. MATERIALS AND METHODS | 50 |
| Cloning and Expression | 50 |
| Protein Purification | 52 |
| Protein Electrophoresis..... | 55 |
| LC-MS/MS | 55 |
| HMGCR activity | 57 |
| Screening for HMGCR inhibitors | 58 |

| | |
|---|-----|
| LC/MS analysis of lovastatin and natural products extract | 60 |
| III RESULTS AND DISCUSSION | 61 |
| IV CONCLUSION | 98 |
| References | 101 |
| CURRICULUM VITAE..... | 109 |

LIST OF TABLES

| Table | | Page |
|-------|---|------|
| 1 | LC-MS-MS Spectra count for the purified wild type HMGCR band..... | 48 |
| 2 | LC-MS-MS Spectra count for HMGCR from crude lysate..... | 54 |
| 3 | LC-MS-MS Spectra count for HMGCR ν -1..... | 67 |

LIST OF FIGURES

| Figure | Page |
|---|------|
| Cholesterol Molecular Structure..... | 2 |
| Cholesterol Biosynthetic Pathway..... | 4 |
| Lipoprotein particle..... | 5 |
| Source and Fate of Cholesterol..... | 8 |
| Cartoon representation of normal versus artery with plaque formation..... | 10 |
| Representation of thrombus formation..... | 11 |
| Location of HMGCR gene..... | 21 |
| HMGCR Transmembrane, Linker and Catalytic domain cartoon representation..... | 22 |
| HMGCR catalytic domain amino acid sequence..... | 23 |
| Crystal structure of HMGCR monomer with labeled domains..... | 25 |
| HMGCR Tetramer contact surfaces..... | 27 |
| HMGCR monomer showing structural elements involved in dimer formation..... | 29 |
| HMGCR dimerization..... | 30 |
| HMGCR dimerization opposite side view..... | 31 |
| HMGCR active site with substrates..... | 32 |
| HMGCR tetramer showing exon 13..... | 34 |
| HMGCR dimer showing exon13..... | 35 |
| HMGCR dimer showing conserved region..... | 36 |
| HMGCR monomer showing exon 13..... | 37 |
| HMGCR monomer with deleted exon 13..... | 38 |
| HMGCR dimer from <i>Pseudomonas mevalonii</i> | 41 |
| Interaction of HMG-Coenzyme A with NADPH and catalytic residues in HMGCR... | 42 |
| First step HMGCR reaction mechanism..... | 43 |
| Second step HMGCR reaction mechanism..... | 45 |
| Hydrogen bonding of important residues in catalysis..... | 46 |
| Binding of 6x-His tagged Protein to Cobalt Metal Affinity Resin..... | 54 |
| <i>E. coli</i> BL21 (DE3) grown on agar plates with inserted HMGCR gene..... | 62 |
| pETDuet-1 plasmid designed with Serial Cloner 2.5 software..... | 63 |
| pETDuet-1 dual expression vector map constructed with Gene Designer software..... | 64 |
| SDS-PAGE showing HMGCR protein bands..... | 66 |
| HMGCR monomers shown with intact and deleted exon for comparison..... | 67 |
| HMGCR monomer showing post exon 13 deletion contacts..... | 68 |
| SDS-PAGE from crude lysate showing HMGCR and HMGCR- <i>Δ1</i> | 69 |

| | |
|---|--------|
| HMGCR activity plot..... | 74 |
| Lovastatin and its fragmentation patterns..... | 79, 80 |
| LC-MS chromatograms from blank..... | 81-84 |
| LC-MS chromatograms from lovastatin standard..... | 85-88 |
| LC-MS chromatograms of lovastatin extracted from immobilized HMGCR..... | 89-95 |
| UV-Vis spectrum of extracted analyte from bound HMGCR..... | 96 |
| DAD spectrum of deconvoluted signal of unknown library..... | 97 |
| MS fragments showing HEPES extracted from HMGCR..... | 97 |

ABSTRACT

VARIATION IN INTERPERSONAL RESPONSE TO STATIN DRUGS IN HYPERCHOLESTEROLEMIA.

Hameed A. Khan, M.S.

George Mason University, 2012

Thesis Director: Dr. Robin D Couch

Cardiovascular disease (CVD) is ranked as the number one cause of mortality and morbidity worldwide. High blood cholesterol is the number one risk factor for CVD events. Statins class of drugs is the first-choice agents prescribed in medical treatment for lowering cholesterol. Statins inhibit 3-hydroxy-3-methylglutaryl-coenzyme A (HMGCR), the rate limiting enzyme in the biochemical pathway leading to endogenous cholesterol synthesis. There is however significant inter-individual variation in the magnitude of response to statin use. This variation in LDL-cholesterol response to statin has been linked to several phenotypic parameters including diet; in addition, there has been an ongoing investigation into the genetic determinants of the response to statin therapy. Single nucleotide polymorphisms (SNPs) in several genes are linked to reduced efficacy of statin therapy. From pharmacogenomic investigations it has been deduced that 37 different genetic loci contribute to an individual's response towards statin therapy, this

includes the gene encoding HMGCR. It has been recently suggested that HMGCR ν _1 is an alternatively spliced transcript of HMGCR which is conceptualized to be a catalytically active, statin-resistant isoform of HMGCR. We did several expression analyses using pETDuet-1 vector in a host *E. coli* strain BL21 (DE3). Both wild type HMGCR expression and a coexpression involving a dual expression of wild type HMGCR and the hypothetical HMGCR ν _1 were performed. The wild-type enzyme was soluble and catalytically active in each case. HMGCR ν _1 was however neither active nor soluble in the co-expression vector. Based on structural analysis, it is possible that since residues involved in dimerization were missing in the conceptual HMGCR ν _1 construct, subunits association for a functional enzyme formation could not be accomplished, and the expressed protein settles insoluble. The US Food and Drug Administration emphasizes appropriate diet with conventional statin drugs indicating that their combined effect reduces the risk of cardiovascular disease. We therefore propose that an inhibitor with high hepatoselectivity could potentially result in an improved therapeutic window. Bioprospecting has been the source of most of the active ingredients of medicines. To stress upon the use of appropriate diet along with the use of statins we screened for HMGCR inhibitors from dietary extracts. We avoided the use of brute-force high throughput screening approaches which sometimes fail to detect important secondary compounds and agents that go undetected due to high velocity flow through techniques.

The proposed method is cost effective and without the need of robotic devices in identifying lead compounds.

I. INTRODUCTION

The Physiology and Pathophysiology of Cholesterol:

Epidemiological studies indicate that hypocholesterolemia, or very low cholesterol level is associated with increased mortality, arising from hemorrhagic stroke, depression, cancer, and respiratory diseases.^{1,2} Cholesterol composition in membranes is essential for membrane organization and properties, which in turn affects its biological functions such as cellular trafficking and signal transduction.³ In addition to its being a main component of cell membranes and structures, cholesterol serves as a precursor of bile acids and steroid hormones, that includes hormones of the adrenal cortex and sex hormones.⁴ It is therefore, very evident that disorders in lipid metabolism and transport have associated risk factors in humans.⁵

Cholesterol Structure:

The molecular formula of cholesterol is $C_{27}H_{45}OH$. Structurally it is composed of three regions, a hydrocarbon tail, a ring structure region with 4 hydrocarbon rings, and a hydroxyl group attached to one of the rings. Cholesterol owes its hydrophobicity to the 4 hydrocarbon rings and the hydrocarbon tail, making it insoluble in water. It has a very slight hydrophilic character at the end bearing the hydroxyl group (Fig. 1). The 4 hydrophobic rings make cholesterol a precursor of several other steroids, namely vitamin

D, sex hormones, corticosteroids and bile acids. Because cholesterol contains both a hydrophilic and a hydrophobic region, it is called an amphipathic molecule.⁶⁻⁸

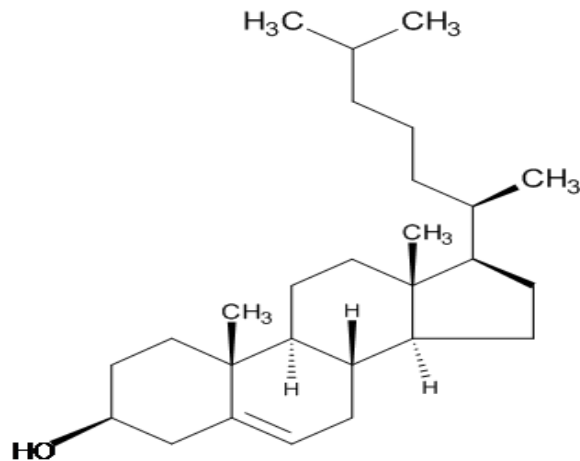


Fig (1) Molecular structure of cholesterol showing four rings, the hydrocarbon tail and the hydrophilic OH group at the opposite end to the hydrocarbon tail.

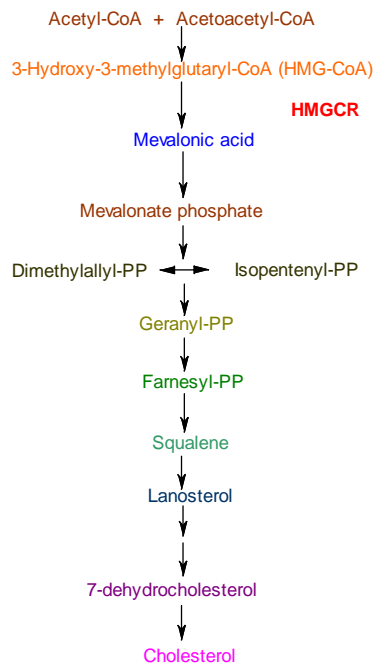
Cholesterol Synthesis:

Endogenous cholesterol synthesis is evolutionary a well conserved multistep biochemical pathway. Considerable amount of energy is consumed to complete more than 20 reactions involved in cholesterol biosynthesis. Endogenous cholesterol synthesis takes

place in all cells, but its synthesis rate in tissues varies depending on the cells need under the physiological conditions. Liver cells produce most of the required cholesterol which are then secreted from the hepatocytes into the blood stream after necessary modifications, and eventually reach the tissues that are slow on de novo cholesterol synthesis. Generally its demand is higher in dividing cells, cells synthesizing lipoproteins, bile and steroid hormones. Since cholesterol is very hydrophobic, therefore it is transported in the blood by lipoproteins.⁹

Cholesterol synthesis initiates from the two carbon acetate group of acetyl-CoA. The process has five major steps. In the first step two molecules of acetyl CoA condense to form acetoacetyl CoA, which further condenses with a third acetyl CoA, resulting in a 6 carbon compound β -hydroxy- β -methylglutaryl-CoA (HMG-CoA). In the second step HMG-CoA is converted to mevalonate. This step is the most committed step, and the major regulatory point of cholesterol biosynthesis. This step involves the reduction of HMG-CoA to mevalonate and is catalyzed by HMG-CoA reductase (HMGCR). This enzyme belongs to the prenyltransferase family that are involved in the synthesis of isoprenoids, cholesterol, steroids, prenylated proteins, heme A, dolichol, ubiquinone, carotenoids, retinoids, chlorophyll and natural rubber etc.¹⁰ This enzyme is the focus of this paper and its reaction mechanism is described in more detail in the preceding sections. In the third step mevalonate is converted to isopentenyl pyrophosphate (IPP), an isoprene based molecule. Three phosphate groups for this step are provided by three molecules of ATP, which allows for the decarboxylation of mevalonate with the concomitant loss of CO₂. Some of the IPP is further isomerized to

dimethylallylpyrophosphate (DMPP). The fourth step begins with the head-to-tail condensation of IPP and DMPP forming geranyl pyrophosphate (GPP). Another IPP then undergoes a further head-to-tail condensation with GPP to form a 15-carbon intermediate farnesyl pyrophosphate (FPP). Next Squalene synthase catalyses the removal of two pyrophosphate groups from two molecules of FPP, resulting in their head-to-tail fusion to form squalene. In the fifth step squalene is cyclized to form lanosterol, a four-ring structure common to all steroids. Similar to HMGCR, squalene synthase is tightly connected to the endoplasmic reticulum. Finally lanosterol undergoes a series of 19 additional reactions to form cholesterol Fig (2).^{7,11}



The Fate of Cholesterol:

After their synthesis or absorption from diet, cholesterol, triacylglycerols (TG) and phospholipids cannot be easily transported freely in the blood. Unlike the anionic form of the fatty acid that can bind to albumin, cholesterol are too hydrophobic to bind to plasma albumin.¹² They are therefore packaged together into droplets of lipoprotein molecules (≈ 20 -1000 nm in diameter) that are composed of lipid and protein. The inner core of lipoproteins is filled by different composition of esterified cholesterol (fatty acid bound to the hydroxyl group on cholesterol) and TG. The inner hydrophobic core is surrounded by a layer of phospholipids, free cholesterol and special proteins called apolipoproteins. The hydrophilic phosphate groups with the embedded proteins make contact with the outer aqueous environment (fig 3).¹³

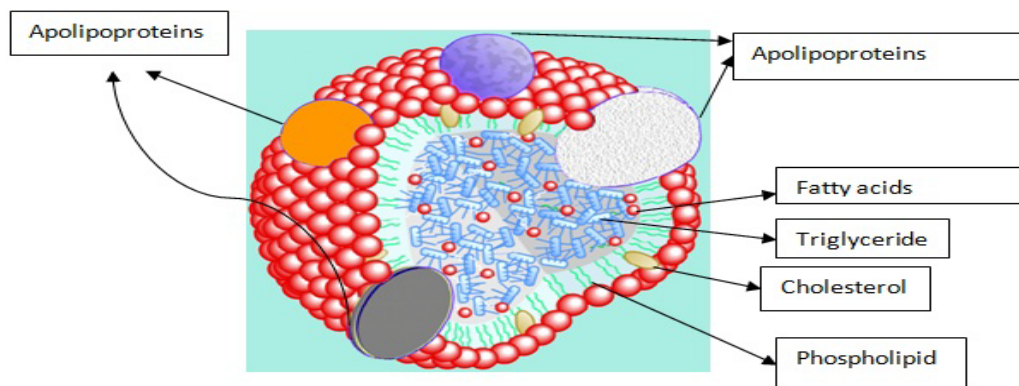


Fig (3) Cartoon representation of a lipoprotein particle.

Lipoproteins are classified based on their density, which varies based on its fat and protein composition. Fat is less dense than proteins and therefore, their ratio gives the overall density of a lipoprotein particle. Thus more fat means lower density. The largest lipoproteins with the lowest density are chylomicrons. Their synthesis begins in the small intestine (enterocytes) from lipids acquired from digested food. They contain apolipoprotein B-48. From the epithelial cells of the small intestine, the lipoproteins are secreted into the lymphatic vessels draining the gut. Chylomicrons bypass the liver and enter the systemic circulation. Chylomicron comes in contact with HDL, another lipoprotein, and receives apolipoproteins particles from the HDL. These apoproteins function as receptor proteins and upon making contacts with tissues (e.g adipose tissue) free fatty acids from chylomicrons are released into these tissues. After losing most of their triglyceride content, chylomicrons are taken up by the liver via a process of receptor-mediated endocytosis, and are broken down.⁹

The liver also produces its own lipoproteins known as very low density lipoproteins or VLDL. These are reservoirs of TG and cholesterol synthesized in the liver. They carry apolipoprotein B-100, and have a life quite similar to that of chylomicrons. In the blood stream VLDL also receive apolipoproteins from HDL. When peripheral tissues removes fat from VLDL, its protein/fat ratio increases and so does its density. This process results in VLDL changing into intermediate density lipoproteins or IDL. Further loss of fats finally changes IDL to low density lipoproteins or LDL. LDL contains mostly cholesterol, which is meant to be targeted to extra hepatic tissues which cannot synthesize their own cholesterol. LDL is then endocytosed into the target tissues. The high density

lipoproteins or HDL, as mentioned before, bears the highest density of all. It has a double function to perform, first it donates some of its apolipoproteins to chylomicrons and VLDL, second which is its main function, is to transport excess cholesterol from peripheral tissue back into the liver. This backward flow of cholesterol makes HDL opposite to other members of the lipoprotein family. Initially HDL has some phospholipids and a lot of proteins, making it the densest of the family, but smallest in size. These proteins on the HDL surface stimulate peripheral cells to lose their cholesterol to the HDL. Some of its apolipoproteins also activate other enzyme, which in turn esterifies cholesterol to make it more hydrophobic. These cholesteryl esters are then packed into the lipoprotein core of HDL and transported back to the liver for further processing and metabolism.^{14,15,16}

Cholesterol biosynthesis is an expensive pathway; therefore the body has evolved to retain it, and no effective way exists for its excretion from the body. A fraction of cholesterol synthesized in the liver is used in making hepatic membranes; the majority of synthesized cholesterol is modified into cholesterol esters and bile acids. Cholesterol esters are packed into VLDL and secreted from the hepatocyte into the blood stream, which are targeted to tissues that do not synthesize sufficient amount of cholesterol. Tissues that receive cholesterol from VLDL use them for the synthesis of membranes, steroid hormones, and vitamin D. Excess cholesterol is stored in the liver as cholesterol esters or converted into hydrophilic bile acids and their salts which are stored in the gallbladder and later excreted into the gut to be used as detergents that aid in the

digestion of dietary lipids. Some of the bile acids is excreted out of the body in the feces while the remaining is reabsorbed and finds its way back to the liver (fig 4).⁹

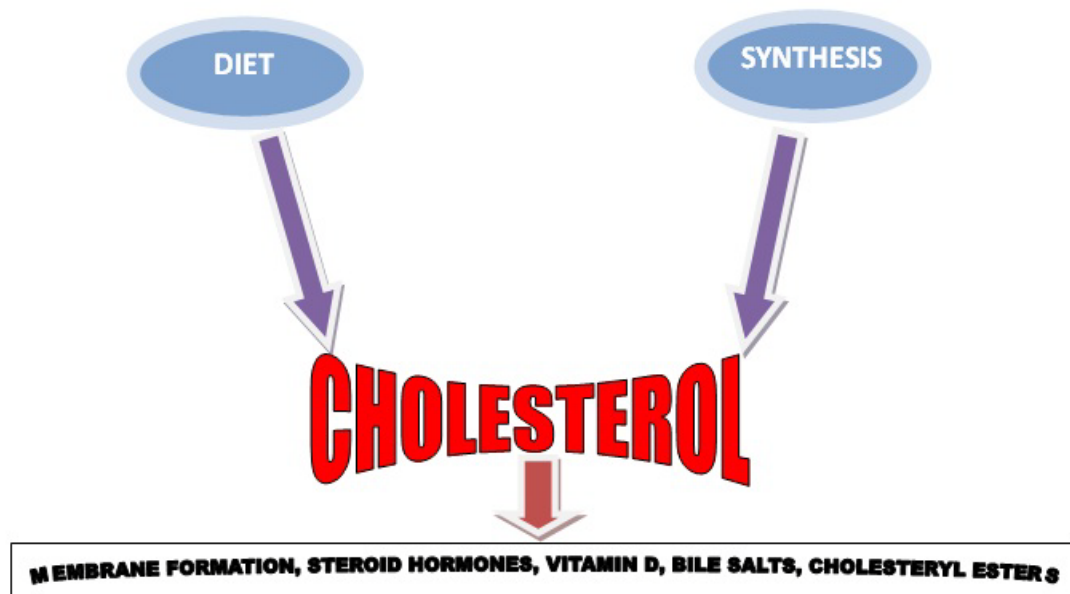


Fig (4) Cholesterol cycle from synthesis to products.

Cholesterol pathophysiology arises when there is too much of it in the blood circulatory system. Circulating cholesterol transported by apolipoprotein B100 (ApoB100)-

containing LDL binds to negatively charged extracellular matrix proteoglycans (due to the occurrence of sulfate and uronic acid groups) and gets trapped in the intima (inner most layer of an artery). Once trapped, LDL becomes susceptible to oxidative damage by reactive oxygen species, or undergoes oxidative modification by enzymes such as myeloperoxidase or lipoxygenases secreted by inflammatory cells. Oxidized lipids and lipoprotein particles initiate the expression of adhesion molecules and the secretion of chemokines, which in turn triggers the body's immune system. The immune system responds by targeting specialized white blood cells (macrophages and T-lymphocytes) to the site in order to absorb the oxidized-LDL. These white blood cells absorb the oxidized-LDL but are not able to process it. Further accumulation of oxidized-LDL causes the white blood cells to grow in size forming foam cells which ultimately rupture. This triggers more white blood cells to the artery walls and further accumulation of cholesterol, fats and even calcium and other substances from the blood at the inflamed site. The same cycle continues again until the site contributes to the formation of tough blockages called plaques. Over time, plaque hardens and narrows the arteries. This buildup of plaque is called arteriosclerosis, and hardening of the arteries is called atherosclerosis.¹⁷ Fig (5) shows formation of plaque and constriction of the artery in a cartoon representation.

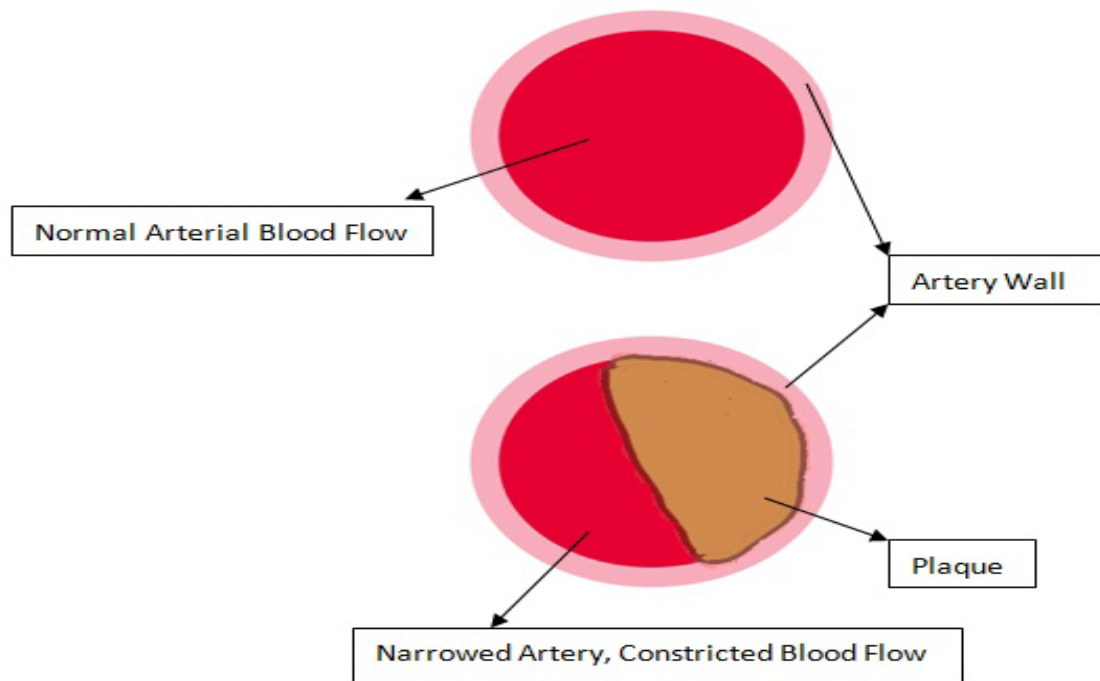


Fig (5) Cartoon representation of normal versus artery with plaque formation.

Lesions at the point of plaque proliferates resident smooth cells (SMCs) in the arterial intima and even targets media-derived SMCs from the media to the intima (intima, medial are layers of arterial wall). Synthesis of extracellular matrix macromolecules such as collagen, elastin and proteoglycans penetrates into the core of the plaque. Increased lesions often results in apoptosis of macrophages and SMCs. Extracellular lipids, cholesterol crystals and microvessels can extend into the lesions (Fig 6 a). At a critical

stage the process ultimately results in thrombosis, and a physical disruption of the plaque's fibrous layer, enabling blood coagulation and platelet aggregation and triggering thrombosis that extends into the vessel lumen (Fig 6 b), where it can impede the flow of oxygen-rich blood to the heart, brain and other parts of the body, causing coronary artery disease and myocardial infarction, stroke and organ failure respectively.¹⁸

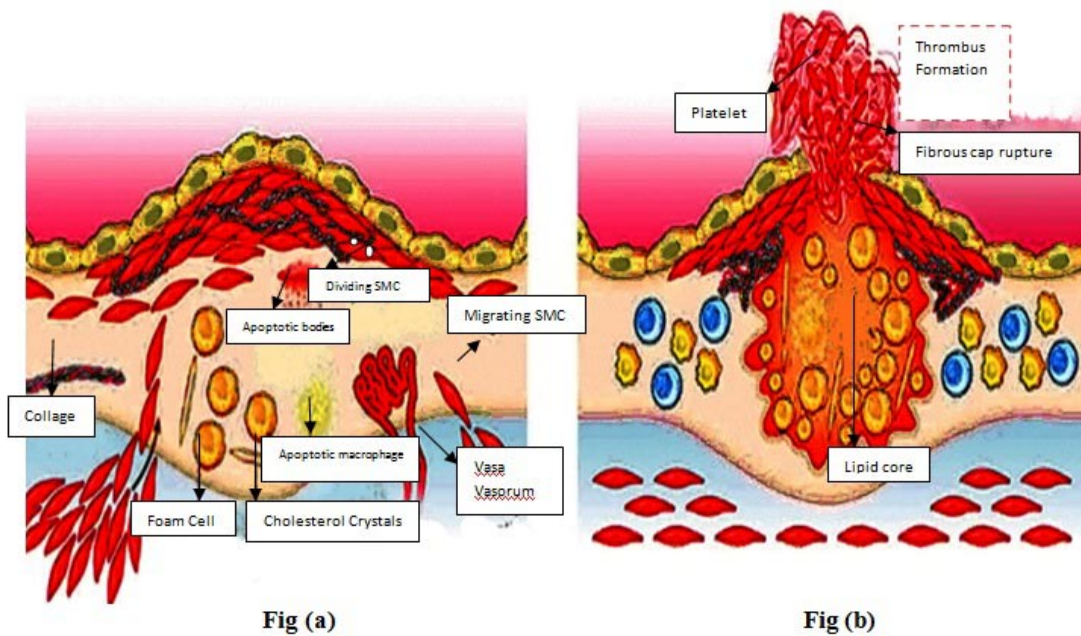


Fig 6 (a) Showing early stages in atherosclerosis, and Fig 6 (b) showing atherosclerosis leading to thrombus formation.

Cholesterol Synthesis Regulation:

Regulation of cholesterol in humans is important to avoid the critical risk factors associated with hypercholesterolemia. Cholesterol synthesis from acetyl Co-A involves more than 10 enzymes of which the important ones are Acetoacetyl Co-A thiolase, HMG Co-A synthase, HMG Co-A reductase, mevalonate kinase, phosphomevalonate kinase, mevalonate-5-pyrophosphate decarboxylase, isopentenyl pyrophosphate isomerase, geranyl pyrophosphate synthase, farnesyl pyrophosphate synthase, squalene synthase, squalene epoxidase, and squalene epoxide cyclase.¹⁹ Knowledge about the kinetic mechanisms and the role of the intermediate products of these enzymes is important for understanding the regulation of the mevalonate pathway that leads to cholesterol synthesis.²⁰

The mevalonate pathway performs several key functions within cells that include production of sterols such as cholesterol, formation and the post-translational modification of proteins from the mevalonate metabolite farnesyl pyrophosphate such as Ras and other small G proteins, which are important secondary messengers of growth signals from membrane growth factor receptors. There is therefore considerable interest in inhibiting the mevalonate pathway to treat not only cardiovascular diseases but also to halt growth signals for the proliferation of cancers.²¹

The first glimpse in understanding endogenous cholesterol homeostasis came during the identification of lead compounds ML-236A, ML-236B, ML-236C isolated from a fungus (*Penicillium citrinum*). These metabolites were found to reduce serum cholesterol levels

in rats. This work was done by Akira Endo and his colleagues at the Fermentation Research Laboratories, Tokyo, Japan. Their research findings indicated that these fungal metabolites had no effect on post mevalonate intermediates in the biosynthetic pathway. This led them to the conclusion that their action was somewhere between the conversion of HMG-CoA to mevalonate, and since the enzyme catalyzing this step was HMGCR, therefore it was identified as the rate limiting enzyme in cholesterol biosynthesis.²²⁻²⁴

Multiple feedback mechanisms harnessed by sterol and nonsterol isoprenoids are involved in regulating the activity of HMGCR. The first regulatory mechanism of cholesterol synthesis occurs when accumulation of sterols results in their binding and subsequent inhibition of sterol regulatory element-binding proteins (SREBPs). SREBPs are membrane bound transcription factors that accelerate cholesterol synthesis and uptake by regulating genes encoding cholesterol biosynthetic enzymes (including HMGCR) and the low density lipoprotein receptor (LDLR). LDLR is a hepatocyte cell surface protein whose physiological role is to assist in the endocytosis of cholesterol-carrying lipoprotein particles into the cells.²⁵

A nonsterol mevalonate-derived product is also involved in the feedback control mechanism that is not clearly understood, but is believed to control the translation of the HMGCR's mRNA by forming a complex with the 5'-untranslated region of the mRNA.²⁶ Both sterol and nonsterol end products of the mevalonate pathway enhances degradation of HMGCR through its ubiquitination by the ubiquitin-proteasome pathway. Through a

knowledge of these mechanisms, it has become clear that sterol accumulation triggers reactions that makes HMGCR susceptible to proteolytic degradation..²⁷⁻²⁹

The third means of regulating HMGCR is via covalent modification achieved by phosphorylation (of Serine 872, in humans). When glucagon concentration is high, phosphorylation of HMGCR increases, which inactivates it, whereas high insulin level increases the activity of reductase by activating phosphatases, which dephosphorylate the reductase. The enzyme that catalyzes phosphorylation of HMGCR is the adenosine monophosphate (AMP) activated protein kinase, which itself is regulated by phosphorylation by the AMP-activated protein kinase kinase.^{30,31} Thus, cholesterol synthesis decreases when adenosine triphosphate (ATP) levels are low and adenosine monophosphate (AMP) levels are high, and increases when ATP levels are high and AMP levels are low.³²

The search for Inhibitors:

Coronary heart disease (CHD) and cardiovascular disease is the leading cause of deaths in 40 % of people in the United States. 1 out of 5 deaths in 2006 were caused by coronary heart disease, which claimed a total of 60700 lives. Even today cardiovascular disease continues to be the leading cause of mortality and morbidity among North Americans. High levels of low density lipoprotein cholesterol (LDLc), or hypercholesterolemia has been the major cause of coronary heart disease.³³ According to The American Heart Association an average American consumes 217-337 mg of cholesterol daily from diet, while 1000 mg cholesterol is synthesized in cells de novo. Thus up to 70% of cholesterol

can be produced by the liver. Although some of the excess cholesterol is removed through the liver, yet a large amount stays in the body. For healthy people of all ages, the World Health Organization (WHO) recommends restricted diet of less than 300 mg cholesterol daily intake and a rigorous exercise to tackle the high mortality rate resulting each year from hypercholesterolemia.³⁴

Diet therapy (with exercise) alone is not always adequate for prevention or normal development. High risk individuals with ≥ 2 risk factors, as well as patients with coronary artery disease and genetic diseases such as familial hypercholesterolemia need a very rigorous approach in controlling plasma LDL levels. These individuals are potential candidates for drug therapy including conventional prevention methods depending on their LDL cholesterol levels.^{35,36,37}

The quest for the development of novel approaches to curtail hyperlipidemia began with the work done by the Japanese microbiologist Akira Endo while searching for antimicrobial agents.²² Endo and others then targeted HMGCR, to search for an agent that could inhibit the rate-limiting step in the cholesterol biosynthesis pathway. Although other enzymes in the mevalonate pathway have been targeted, the results have not been really convincing. Inhibitors of post HMGCR enzymes of the mevalonate pathway, for instance, leads to accumulation of isoprenoid intermediates that has additional effects on other enzymes of the pathway either directly or indirectly.³⁸ These inhibitors are insufficient to prevent the action of one enzyme on the other,³⁹ or have limited clinical activity.^{40,41} Inhibitors for Acetoacetyl Co-A thiolase, a pre HMGCR enzyme is believed

to be targeting other enzyme systems, or showing differential disposition activity in vivo.⁴² Lofibrol, an inhibitor of HMG Co-A synthase, has shown to have some clinical efficacy, but its therapeutic concentrations do not interfere with the production of mevalonate, the product of the committed step in the mevalonate pathway.⁴³ Inhibiting some enzyme in the cholesterol biosynthesis pathway can also lead to diseases like mevalonic aciduria, which is naturally caused by a mutation in the gene coding for mevalonate kinase.⁴⁴ Inhibitors of other enzymes in the pathway like mevalonate kinase and mevalonate 5-diphosphate decarboxylase, are still in the experimental phase and may become useful lead compounds for the treatment of cardiovascular disease and cancer.⁴⁵

HMGCR has become a pharmacological target once it was known to be the rate-limiting enzyme in the cholesterol biosynthetic pathway. Unlike other intermediates of the pathway, HMG-CoA, one of the two substrates for HMGCR, is water soluble and can be broken down by alternative metabolic pathways when HMGCR is inhibited, so that preventing its build-up can prevent potential toxicity. HMGCR was, therefore, an attractive target. The first line of inhibitors for HMGCR came from natural products that had powerful inhibitory effect on HMGCR. ML236B (compactin), the first potent inhibitor, was discovered by the previously mentioned work of Akira Endo and his colleagues, and this work was subsequently appreciated by others.⁴⁶

The current group of drugs called statins is being produced by slight alteration of the basic structure of compactin. Currently the available statins include lovastatin, fluvastatin, simvastatin, pravastatin, cerivastatin, atorvastatin and Rosuvastatin. Although

less potent than compactin, these modified compounds have greater bioavailability and reduced hepatotoxicity.⁴⁷ All statins share an HMG-like moiety to which are covalently linked hydrophobic groups of variable hydrophobicity. The HMG-like moiety extends into a narrow pocket in HMGCR where HMG is normally bound while the hydrophobic groups make contacts with other residues in the enzyme for tight binding.¹¹ The most important effect of HMGCR inhibition is the lowering of circulating LDL in serum. Once statins reduce intracellular cholesterol synthesis and their levels go down, a protease gets activated, which then cleaves SREBPs from the endoplasmic reticulum. The SREBPs then enters the nucleus where they activate the expression of the LDL receptor gene. Greater number of LDL receptors on liver cells upregulate the endocytosis of LDL, thus lowering serum LDL concentration.⁴⁸ Statins can reduce plasma LDL cholesterol levels by as much as 63 %, total cholesterol by 46 %, and triglycerides by 35 %. They can also increase the concentration of HDL, the so called good cholesterol by 14 %.⁴⁹

Statins Related Toxicity:

Although statins continue to dominate the lucrative drug market and have proven to be very efficacious in lowering cholesterol, there is still significant toxicity, especially at high doses associated with them. These effects include increases in hepatic transaminases, atypical focal hyperplasia of the liver, cataracts, vascular lesions in the central nervous system (CNS), skeletal muscle toxicity, testicular degeneration and, although the statins are clearly not genotoxic, tumours of the liver and other sites have been reported, however this claim has not been verified (warning signs for each can be found in the product circulars of the individual statins).^{50,51} Although most of the adverse

effects found in animals during clinical trials did not exist in humans other than minor incidence of myopathy and a slight increase in hepatic transaminases, the possibility of severe side effects cannot be ruled out, especially at higher doses for people who do not respond well enough at therapeutic doses. In addition to dosage dependent toxicities, it is also vital to keep track of treatment duration effects, since previous clinical trials have not been more than five years long, as has been the case with published clinical trials with lovastatin, pravastatin and simvastatin.⁵²⁻⁵⁸ Minor incidences of cancer have also been reported, but statins have largely been ruled out as its causative agents due to the lack of good evidence.^{55,59} Myopathy is believed to be the number one concern in a number of patients who receive statin monotherapy. If myopathy is not detected and therapy is continued, it can progress further to rhabdomyolysis and death.^{33,60}

Interpersonal Variation in Statin Response:

Despite improvements in diagnosis and treatment, cardiovascular heart disease (CHD) remains a major cause of deaths worldwide. The statins class of drugs represents the most common source of treatment for patients with risk factors for CHD. Clinical findings suggest that these drugs are well tolerated and very effective. However, according to the new revisions to National Cholesterol Education Program (NCEP) cholesterol treatment guidelines, more aggressive LDL lowering in at-risk patients (LDL < 70 mg/dl for highest risk patients) is required. Therefore, there is continued requirement for novel HMG-CoA reductase inhibitors with increased efficacies since higher doses of statins

monotherapy or in combination with other drugs such as fibrates and niacin have shown some side effects.^{33,61}

There is significant inter-individual variation in the magnitude of response to statin use. Inter-individual variation in LDL-cholesterol response to statin has been linked to phenotypic parameters such as age, smoking status, diet, body weight, and physical activity; in addition, a number of genetic factors have also been identified. There has been an ongoing investigation into the genetic determinants of the response to statin therapy. From pharmacogenomic investigations it has been deduced that 37 different genetic loci contribute to an individual's response towards statin therapy, this includes the gene encoding HMGCR. Single nucleotide polymorphisms (SNPs) in several genes such as SNP12, SNP29 and the H7 haplotype (groups of SNPs) in *HMGCR*, the ϵ 3 and ϵ 4 alleles in *APOE*, and several other SNPs in genes PCSK9, ACE, LDLR and ABC B1 are linked to reduced efficacy of statin therapy.⁶²⁻⁶⁵ However the reduction efficacy of statins in these variants is small, and of lesser clinical concern.

mRNA alternative splicing is a mechanism of generating variation in several enzymes and HMGCR is not an exception. It has been recently suggested that *HMGCR ν _1* is an alternatively spliced transcript of HMGCR which is conceptualized to be a catalytically active, statin-resistant isoform of HMGCR.⁶⁶ Medina and her colleagues at the Children's Hospital Oakland Research institute, Oakland, CA, hypothesize that the upregulation of expression of the *HMGCR ν _1* transcript in response to statin treatment is related to the drug's significantly varying efficacy in its ability to reduce total cholesterol and LDL and

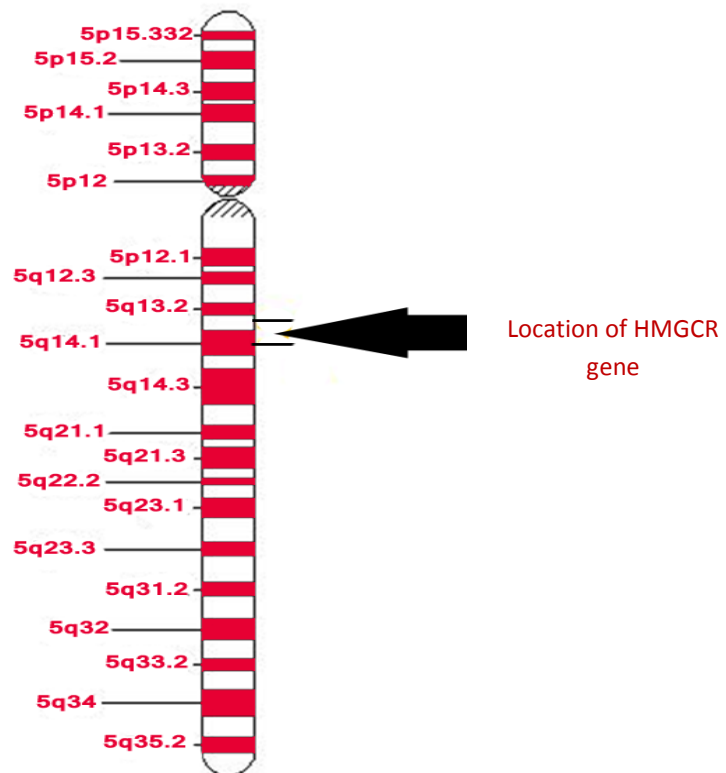
even raise HDL-cholesterol. *HMGCR ν _1*, the alternatively spliced variant of HMGCR is believed to be expressed as a result of rs3846662, one of three SNPs in the H7 haplotype. HMGCR consists of 20 exons (exon 1 – exon 20), and *HMGCR ν _1* is alternatively expressed with the complete deletion of exon 13, but is still conceptualized to be catalytically active, statin-resistant isoform.⁶⁶⁻⁶⁸ However evidence suggests that deletion of exon 13 would result in the deletion of important residues involved in catalysis that would yield the enzyme catalytically inactive.⁶⁹

However splicing events can result in entirely different folds in the protein sequence–structure space, which can be translated in disease state, enhanced or reduced activity of proteins and even insoluble proteins.⁷⁰ Since *HMGCR ν _1* lacks exon 13 that includes important catalytic residue Glu559 and a number of residues involved in dimerization, we therefore believe that based on structural analysis it is possible that since residues involved in dimerization are missing in the conceptual *HMGCR ν _1* construct, subunits association for tetramer formation (explained in the next sections) could not be accomplished, and the expressed protein could possess an entirely different fold or settle insoluble. Thus, in this study, we sought to determine that the expressed protein may not be structurally viable. The focus of this thesis project is on the expression and characterization of HMGCR, and *HMGCR ν _1*.

HMGCR Structure and Classification:

Phylogenetically the HMGCR protein family is branched into two classes, class I and class II HMGCR's. The human HMGCR belongs to the eukaryotic Class I enzyme.⁷¹

Using cDNA probes, in situ hybridization and Southern blotting, the LDLR gene is regionally mapped to the short arm of chromosome 19 in bands p13.1-p13.3, and the HMGR gene to chromosome 5 in bands 5q13.3-5q14.3 (Fig 7).⁷²



(7) Chromosome 5, showing location of HMGR gene on the long (q) arm of chromosome 5 between positions 13.3 and 14. Figure adopted from Genetics

Home Reference, a service of the U.S. National Library of Medicine.

Istvan and Deisenhofer determined structures of HMGCR forming complex with 6 statin inhibitors at its catalytic site. Active site of the HMGCR is occupied by its normal substrates 3-hydroxy-3-methyl-glutaryl-coenzyme-A (HMG-CoA) and NADP(H), where CoA and NAD are the cofactors. Structurally the eukaryotic HMGCR is a tetramer of homodimers. The different monomers are named as chain A, chain B, chain C, and chain D. Each monomer consists of N-terminal membrane anchor domain, a linker domain, and a C-terminal catalytic domain as shown in the cartoon image (Fig 8 (a)), and the amino acids sequence (Fig 8 (b)).

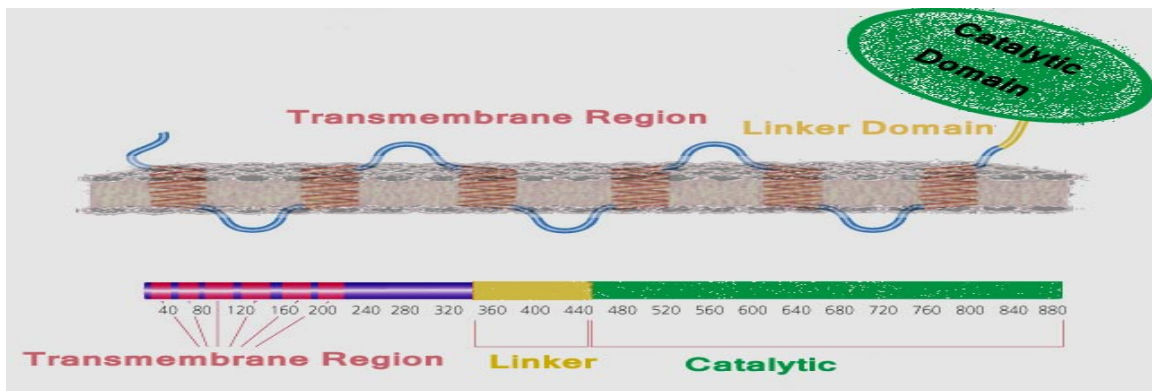


Fig 8 (a) HMGCR (human) represented with both transmembrane region, and the cytosolic linker and catalytic region. Figure adopted from Sigma Aldrich.

MLSRLFRMHGLFVASHPWEVIVGTVTLTICMMSMMFTGNNKIC
 GWNYECPKFEEDVLSSDI I I L T I T R C I A I L Y I Y F Q F Q N L R Q L G S
 KYILGIAGLETFIFSSVFVSTVVIHFLLDKELTGLNEALPFFLLLI
 DLSRASTLAKFALSSNSQDEVRENIARGMAILGPTFTLDALVEC
 LVIGVGTMSGVRQLEIMCCFGCMSVLANYFVFMFFPACVSLVL
 ELSRESREGRP IWQLSHFARVLEEEENKPNPVTQRVKMIMSLGL
 VLVHAHSRWIADPSPQNSTADTSKVS LGLDENVSKRIEPSVSLW
 QFYLSKMI SMDIEQVITLSLALLLAVKYI FFEQTETESTLSLKN
 PITSPVVTQKKVPDNCCRREPMLVRNNQKCD SVEEETGINRERK
 VEVIKPLVAETDTPNRATFVVGNS SLLDTSSVLVTQEPEIELPR
 EPRPNEECLQILGNAEKGAKFLSDAEI IQLVNAKHI PAYKLETL
 METHERGVSIRRQLLSKKLSEPSLQYLPYRDYNYSLVMGACCE
 NVIGYMPI PVGVAGPLCLDEKEFQVPMATTEGCLVASTNRGCRA
 IGLGGGASSRVLADGMTRGPVVRLPRACD SAEVKAWLETSEGFA
 VIKEAFDSTS RFARLQKLHTS IAGR NLYIRFQSRSGDAMGMNMI
 SKGTEKALS KLHEYFP EMQILAVSGNYCTDKKPAAINWIEGRGK
 SVVCEAVI PAKVVREVLKTTTEAMIEVNINKNLVGSAMAGS IGG
 YNAHAANI VTAIYIACGQDAAQNVGS SNCITLMEASGPTNEDLY
 ISCTMPSIEIGTVGGGTNLLPQQACLQMLGVQ GACKDNPGENAR
 QLARIVCGTVMAGELSLMAALAAGHLV KSHMIHNRSKINLQDLQ
 GACTKKTA

Residues 1-339
Membrane anchor domain

Residues 340-459
Linker domain

Residues 460 -863
Catalytic domain

Flap domain

Fig 8 (b) Amino acid sequence of human HMGCRC with each domain color coded.

The catalytic domain further consists of three domains: an N-terminal ‘N-domain’, a large ‘L-domain’ and a small ‘S-domain’. The N-domain (residues 460-527) is the smallest of the three domains consisting of 5 α -helices numbered N α 1 to N α 5. The L-

domain is the largest of the three domains (residues 528-590 and 694-872) and consists of 6 beta sheets numbered L β 1 to L β 6 and 11 alpha helices numbered L α 1 to L α 11. The L-domain resembles a prism in its architecture. A 27-residue helix (L α 10) is at the center of the prism surrounded by three subdomains. The S-domain (residues 592-682) is formed by 4 beta sheets numbered S β 1 to S β 4 and 3 alpha helices numbered S α 1 to S α 3. L-domain is not continuous as it starts at residue 528 and ends at residue 590, then starts again at residue 694 ending at residue 872. The discontinued residues (residues 591-693) are mostly filled by residues coming from the S-domain's helices and beta sheets (residues 592-682). This insertion of the S-domain into the L-domain together forms the binding site for NADP (H) and folds into an α/β sandwich that resembles ferredoxin. Another important feature of the L and S domains is the formation of the binding site for HMG. This binding site gets its structure from the continuation region that is formed by these two domains. This continuation of one domain into the other is brought about by beta strand (L β 3 and S β 1) and a 'cis-loop' formed by a cis-peptide (residues 682-694). The cis-loop between residues C688 and T689 consists of important residues involved in HMG binding (Fig 9).⁷¹

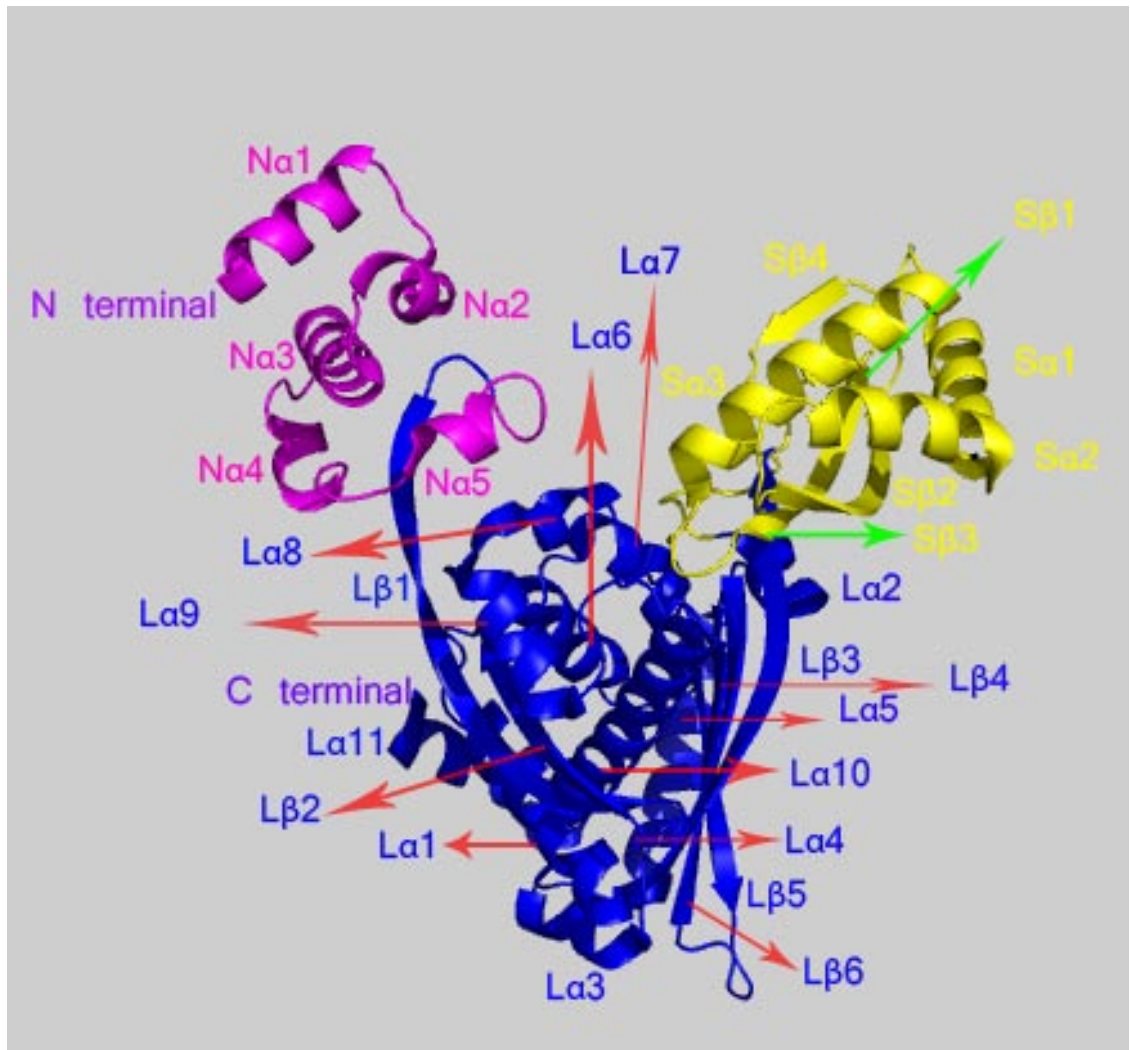


Fig (9) Crystal structure of HMGCR monomer with all three domains labeled.

Crystal structures have shown an important mobile element of the human HMGCR that comprises of N870, R871 and the C-terminal residues (25-30 amino acids) that includes helix $\text{La}11$. This element called as the flap domain alternates between ordered and disordered conformation depending on the binding of the substrate NADP(H). Our

previous work has shown how slight alterations to the flap domain can influence enzyme activity and confer sensitivity to statins, the target inhibitors of HMGCR (Fig 20).⁷³

Oligomerization:

Catalytically active HMGCR is found as a dimer of dimers where protein-protein interactions in the formation of a tetramer are known to be brought by hydrophobic forces, hydrogen bonds and salt bridges between residues in each chain. The interface is predominantly hydrophobic where carbon atoms contribute 64 % while N, O, and S contribute the remaining 36 % in the form of polar contacts. Thus although the interface is mostly hydrophobic, buried salt bridges participate in establishing the anchor points in forming a catalytically active enzyme (Fig 10).

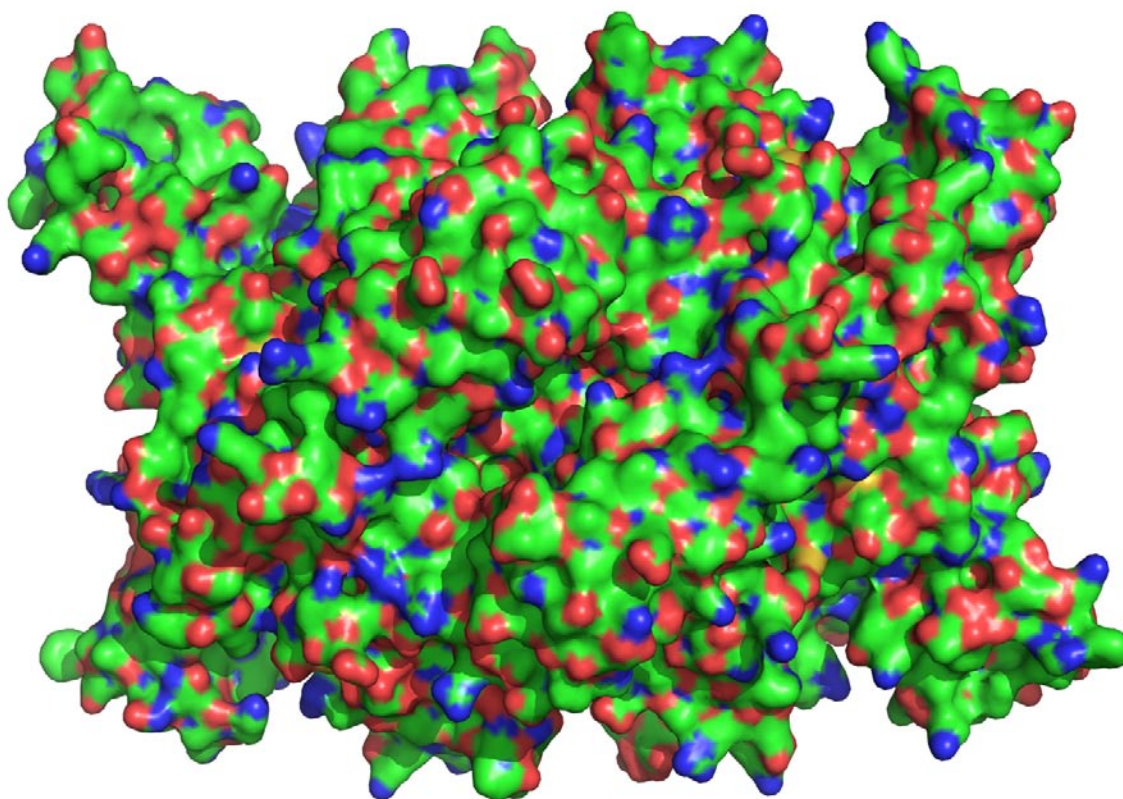


Fig (10) HMGCR tetramer contact surfaces, showing green predominant color (hydrophobic contacts), polar contacts involving oxygens (red), nitrogens (blue) and couple of yellow (disulphide sulphur bridge).

Starting with the N-terminal of the Catalytic portion (residues 426-888) of the enzyme the first important interdimer contact that has been well conserved in both class I and class II HMGCR's is the sequence element ENVIGX₃I/P starting at Glu528 and ending at Pro537 resulting with 9 important hydrogen bonds between the two monomers (Fig11). The second dimerization element exists between alpha helices L α 6 and L α 7 of the L-domain with similar but antiparallel helices from the neighboring monomer. This

sequence can be found at His752-Cys764 and Asp767-Ser775, and the interactions results in a buried four helix bundle. Interactions between the L and S domains comes from the four-stranded antiparallel β -sheets of one monomer (Pro592-Arg595, Arg630-Ala639, Asn642-Arg650, and Gln679-Val683, from S-domain) with L α 4 (Thr723-Ala743) of the neighboring monomer, which includes an important salt bridge between Arg595 and Glu730 along with several hydrogen bonds. In the N-domain interactions between monomers is brought about by the 3_{10} -helix N α 4 packed against the L-domain helix L α 9 (Figures 11, 12 and 13).⁷¹

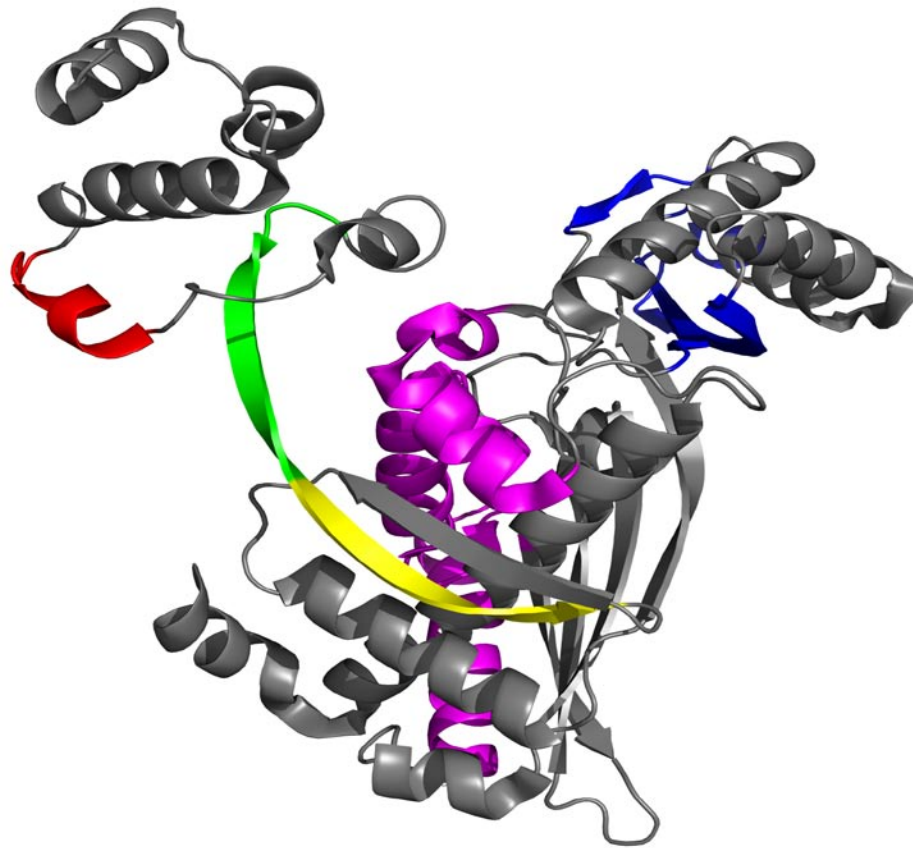


Fig (11) HMGCR monomer showing important structural elements involved in dimer formation. N domain's $N\alpha 4$ 3_{10} -helix (red). L domain's elements include $L\beta 1$ (green, yellow) that includes ENVIGX₃I/P conserved region (green) and $L\alpha 4$, $L\alpha 6$ and $L\alpha 7$ (purple). Antiparallel β -sheets of S domain (Blue).

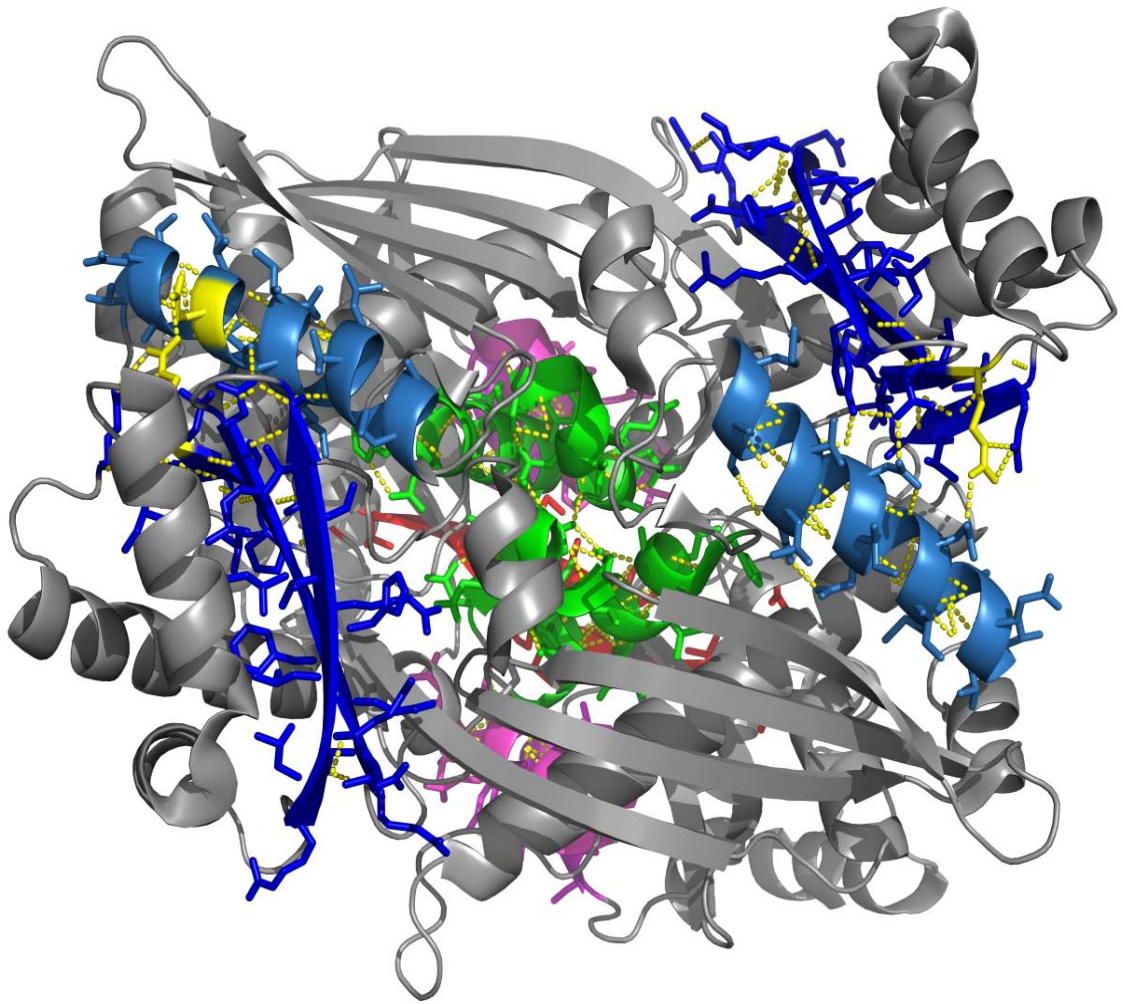


Fig (12) HMGCR dimer showing dimerization elements of four-stranded antiparallel β -sheets of S domain (dark blue) with $L\alpha 4$ of L-domain (light blue) of the neighboring monomer, $L\alpha 6$ and $L\alpha 7$ of the L-domain with similar but antiparallel helices from the neighboring monomer (green) also showing important salt bridge (yellow). 3_{10} -helix $N\alpha 4$ packed against the L-domain helix $L\alpha 9$ (purple) and $L\beta 1$ (red) with similar but opposite beta sheet from the neighboring monomer.

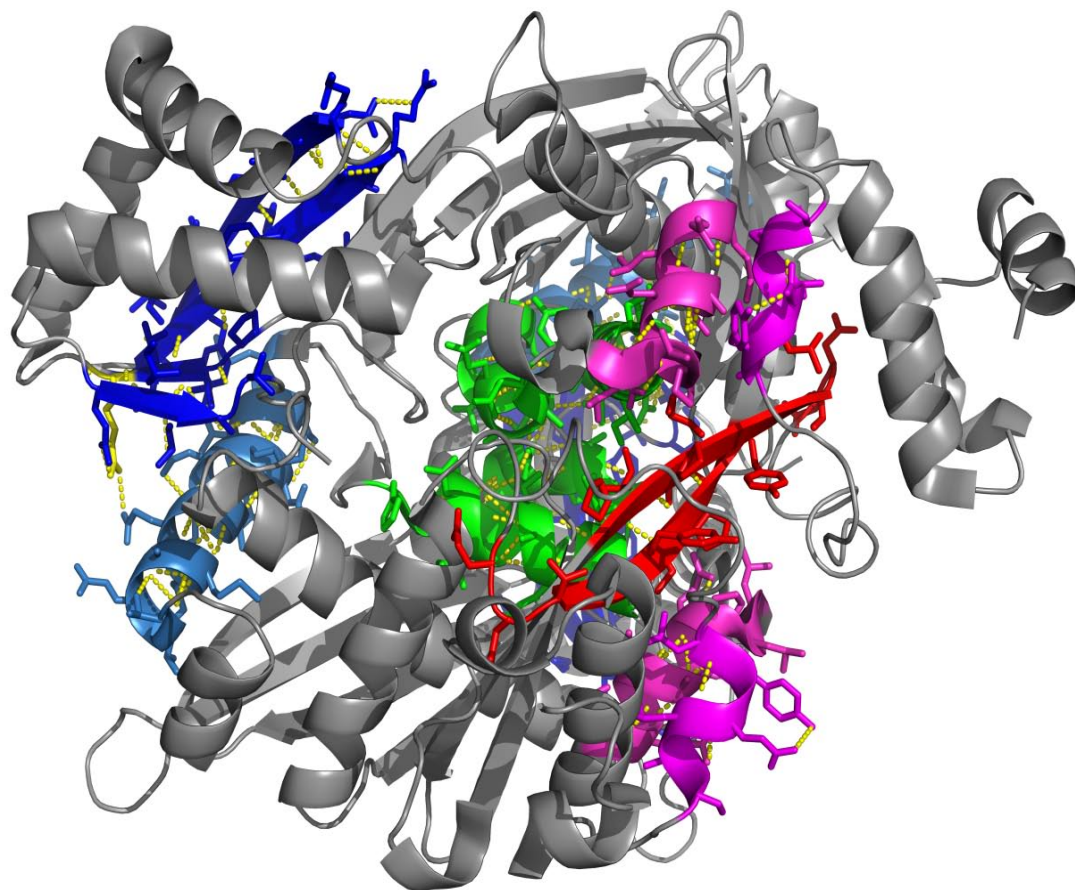


Fig (13) Opposite side view of fig (12), HMGCRCR dimer contacts.

Each monomer has active sites for the binding of NADPH and HMG-CoA (Fig 14). These binding sites are located at the interface of the two monomers of a dimer. The tetrameric structure is not involved in the formation of the active site, but instead gives structural stability to the enzyme, whereby each monomer of a dimer makes contacts with two monomers of the neighboring dimer in forming the D_2 symmetry. ¹¹

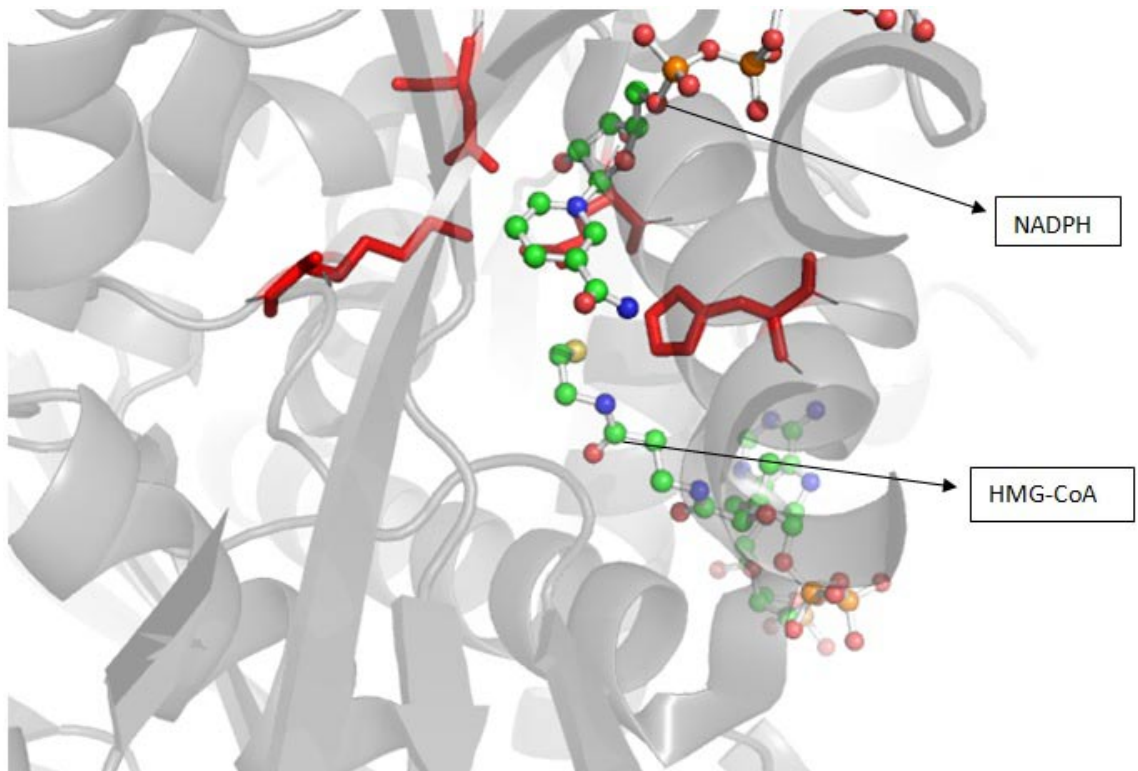


Fig (14) HMGCR active site showing substrates NADPH and HMG-CoA, and residues involved in catalysis (red).

The spliced variant isoform HMGCR ν _1 has a deletion of 53 important residues in its probable structure (Fig 19). These 53 residues are deleted as a result of alternative splicing which results with the depletion of exon 13. Exon 13 encodes approximately 5 residues in the N domain (Val522-Cys526) and 46 residues in the L domain (Cys527-Gly574) (Fig 18). This sequence contains an important dimerization region ENVIGX₃IP

(Fig 17), and as has been mentioned before, is highly conserved in both class I and class II enzymes. It also includes Glu559 an important residue involved in catalysis that will be mentioned in the preceding sections. Exon 13 has all three elements of a secondary structure, loop, beta sheets and helix, and as seen in the HMGCR tetramer figure (18), makes vital surface to surface contacts in the dimeric structure. The dimer structure in fig (16) shows that especially its beta sheets intertwine with each other while extending into the center of the contact surfaces.

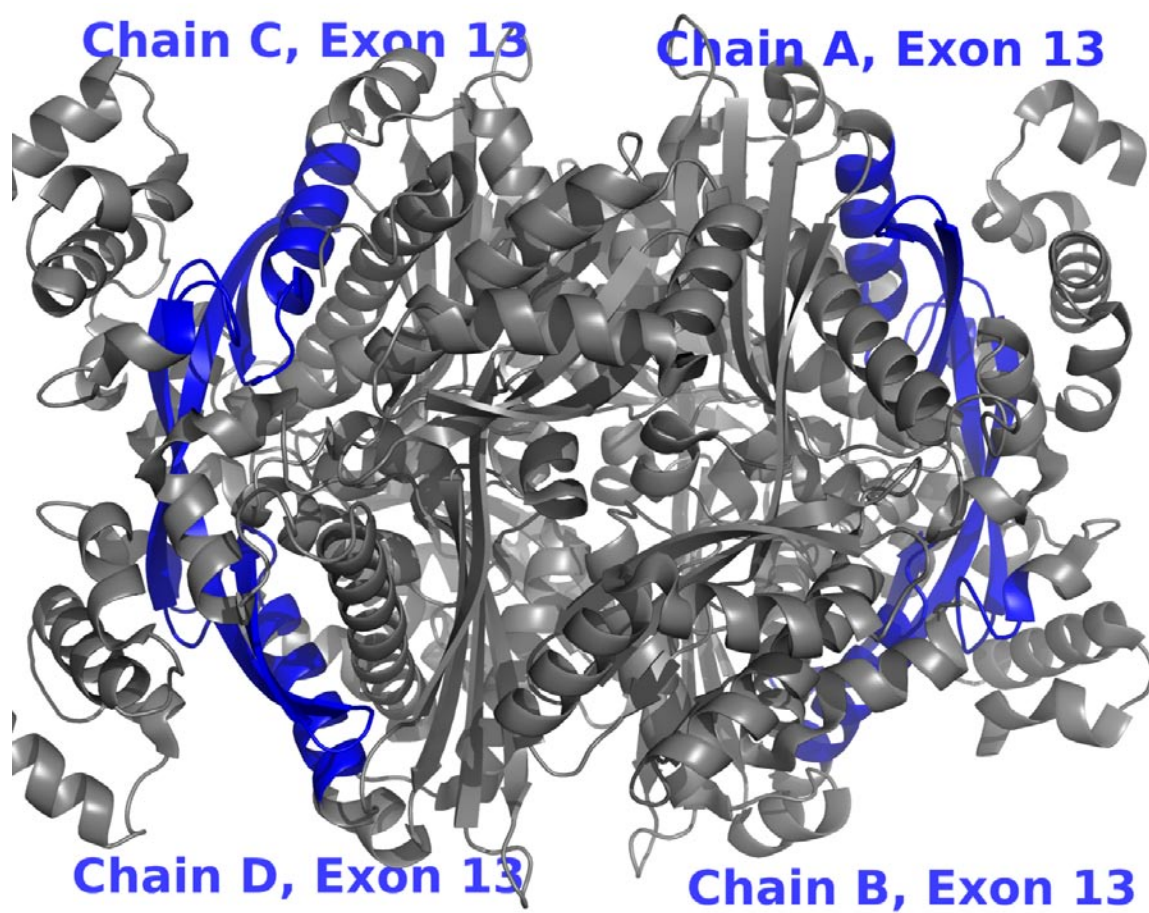


Fig (15) HMGCR tetramer showing exon 13 in blue.

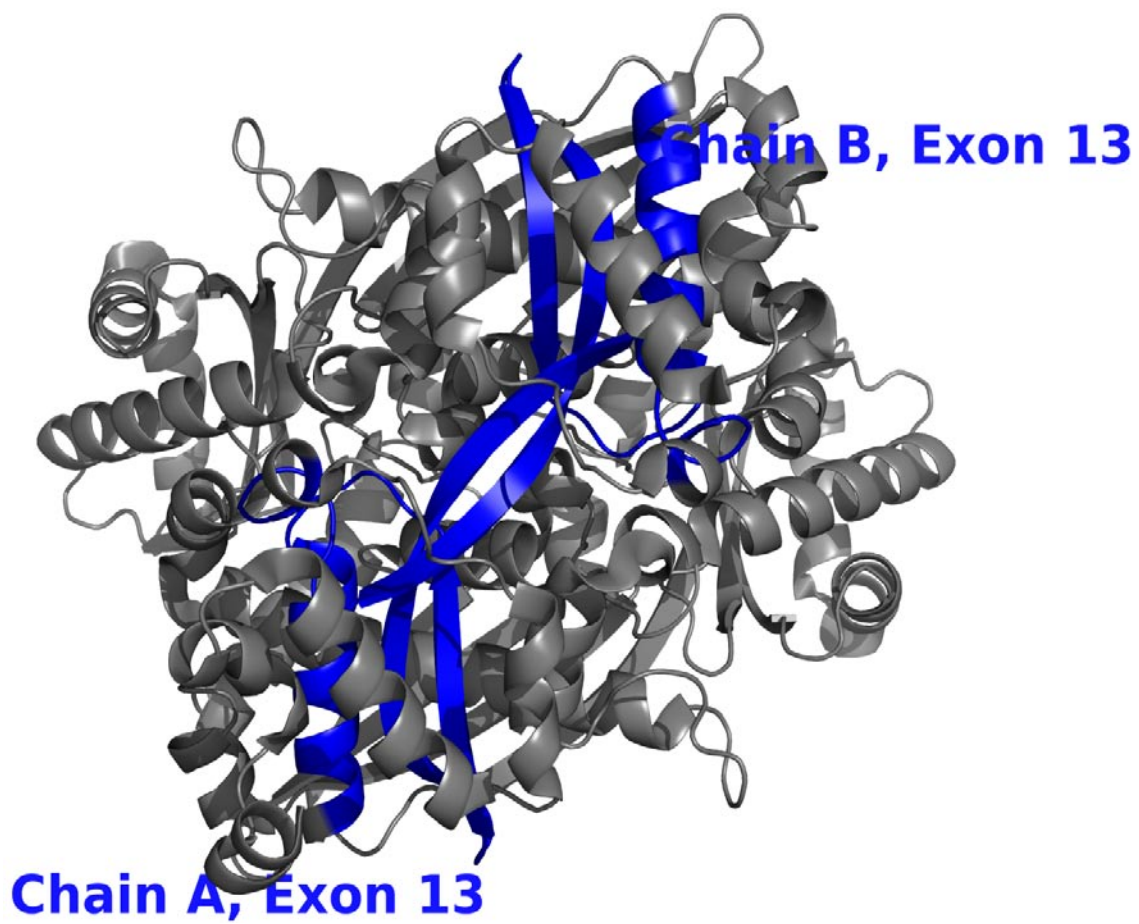


Fig (16) HMGCR dimer showing exon 13 in blue.

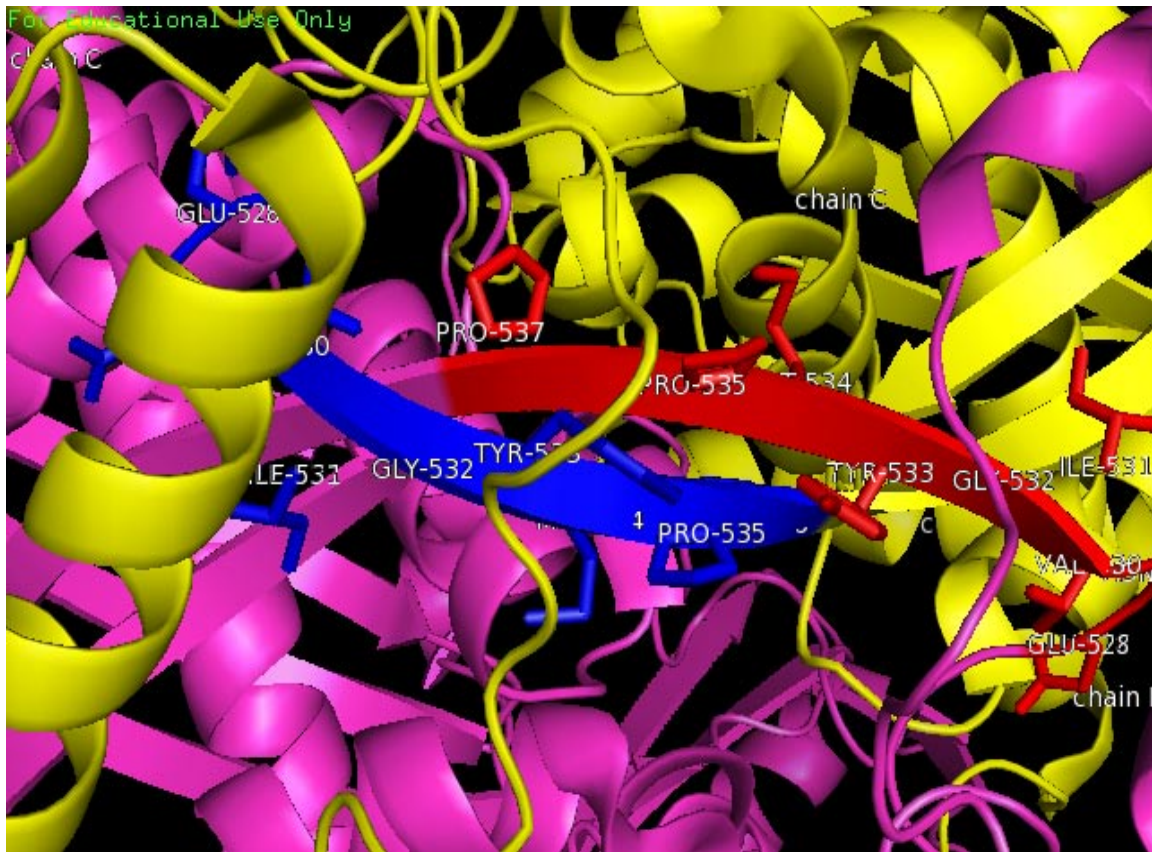


Fig (17) Conserved region ENVIGX₃I/P in exon 13 involved in dimerization, red from one monomer and blue from the neighboring monomer wrapping against each other.

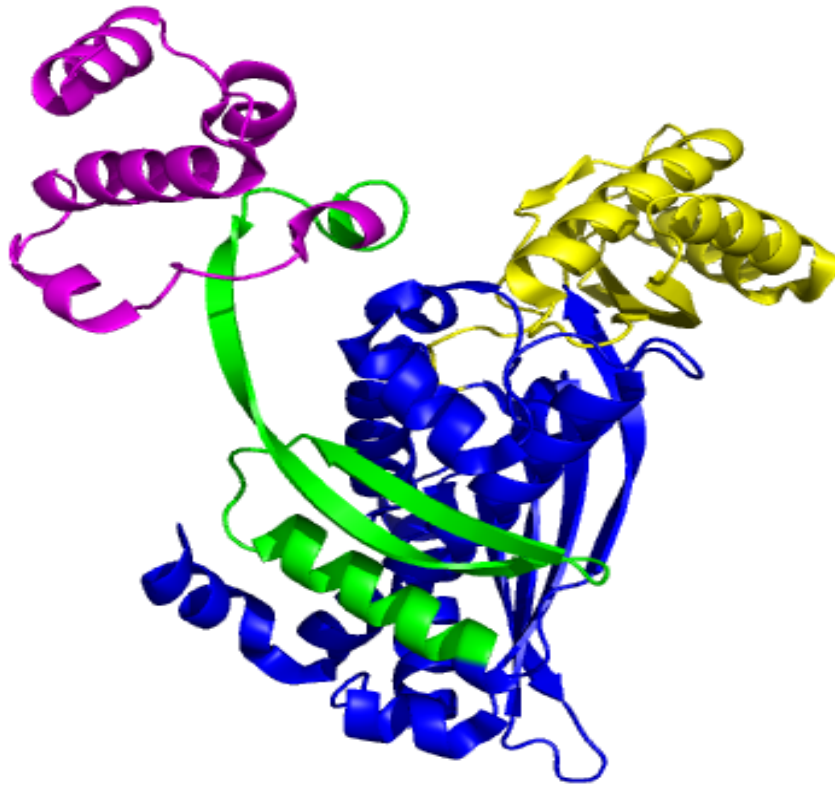


Fig (18) HMGCR monomer showing all three domains and exon 13, N domain (purple), L domain's exon 13 (green), remaining L domain (blue) and S domain (yellow).

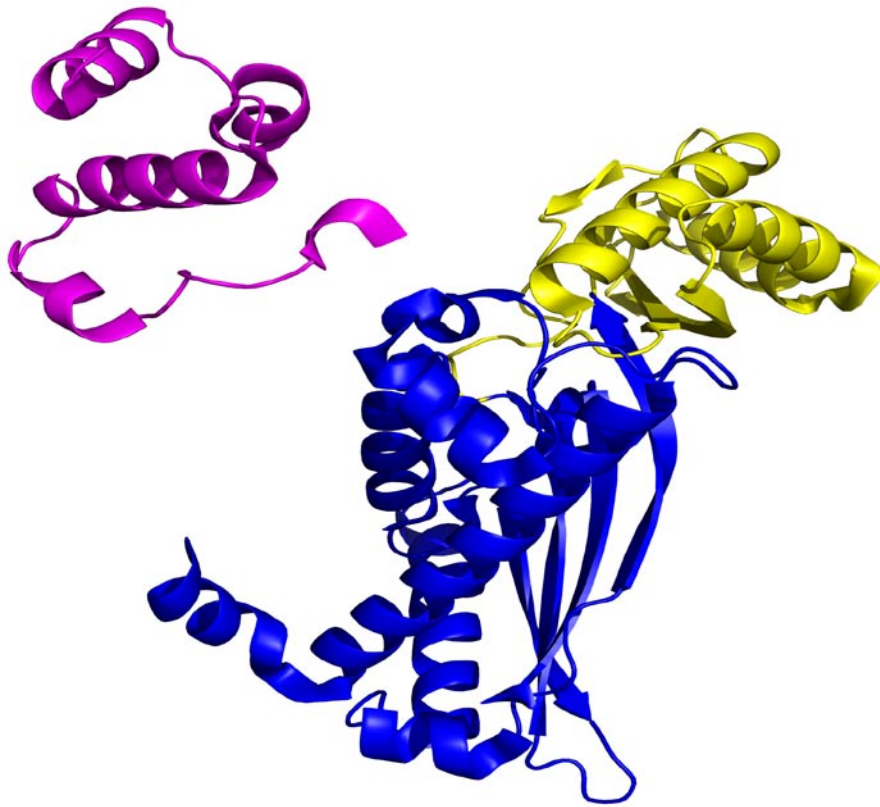


Fig (19) Same HMGCR monomer as fig (18) but with exon 13 deleted (green missing).

Catalysis:

The HMGCR reaction mechanism has been studied since 1960's. In 1959 Knappe *et al*⁷⁴ found that the rate limiting step of cholesterol biosynthesis is catalyzed by HMGCR, and pointed out mevalonate as a product of HMG-CoA. The role of NADPH as a reducing agent in this reaction was elucidated by several others (Durr *et al.* 1960, Bensch *et al.* 1970, Kleinsek *et al.* 1977, Edwards *et al.* 1979)⁷⁵⁻⁷⁸. From kinetic studies it was made

evident that the reaction mechanism involves the formation of two intermediate steps, a thiohemiacetal and an aldehyde (Retey *et al.* 1970, Qureshi *et al.* 1976)^{79,80}. Active site residues in HMGCR were determined, and point mutation studies revealed the important catalytic activity of Lys, His, Glu, and Asp (Frimpong *et al.* 1994, Bochar *et al.* 1999)^{81,82}. HMGCR has been studied extensively because of its biological importance, especially for enzymologist it has been an interesting enzyme. The first x-ray crystallographic structure of HMGCR was determined from class II enzyme of *Pseudomonas mevalonii* (Lawrence *et al.*, 1994)⁸³. The catalytic portion of HMGCR both from class II and class I enzyme was elucidated with the crystal structures from 2.0 to 2.8 Å. (Taberero *et al.*, 1999, Istevan *et al.*, 2000)^{84,85}. Based on all the accumulated results from these studies a reaction mechanism was proposed for the catalysis taking place at the active site of HMGCR.

First, HMG-CoA binds to the enzyme followed by NADPH, and a hydride transfer from NADPH results in formation of mevaldyl-CoA intermediate also known as hemithioacetal. This reduction of thioester bond in HMG-CoA by residues in the active site occurs due to the fact that thioester bonds (R-S-(C=O)-R') are extremely labile. In the next step mevaldyl-CoA decomposes to mevaldehyde and CoASH, and conformational changes in the enzyme permits the dissociation of NADP⁺ thus allowing another NADPH molecule to bind. In the final step, mevaldehyde is reduced to mevalonate followed by the dissociation of all three products (mevalonate, CoASH, and NADP⁺) from the enzyme.

NADPH molecules are created in catabolism when a negative hydride anion is bonded to a molecule of NADP^+ . A "hydride anion" (H^-) is a hydrogen atom with an extra electron (two e^- instead of one e^-) and therefore a negative charge. When used as a reducing agent, each NADPH molecule gives up the hydride anion (H^-), providing two electrons ($2 e^-$) to help move the reaction forward. In the process, a NADP^+ molecule is also released.

The orbital overlap between a carbonyl group and sulphur is not as good as the resonance overlap between oxygen and carbonyl group in esters due to larger atomic size of sulphur compared to oxygen. This means that the C-S bond is longer and more easily polarized. The hydrolysis of thioester bond results in lower free energy of the products compared to hydrolysis of a normal ester bond. This makes the thioester bond in HMG-CoA very prone to nucleophilic attack. The hydride anion in NADPH acts as a nucleophile in the conversion of HMG-CoA to mevaldyl-CoA.

Investigation demonstrated the importance of a three-helix C terminal flap domain (residues 858-888), which appears to be disordered upon binding of HMG-CoA, and is ordered during the first hydride transfer. This ordering positions the catalytic histidine His-888, which resides on the first helix of the flap, in the active site. No crystal structures are available showing the mobile element flap domain of the C-terminal for any class I HMGCR enzyme, however crystal structures for Class II enzyme are available showing the closure of this mobile element upon substrate binding.⁸⁴ The disordered versus ordered C-terminal flap domain is shown in Fig (20). Our previous work⁷³ showed

how alteration to the flap domain imparts enhanced catalytic activity to the enzyme by affecting the alignment of the histidine located in the first helix of the flap domain.

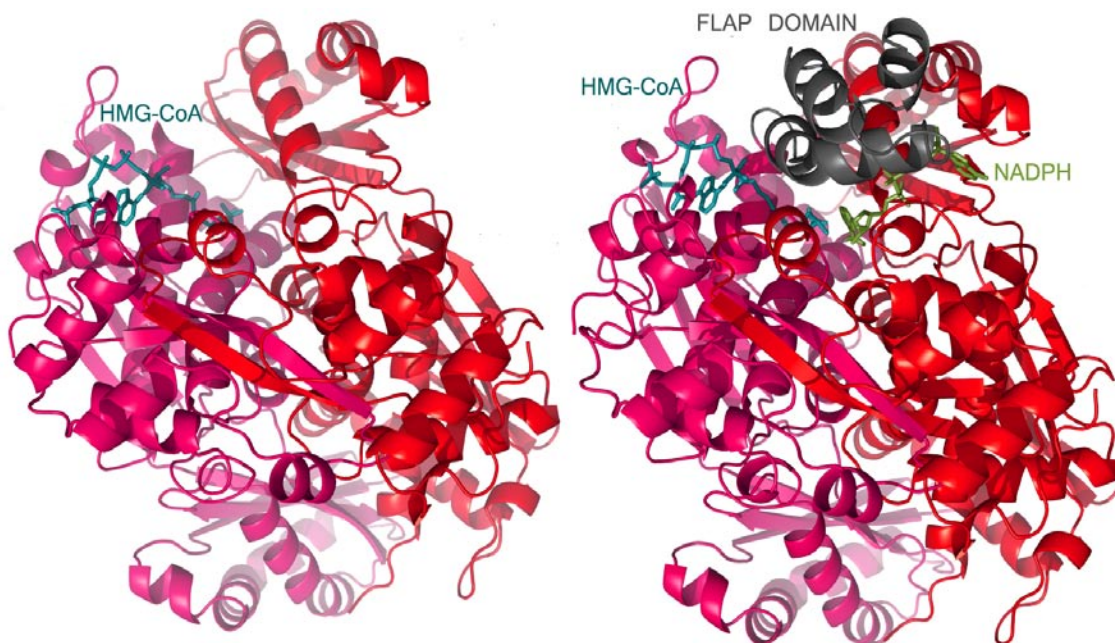


Fig (20) HMGCR dimer from *Pseudomonas mevalonii* showing the closure of flap domain (grey) upon binding of NADPH. PDB ID 1QAX.

Particular amino acids in HMGCR are responsible for helping lower the activation energy barrier for the transition state that has to be overcome in order to convert HMG-CoA to mevalonate. Once inside the active site, the negatively charged carboxylate group of HMG-CoA forms an ionic bond with a lysine residue (Lys-735). A hydrogen bonding network is formed between the alcohol group of HMG-CoA and Ser-684, Asp-690 and

Lys-691 forming a hydrogen bond to the negatively charged carboxylate of HMG-CoA, it also plays a vital role in stabilizing the negatively charged oxygen of mevaldyl-CoA through hydrogen bonding and ionic interactions. This serves a two face advantage, first stabilizing the intermediate mevaldyl-CoA, and second stabilizing the transition state leading to it. Consequently the activation energy for the first step in the biosynthesis reaction is lowered, allowing for the reaction to proceed to the formation of the intermediate product in this step (Fig 22).

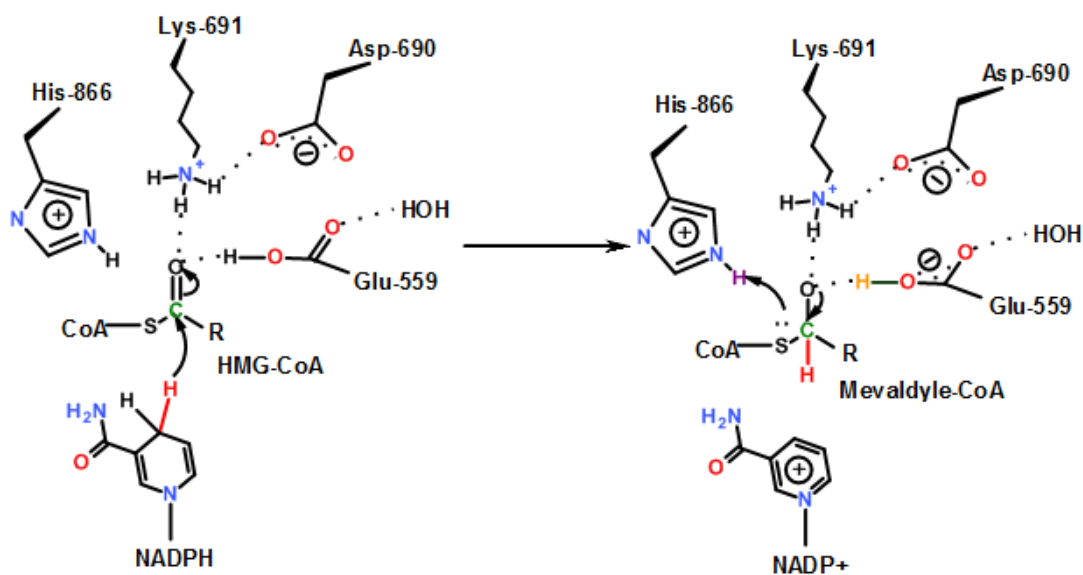


Fig (22) First step in the reaction mechanism of HMGCR leading to the formation of the intermediate product Mevaldyl-CoA

In the second step enzyme-bound mevaldyl-CoA is deacylated to enzyme-bound mevaldehyde and coenzyme-A. The ionic and hydrogen bonding network between the negatively charged oxygen of mevaldyl-CoA and Lys-691 and Glu-559 facilitates conversion of mevaldyl-CoA to bound mevaldehyde and the CoAS⁻ anion. NADPH then replaces NADP⁺. Coenzyme A gets a proton from His-866, which serves as an acid catalyst, to let the CoA depart as a leaving group (Fig 23).

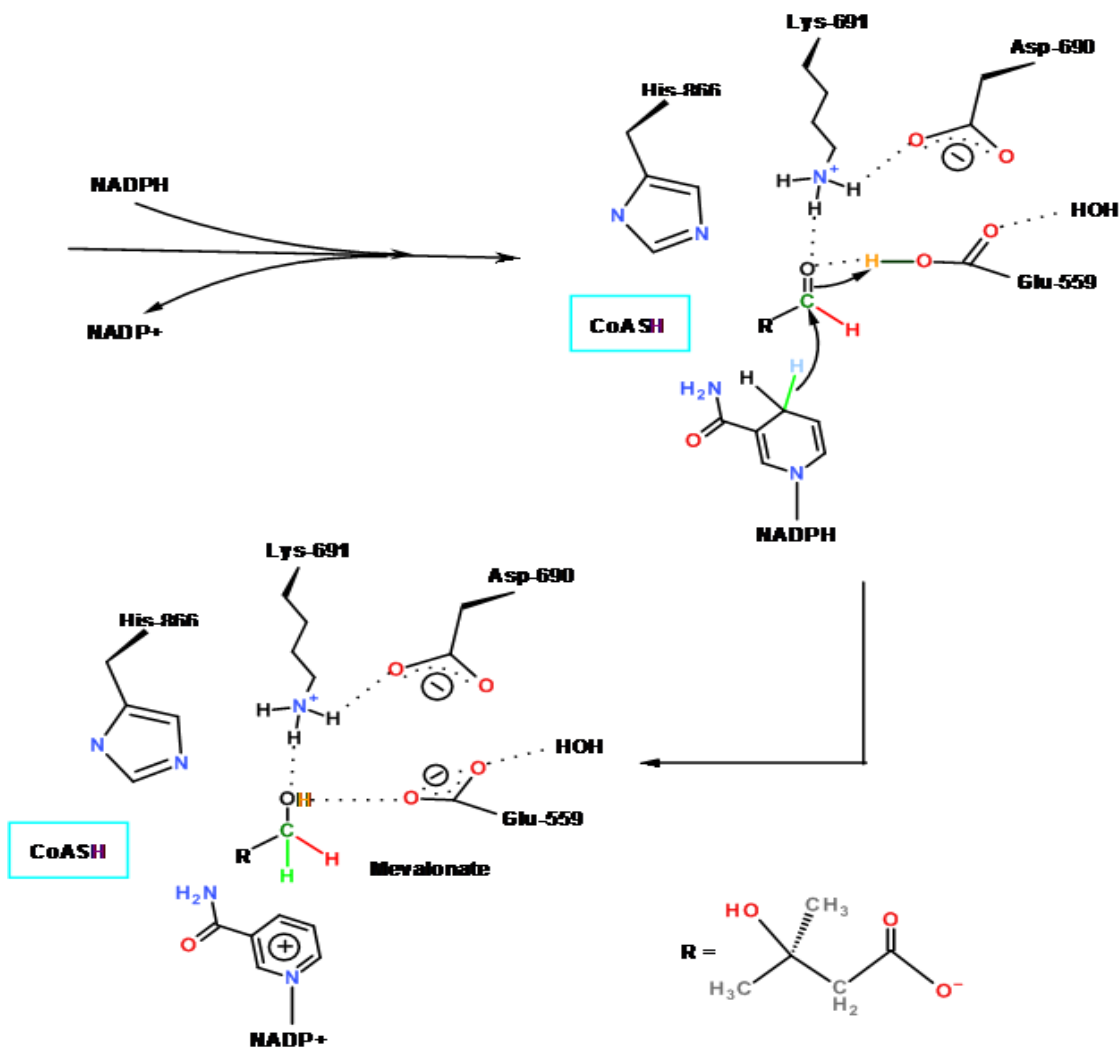
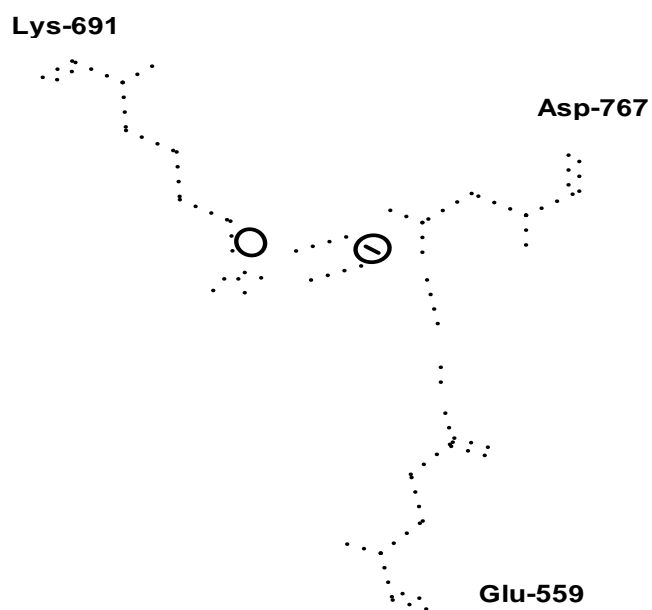


Fig (23) Showing the conversion of mevaldyl-CoA to bound mevaldehyde and CoASH (step 2), and the ultimate conversion of mevaldehyde to mevalonate (step 3)

Special attention needs to be made regarding an important role played by a protonated glutamic acid Glu-559 in the reaction. First the presence of a neighboring aspartate residue (Asp-767) affects the pK_a of Glu-559, which results in protonating the ionic Glu-

559. In the final stage of the reaction this protonated Glu-559 acts as an acid catalyst and provides this proton for the reduction of mevaldehyde to mevalonate. Asp-767 also forms a hydrogen bonding network with Lys-691 which results in stabilizing the ionic form of Lys-691 (Fig 24).^{71,81}



Structurally the components of all statins are a dihydroxyheptanoic acid unit and a ring system with variable substituents. The variability in the ring structure and substituents lead to the variations of physicochemical, pharmacokinetic, and pharmacodynamic properties of all statins. Lipophilicity is one of the important physicochemical properties of statin drugs. It was found that not only ADME properties, but also the hepatoselectivity of the statins, are linked to their physicochemical properties. The more lipophilic statins tend to hit non-hepatic tissues, while the hydrophilic statins are more hepatoselective. The lipophilic statins tend to passively diffuse into both hepatocyte and non-hepatocyte, the hydrophilic statins on the other hand depend mostly on active transport into hepatocyte for its activity. High hepatoselectivity has been linked to reduced risk of adverse effects and therefore it was concluded that lipophilicity of statins also affects their toxicity.⁸⁶

Thus, an inhibitor with high hepatoselectivity could potentially result in an improved therapeutic window. Bioprospecting has been the source of most of the active ingredients of medicines. Natural products were the major source of drug discovery before the advent of high-throughput screening and the post-genomic era. More than 80% of drugs are based on natural products or inspired by natural compounds. Almost all new drugs from 1981 to 2007 indicate that half of the drugs approved since 1994 are based on natural products. Thirteen natural-product-related drugs were approved from 2005 to 2007 that included peptides, exenatide and ziconotide, and small molecules such as ixabepilone, retapamulin and trabectedin. More than a 100 natural-product-derived compounds are

currently undergoing clinical trials and as many projects are in preclinical development. Most of these lead compounds are derived from plants and microbial sources.⁸⁷

Genes may change the response to diet and drugs. A combination of drugs and diet alterations has been shown to be effective in reducing cardiovascular disease risk and mortality. However, the convenience of application, the consistency and magnitude in lowering of LDLc achieved, and benefits associated with statins in large randomized clinical controlled trials has ignored the importance of diet even in primary prevention of CHD. The National Cholesterol Education Program Adult Treatment Panel III (ATPIII) and the American Heart Association have recently recommended the use of appropriate diet, high in components that reduce cholesterol as an extra option to enhance the effectiveness of cholesterol-lowering therapy. These dietary ingredients include viscous fibers, soy protein, plant sterols, and nuts. The US Food and Drug Administration now emphasizes appropriate diet with conventional statin drugs indicating that their combined effect reduces the risk of cardiovascular disease.⁸⁸

Proteomic and genomic laboratory research approaches have served to provide new insights into the molecular and physiological pathways of disease pathogenesis and its health effects on drug targets. Traditionally, high-throughput screening approaches use brute-force robotic analytical and sampling devices to detect potentially therapeutically useful lead compounds and agents against a particular target. During this screening process, important secondary compounds and agents go undetected due to high velocity flow through techniques which results in escape from the scene of important bioavailable

compounds that can have important pharmacokinetic properties, for example the absorption, distribution, metabolism and excretion properties of that compound. Despite these drawbacks approaches in finding important therapeutic compound for drug discovery, the screening process for effective drugs candidate is highly reliant on natural products from diverse species of plants and animals.⁸⁹

Personalized medicine based on an individual's molecular profile, will revolutionize the way drugs are developed and medicine is practiced. Molecular basis of disease will lead to novel target identification, toxicogenomic markers to screen compounds and improved selection of clinical trial patients, which will have a positive effect on pharmaceutical industry. There has been a decline in pharmaceutical productivity in recent years, where despite increases in research and development expenses, there has been a decline in submission and approval of new drugs to treat disease and benefit patients.⁹⁰

The purpose of this thesis is thus to propose a simple and cost effective way to determine lead compound identification of natural inhibitors of wild type HMGCR using bioprospecting. The method we propose for screening ligands for our wild type HMGCR target is very simple and cost effective. The apparatus can be easily set up in a small space in any laboratory work bench area. The techniques and instrumentation utilized in the proposed project are ion exchange column chromatography (cobalt resin), LC/MS, LC-MS/MS tandem mass spectrometry, UV-Vis spectrophotometry, growing E.Coli host cells with a petDuet vector for the expression and isolation of HMGCR and its isoform HMGCR_v_1.

II. MATERIALS AND METHODS

Cloning and Expression:

To construct a bacterial coexpression plasmid containing HMGCR and HMGCR_v_1 fragments, we used the pETDuet-1 vector (Novagen) which has two multiple cloning sites (MCS1 and MCS2), both under the control of the bacteriophage T7 transcription promoter.

One pETDuet-1 plasmid was constructed with the insertion of wild type HMGCR gene alone into MCS1, while another pETDuet-1 vector was constructed such that wild type HMGCR gene was inserted into MCS1 while the spliced variant HMGCR_v_1 gene was inserted into MCS2. Both vectors were commercially cloned and their recombinant molecules amplified at GenScript USA Inc. The first plasmid prepared was restriction enzymes digested with *SalI* *NotI* and ligated with DNA ligase into the MCS1 site of pETDuet-1. The second coexpression pETDuet-1 vector was restriction enzymes digested with *SalI* and *NotI* and ligated with DNA ligase into the MCS1 site and the same was done with the splice variant isoform HMGCR_v_1 gene sequence into the MCS2 site with DNA ligase and *NdeI-XhoI*. Both plasmids were amplified at GenScript and sent to us in special frozen packages for transformation. The MCS1 site contained a His tag sequence at the N-terminus for isolation at purification using affinity chromatography.

Virtual genetic recombination was performed using Serial Cloner 2.5, a software for designing plasmids. A restriction digest was performed on the vector plasmid for the insertion of the appropriate genes into the pETDuet-1 vector sequence. Similarly restriction enzyme digestion was performed on PCR product sequences of the wild type HMGCR and the HMGCR_v_1 DNA sequences that included primers at both ends followed by sequences identified by the restriction endonucleases. For verification purposes the construct was also designed using Gene Designer by DNA 2.0, another plasmid designing software but no differences were seen other than special features specific to each software.

Plasmids pETDuet-1 HMGCR and pETDuet-1 HMGCR+HMGCR_v_1 were transformed into competent *E. coli* cells with BL21(DE3) strain . This *E. coli* strain lacks many of the protease enzymes present in other bacterial strains and is thus well suited for protein expression.

The transformed cells were plated on LB-agar Petri dishes containing 50 µg/mL ampicillin and 34 µg/mL chloramphenicol and incubated overnight at 37°C. Three colonies were aseptically picked up from these plates and separately inoculated into 10 mL culture of LB medium containing the same concentration of antibiotics and then incubated at 37°C overnight. This, in turn, was used to inoculate four 1 L volumes of LB liquid media with antibiotics. The optical density (OD) of these cultures was monitored at 600 nm over a period of ~3 hours. After the OD reached 1.1, protein expression was induced by adding 5 mL of 100 mM isopropyl-β-D-thiogalactopyranoside (IPTG) to each

flask to a final concentration of 0.5 mM. Expression was allowed to continue for 16 hours at 37°C, after which the cultures were harvested by centrifugation at 6000 X g for 20 minutes at 4° C. The supernatant was discarded and the pellets then stored frozen at -80°C. The cells were lysed using a mixture of buffer A (100 mM Tris pH 8, 0.032 % lysozyme); 3 mL of buffer A was used per 1 g of cell pellet, and buffer B (0.1 M CaCl₂, 0.1 M MgCl₂, 0.1 M NaCl, .020 % DNase); 0.3 mL buffer B was used per 1 g of cell pellet. Preparation of a clear supernatant cell lysate was performed with centrifugation of the crude lysate at 4° C, 48000 X g for 20 min.

Protein Purification:

His-tagged protein was purified at room temperature using a gravity flow column containing TALON immobilized metal affinity chromatography (IMAC) resin. This resin is used for the purification of histidine tagged protein. Adjacent, specially positioned, or neighboring histidines bind to the TALON cobalt ligand core with greater affinity. Cobalt (Co³⁺) ion can accept lone pair of electrons due to its empty valence-shell orbitals. Co³⁺ has room in its valence shell for 12 more electrons (four electrons can be added to the 3d subshell, two to the 4s orbital, and six to the 4p subshell). Four coordinate covalent bonds from the resin bead cross linker provides 8 of the electrons while the remaining 4 electrons are provided by two coordinate covalent bonds from two of the six His-tag on the expressed HMGCR (Fig 25). Although only two histidines are used out of the six His-tag, the extra four histidines are used to saturate the environment with histidines around Co³⁺. This increased concentration of histidines drives the association with Co³⁺ making

the association too solid in hydrophobic solution such as oils that do not form coordinate bond with Co^{3+} , they therefore, do not interfere with the coordination chemistry between histidine and Co^{3+} . They can however clog chromatography columns and their removal is important before purification of the target protein.⁹¹ TALON cobalt resin is highly selective for his-tagged proteins compared to nickel-based resins, thus background proteins can be prevented from binding, so intense washing procedures are avoided before eluting the desired protein (Fig25). Another advantage of TALON resin is that the desired protein can be eluted with mild, physiological conditions, so as to keep the protein biologically active. Second, His-tagged proteins elute from TALON resin under mild, physiological conditions, which can be crucial for keeping the protein biologically active. TALON resins are also less prone to metal ion leakage because cobalt forms uniform complexes with the chelating ligands, thus preventing co-elution of the protein with the metal ion leakage.

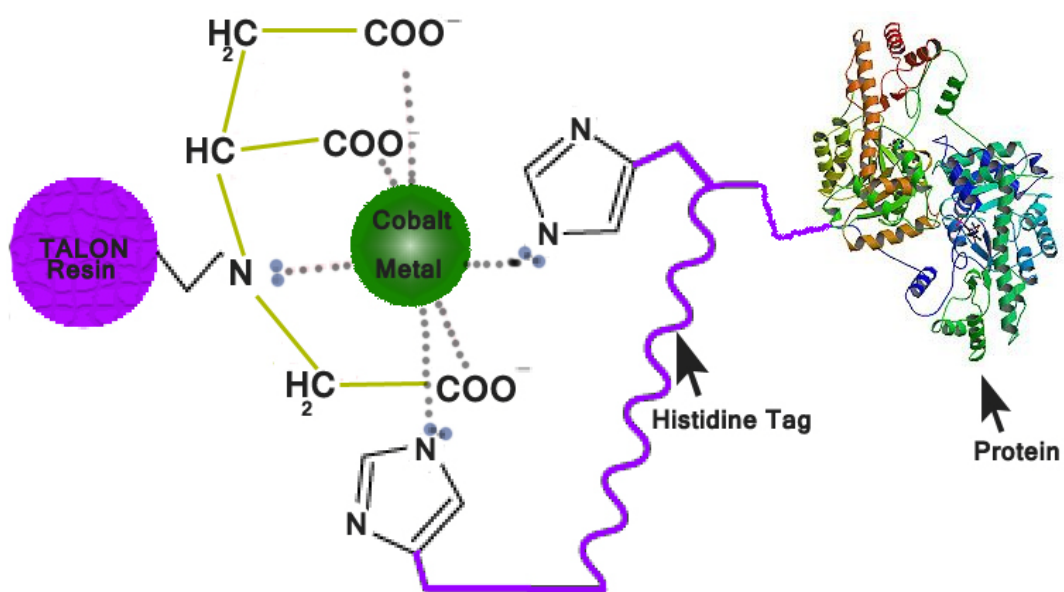


Fig (25) Talon Cobalt resin showing six coordinate covalent bonds, four with the cross linker and two histidines from a His-Tag. Only two histidines are shown for clarity.

The column was equilibrated with 1X equilibrium buffer (50 mM HEPES *pH* 7.5, 0.3 M NaCl). The supernatant was transferred to the TALON cobalt resin column then washed with the same 1X equilibrium buffer followed by a second wash with a 1X wash buffer (50 mM HEPES *pH* 7.5, 0.3 M NaCl, 10 mM Imidazole). The bound protein was then eluted with 1X elution buffer (0.15 M imidazole, *pH* 7.0, 4° C, 0.02 M NaCl). Each eluate was concentrated using an Amicon Ultra centrifugal filter device. The elution

buffer was exchanged by adding aliquots of the 1X wash buffer to the retentate while concentrating. Protein concentration was determined using the Advanced Protein Assay reagent (Cytoskeleton, Denver, CO, USA), with bovine γ -globulins as the standard.

Protein Electrophoresis:

4–12% Criterion™ XT Bis-Tris precast polyacrylamide gel was used with 1X MOPS SDS PAGE running buffer for good protein electrophoresis resolution. The concentrated protein was mixed with 5X SDS dye and run next to Fisher BioReagent EZ-Run Rec protein ladder. The protein gel was covered with staining solution (40 % methanol, 7 % acetic acid, 0.1 % m/v brilliant blue^R) and left until the next day. The gel was covered with destaining solution (10 % methanol, 10 % acetic acid) and visualized.

LC-MS/MS:

For the detection of insoluble protein fraction, half pea size cell pellet left over from the purification step was placed in microcentrifuge tube and dissolved in 45 μ L 5X SDS loading buffer and heat denatured at 75° C for 10 minutes. The tubes were spun at maximum speed (13.2 RPM) in a microcentrifuge tube for 15 minutes. The upper layer supernatant was removed and protein electrophoresis was performed on the supernatant. Bands on the gel were cut out and sent for protein identification to the Center for Applied Proteomics and Molecular Medicine at the Manassas campus, George Mason University for LC-MS/MS analysis.

In-gel digestion by trypsin was performed on the excised gels according to the standard procedure.⁹² The extracted peptides were analyzed by reversed-phase liquid

chromatography nanospray tandem mass spectrometry (LC-MS/MS) using an LTQ-Orbitrap mass spectrometer (ThermoFisher). The reversed-phase LC column was slurry-packed in-house with 5 μm , 200 Å pore size C18 resin (Michrom BioResources, CA) in a 100 μm i.d. \times 10 cm long piece of fused silica capillary (Polymicro Technologies, Phoenix, AZ) with a laser-pulled tip. After sample injection, the column was washed for 5 min with mobile phase A (0.1% formic acid), and peptides were eluted using a linear gradient of 0% mobile phase B (0.1% formic acid, 80% acetonitrile) to 45% mobile phase B in 120 min at 200 nL/min, then to 100% B in an additional 5 min. The LTQ-Orbitrap mass spectrometer was operated in a data-dependent mode in which each full MS scan (60,000 resolving power) was followed by eight MS/MS scans where the eight most abundant molecular ions were dynamically selected and fragmented by collision-induced dissociation (CID) using a normalized collision energy of 35%. Tandem mass spectra collected by Xcalibur (version 2.0.2, ThermoElectron, San Jose, CA) were searched against the NCBI human protein database (released on September 5, 2009, 34 180 sequences) using Bioworks 3.3.1 (ThermoFisher, Extract_msn for peak picking software and SEQUEST for search engine) with full tryptic cleavage constraints, static cysteine alkylation by iodoacetamide, and variable phosphorylation of Ser/Thr/Tyr and methionine oxidation. Mass tolerance for precursor ions was 10 ppm and mass tolerance for fragment ions was 0.5 Da. Confident phosphopeptide identifications were determined using stringent filter criteria “ranked top #1; Xcorr versus charge 1.8, 2.5 for 2+, 3+ ions; mass accuracy 3 ppm; probability of randomized identification of peptide <0.05” for database match scoring followed by manual evaluation of the results. The estimated

“false discovery rate (FDR)” is lower than 1% by searching a combined forward reversed database. Information about the E. coli host strain was given along with the vector plasmid and the gene of interest.

HMGCR activity:

The HMGCR catalytical activity was determined spectrophotometrically following the method of Kleinsek *et al*⁹³, whereby the oxidation of NADPH was monitored as a rate of decrease in absorbance at 340 nm. The spectrophotometer was equipped with a 1 cm path length analytical cell and maintained at 37° C. The standard assay mixture contained 100 mM K₂HPO₄ pH 7.0, 4 mM dithiothreitol (DTT), 0.15 mM NADPH, 30 nM enzyme and 3.69 μM substrate (HMG-CoA) to a final volume of 120 μL. The reaction mixture containing the enzyme except the substrate was preincubated for 5 min at 37° C prior to adding the substrate, to ensure maximal activity. The spectrophotometer reading was first monitored with the addition of distilled water to the mixture without HMG-CoA to ensure no independent oxidation of NADPH without the substrate. The reaction was then initiated by the addition of the substrate instead of distilled water. The same procedure was repeated for the concentrated enzyme obtained from the dual expression to see any marked difference in the activity. The enzyme substrate dependent activity was reported as micromoles of product per minute based on the change in the absorbance signal using the following equation:

$$\text{Activity} = \frac{\Delta \text{absorbance} / \Delta \text{min}}{6220 \text{ M}^{-1} \text{cm}^{-1}} \times 10^6 \mu\text{M} / \text{M} \times 0.0012 \text{L}$$

Natural products library was created based on previous literature showing effects of certain natural compounds on LDL and triglyceride lowering. Several other random compounds were also added to the library for bioprospecting. The library contained 2.59 g mixture of green tea and cardimium, 100 ml distilled water, 14 g garlic and ginger paste, 200 mL V8 vegetable juice. To this library was added 127.1 g of black seed extract. Grinded black seeds were dissolved in ethyl acetate, vortexed then centrifuged at 3600 RPM 25° C, 15 minutes. Transferred the supernatant to round bottom flask and dried out the solvent ethyl acetate using Buchi Rotavapor R-200 connected to B-490 heating bath, Neslab RTE-140 refrigerated cooling system and AHL CT-60e vacuum chamber. Added the mixture library to 2 mL 1% polyethylene glycol (PEG) and sterilized filtered for binding analysis.

Screening for HMGCR inhibitors:

Bioprospecting for ligands showing affinity to HMGCR was performed using TALON cobalt resin affinity column. 50 μ L, ~ 30.03 mg/ml of His-tagged HMGCR was run under gravity across the cobalt resin column for binding to the cobalt metal. After successful binding of the protein to the column the prepared library was run across the column for the detection of analyte with probable affinity to the protein. To determine the detection level using this procedure for ligand binding, control experiments were performed using lovastatin (mevinolin), a known inhibitor of wild type HMGCR prior to running the natural products library. Several concentrations starting with 5mM of lovastatin was added to 1 mL PEG200 (5 mM stock) in a microcentrifuge tube, heated in a waterbath at 37° C, 10 minutes and inverted periodically to mix and dissolve in the solvent.

Decreasing concentrations of lovastatin were prepared in basic PEG200. To each prepared concentration was added 2.5 μ L of 2 M NaOH to open the lactone ring in the HMG like moiety in lovastatin before running it across the bound HMGCR. The conditions in which the binding occurs were optimized to stabilize the protein-analyte complex, washed off nonbinders using 1X equilibrium buffer (50 mM HEPES *pH* 7.5, 0.3 M NaCl), and then dissociated the complex with 1X elution buffer (0.15 M imidazole, *pH* 7.0, 4° C, 0.02 M NaCl). HMGCR along with bound lovastatin was eluted to 10 K nominal molecular weight limit (NMWL) cut out microcon Millipore ultracentrifuge micro filter. The tube was spun at 13.2 RPM, 10 min, then buffer swapped with 1X equilibrium buffer at the same speed and time. The concentrate HMGCR with bound lovastatin was then heat denatured at 80° C for 5 minutes in a water bath with periodic mixing. The denatured protein was then spun again in the microcon filter and the flow through collected (FT1). The concentrate was transferred to a small centrifuge tube, added 10 mL of 10 % cold ethanol stored at -20° C. The tube was kept in -20° C for 3 hours to further denature HMGCR and free the bound lovastatin. The denatured HMGCR with free lovastatin in ethanol was spun again in the microcon tube and the flow through collected and added to a 5ml polypropylene tube along with the previous flow through (FT1). The combined flow through was then dried using a speed vacuum system (SpeedVac AES-2010; Savant Instruments, Holbrook, NY) speed vacuum.

LC/MS analysis of lovastatin and natural products extract:

The dried analytes were tested for the presence of lovastatin using HP/Agilent 1100 LC/MSD System. A high-pressure reverse phase LC-system was utilized for the separation of the analytes starting with a flow of 70 % solvent A (5mM ammonium formate *pH* 9.0), 30 % solvent B (90 % acetonitrile + 5mM ammonium formate *pH* 9.0) for 30 seconds followed by a gradient increase for 3 min of solvent B until it reached 100 %, then maintaining this flow for the next 7 minutes, and eventually a gradient decrease of solvent B back to the starting condition for the next 10 minutes. The analytes were separated on a Luna C5 column (100 Å pore size, 3 mm internal diameter, 5µm particles, 150 mm in length). In the case of positive electrospray ionization (ESI(+)) 90 % (v/v) acetonitrile was added to the analytes and in the case of negative electrospray ionization (ESI(-)) no acetonitrile was added. Detection was performed by Agilent 1100 fluorescence diode array detector. In the APCI(-) mode, a capillary temperature of 45°C and a vaporizing temperature of 350°C were used. The capillary voltage was set to 30000 V, and the tube lens to 20 V. The nitrogen flow was 30 Psig (pound-force per square inch gauge) for the nebulizing gas, and 13 L/min for the auxiliary (dry) gas at 350° C. In the ESI(+) mode the capillary voltage were set at a range of 170 to 150 V, and in the ESI(-) mode it was set to 70 to 150 V. In order to determine the concentration and quality of lovastatin in the dry extract, the response was correlated against an initially measured LC/MS response for a pure lovastatin (M2147-25MG Mevalonin from Aspergillus, Sigma Aldrich) under similar conditions as those selected for the dry extract.

III RESULTS AND DISCUSSION

The transformed cells were plated on LB-agar Petri dishes containing 50 µg/mL ampicillin and 34 µg/mL chloramphenicol and incubated overnight at 37°C. The wild type HMGCR inserted alone into one of the pETDuet vectors and the second vector with a dual expression of both the wild type and spliced isoform HMGCR_v_1 showed good cells colony growth on their respective plates (Fig 26), thus indicating a successful uptake of plasmid DNA into the *E. coli* host cells during transformation. Three individual colonies were aseptically taken from each plate and inoculated into two production flasks with LB-media for protein expression.

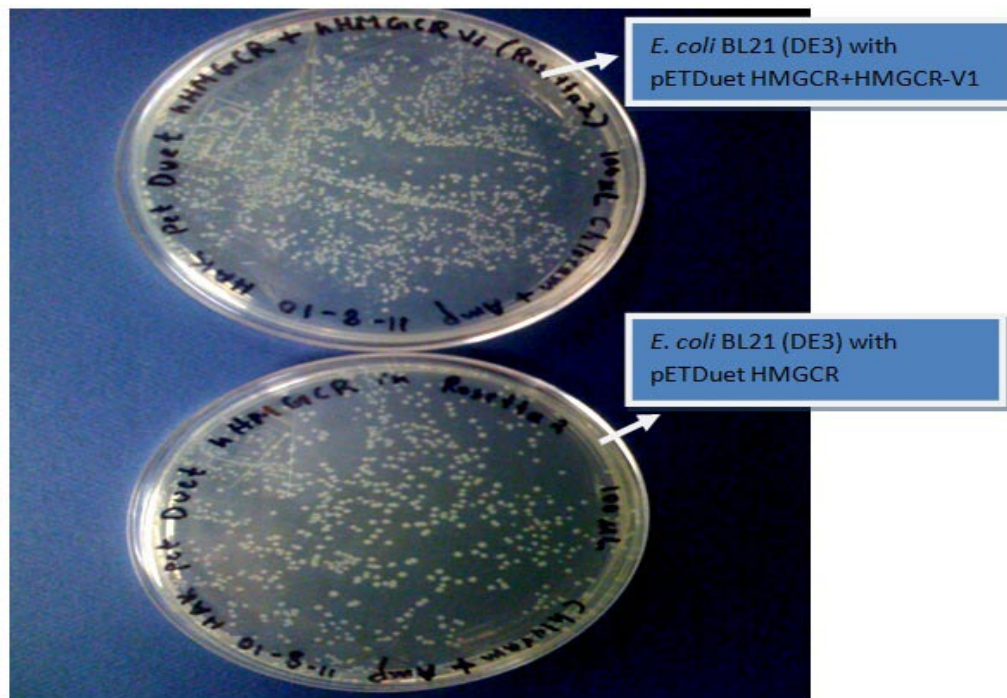


Fig (26) Top plate had the duet vector pETDuet-1 with HMGCR and HMGCR-V1 genes in *E. coli* BL21 (DE3). Lower plate only had wild type HMGCR gene in the same host cell.

Plasmid designed by Serial Cloner software 2.5 (fig 27), shows a map of the recombinant plasmid. The designed plasmid shows the entire construct to be 7979 nucleotides, coding for a total of 2538 amino acids with a molecular weight of 287.11. Fig (28) designed by Gene Designer indicates sizes of the two genes inserted into the pETDuet-1 vector. The HMGCR gene is shown to be 1396 nucleotides, coding for 440 amino acids, with a molecular weight of 50.96 kDa. Similarly the HMGCR_v_1 gene is 1232 nucleotides long, coding for 387 amino acids, with a molecular weight of 44.51 kDa.

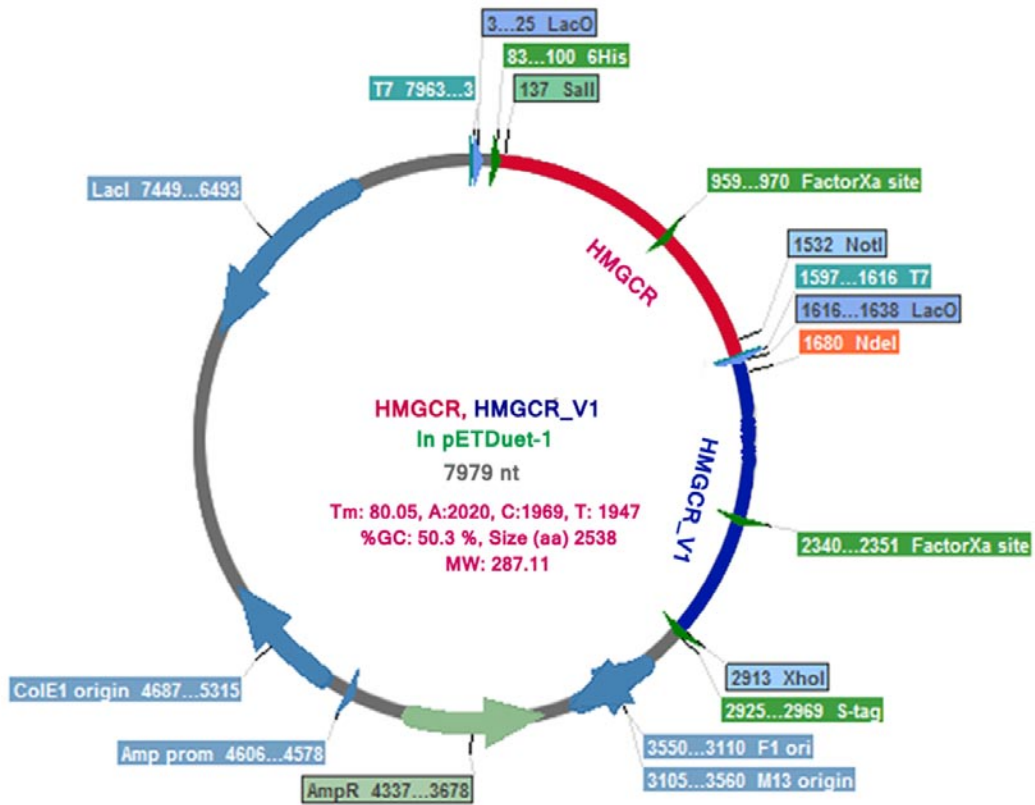


Fig (27) pETDuet-1 plasmid with dual expression gene inserts HMGCR (red) and HMGCRv_1 (blue), and also important regulatory and other gene sites. Plasmid designed with Serial Cloner 2.5 software.

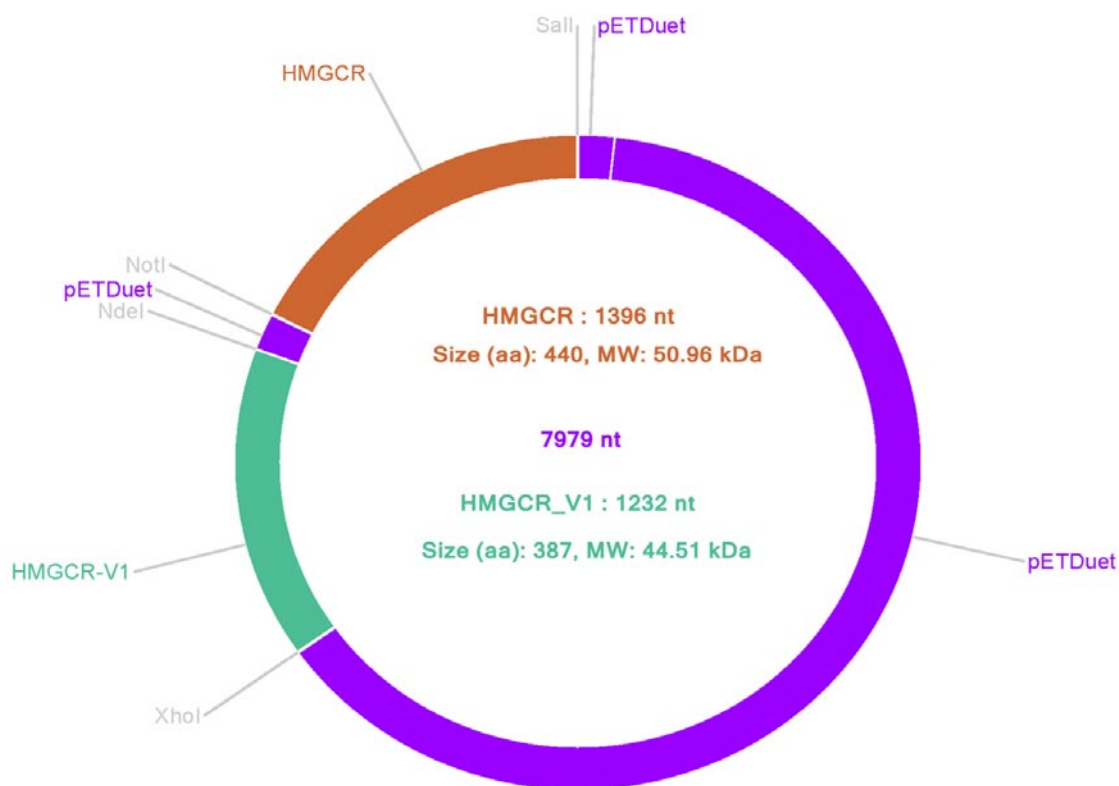


Fig (28) pETDuet-1 dual expression vector map constructed with Gene Designer software.

In order to confirm the validity of the molecular weights predicted by the softwares, an SDS-PAGE was performed on the purified proteins obtained after the elution step from the TALON cobalt resin column chromatography. A scanned image (Fig 29) of the destained gel indicated the success of our protein expression and purification protocol, and clear bands were visible around the 50kDa molecular weight marker. The EZ ladder protein marker shows clear separate bands for the 40 and 50 kDa marks. Based on the

predicted weights from the software and literature, we expected to see at least two bands in the dual expression vector, however only one band was noted at approximately the same location as the wild type HMGCR enzyme. The purpose of the dual expression vector was to confirm protein-protein interactions in the complex between the individual monomers of HMGCR in the homotetramer. In the work done by Medina *et al* it was hypothesized that there could be a possibility that varying compositions of wild type HMGCR with the alternatively spliced isoform HMGCR ν _1 might form heterogenous dimers or tetramers.⁶⁷ However if that were the case, then the dual expression vector we utilized in our work might have shown monomer-monomer protein interactions, and there could have been more than one bands in our protein electrophoresis gel (Fig 29) in close proximity to each other in support of this claim.

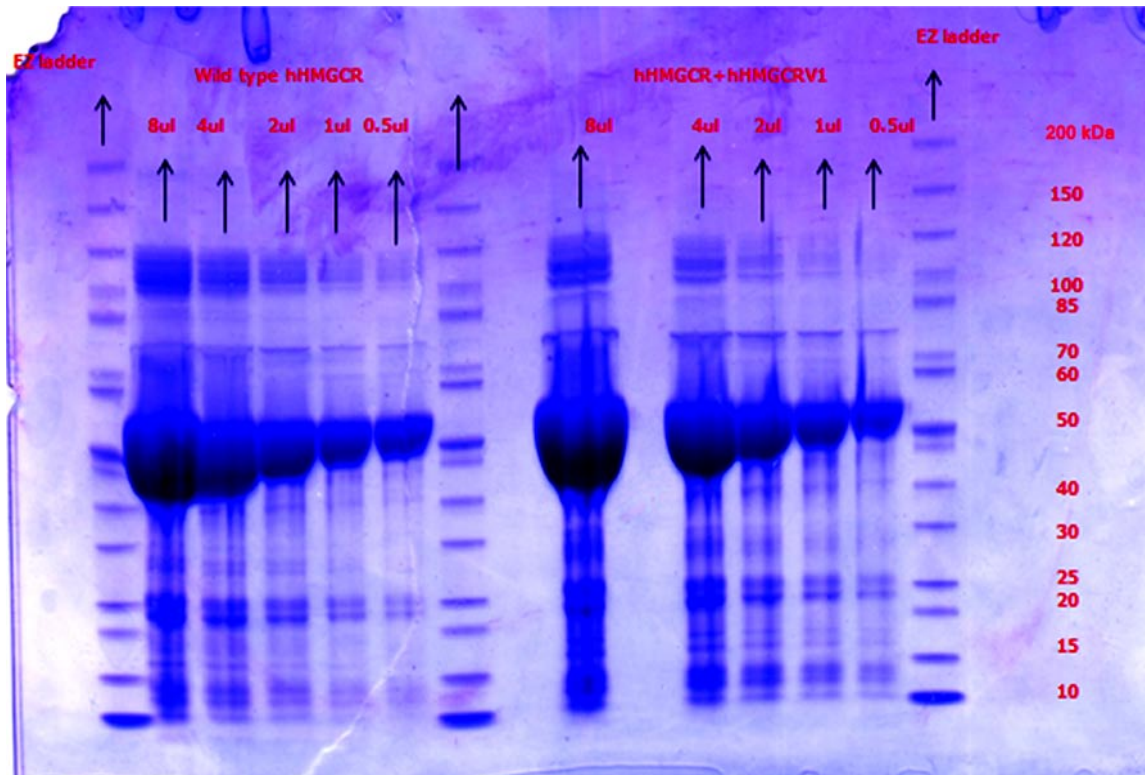


Fig (29) SDS-PAGE from left to right protein bands in the following order: EZ protein ladder, wild type HMGCRCR in decreasing quantity from 8 μ L to 0.5 μ L, EZ ladder, dual expression wild type HMGCRCR+ HMGCRCRV1 in decreasing quantity from 8 μ L to 0.5 μ L and followed by another EZ protein marker ladder.

In our structural elucidation section described before, we have explained that HMGCRCRV1 results from the deletion of exon13 as a result of alternative splicing (Fig 30). Exon13 encodes about 52 residues in the catalytic domain that includes a highly conserved sequence element ENVIGX3I/LP conserved in both class I and class II HMGCRCRs which is believed to participate in dimerization of the enzyme's monomers.⁹⁴ We believe that not only can there be a loss of important residues involved in

dimerization, but it is possible that the newly generated monomer might shift subdomains within the catalytic domain in such a way as to obscure other secondary structure elements within the remaining enzyme involved in dimerization, thus further reducing the possibility of forming a complex with the neighboring monomers. As is shown in Fig 31, the N-domain might form a new contact point with the L-domain, thus obscuring $L\alpha 4$, $L\alpha 6$ and $L\alpha 7$ and preventing them from interactions with other monomers. The importance of these structural elements within the L domain involved in dimerization has been explained in the previous sections.

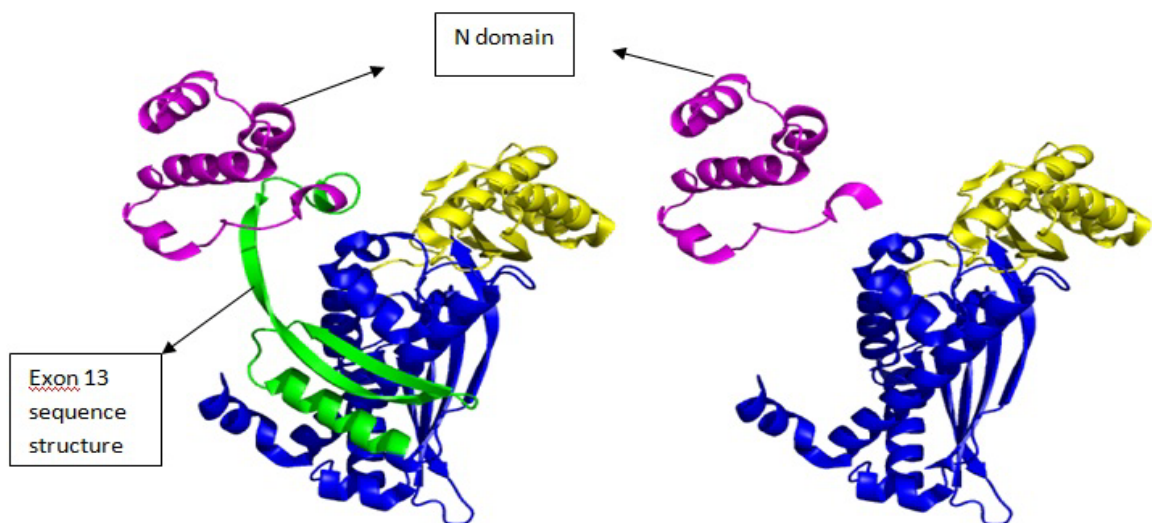


Fig (30) Left side wild type HMGCRCR showing intact exon 13 sequence (green). Right side monomer indicates the loss of exon 13 sequence due to alternatively spliced isoform HMGCRCRv_1.

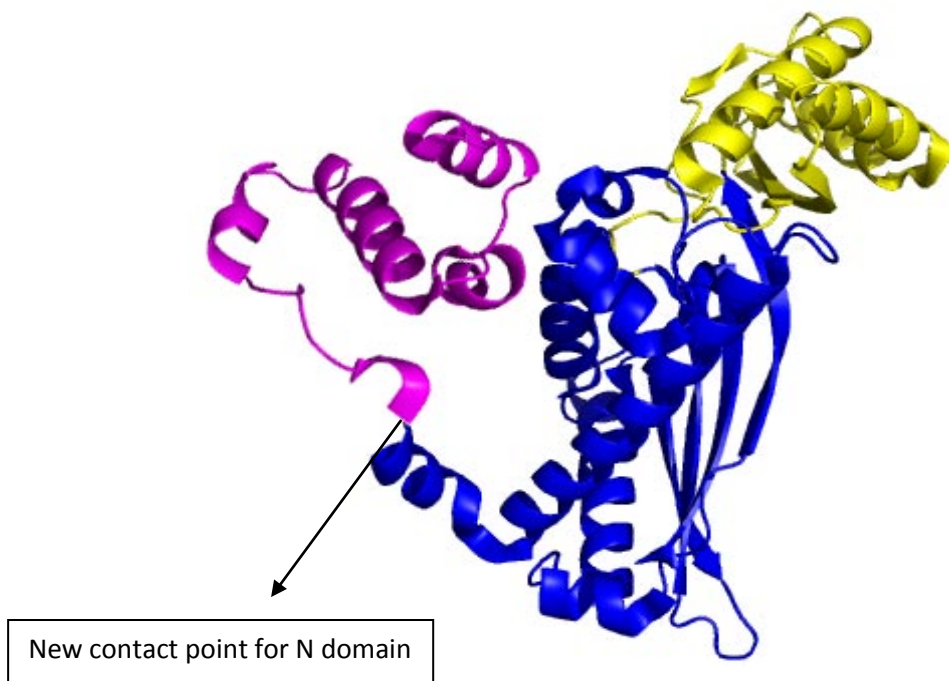


Fig (31) HMGCR_v_1 with a new possible location for the N domain (purple) and possibly obscuring the L domain helices from forming dimers.

Based on structural analysis and SDS-PAGE visualization, we believe that since residues involved in dimerization were missing in the conceptual HMGCR_v_1 construct, subunits association for tetramer formation could possibly not be accomplished, and the expressed protein settled insoluble without forming a complex with the wild type enzyme. In order to detect HMGCR_v_1 in the insoluble lysate fraction, and verify that it was successfully expressed, we denatured small quantity of insoluble lysate fraction with SDS and heat. SDS PAGE was performed on the denatured lysate along with our purified wild type enzyme.

tables 1, 2 and 3 for the wild type HMGR, crude HMGR and crude HMGR_v_1 respectively.

| Sample wild type HMGR | | | | |
|---|----------|---------|-----------|---------------|
| Reference | P (pro) | MW | Accession | Spectra count |
| HMDH_HUMAN 3-hydroxy-3-methylglutaryl-coenzyme A reductase (P04035) | 5.74E-13 | 97412.7 | P04035 | 253 |
| meso-diaminopimelate-adding enzyme [Escherichia coli K12] | 3.89E-15 | 53310.1 | 16128078 | 20 |
| aminopeptidase A/I [Escherichia coli O157:H7 EDL933] | 1.26E-09 | 54845.1 | 15804852 | 11 |
| protein chain elongation factor EF-Tu [Escherichia coli O157:H7] | 2.71E-11 | 43286.4 | 15834157 | 9 |
| lipoamide dehydrogenase (NADH); component of 2-oxodehydrogenase and pyruvate co | 8.21E-10 | 50656.7 | 15799800 | 7 |
| putative ligase [Escherichia coli K12] | 2.21E-09 | 49842.2 | 16132055 | 6 |
| pyruvate kinase II [Escherichia coli K12] | 1.06E-07 | 51324.8 | 16129807 | 6 |
| AHPF_ECOLI Alkyl hydroperoxide reductase subunit F (Alkyl hydroperoxide reductase | 2.21E-08 | 56142.2 | 2507291 | 5 |
| UDP-N-acetyl-muramate:alanine ligase [Escherichia coli K12] | 1.91E-07 | 53592.5 | 16128084 | 5 |
| STHA_ECOLI Soluble pyridine nucleotide transhydrogenase (STH) (NAD(P)(+) transhyc | 2.45E-13 | 51527.9 | 11182439 | 3 |
| isocitrate dehydrogenase [Escherichia coli K12] | 3.92E-09 | 45727.5 | 16129099 | 3 |

Table 1. Spectra count for the purified wild type HMGR band.

| Sample crude HMGR | | | | |
|---|----------|---------|-----------|---------------|
| Reference | P (pro) | MW | Accession | Spectra count |
| HMDH_HUMAN 3-hydroxy-3-methylglutaryl-coenzyme A reductase (P04035) | 1.11E-15 | 97412.7 | P04035 | 243 |
| membrane-bound ATP synthase, F1 sector, alpha-subunit [Escherichia coli O157: | 1.00E-30 | 55187.8 | 15804334 | 140 |
| ketol-acid reductoisomerase [Escherichia coli K12] | 5.90E-11 | 54034.4 | 16131632 | 54 |
| lipoamide dehydrogenase (NADH); component of 2-oxodehydrogenase and pyruva | 8.88E-15 | 50656.7 | 15799800 | 49 |
| trigger factor; a molecular chaperone involved in cell division [Escherichia coli O15 | 7.90E-12 | 48163.0 | 15800166 | 47 |
| protein chain elongation factor EF-Tu [Escherichia coli O157:H7] | 8.43E-12 | 43286.4 | 15834157 | 28 |
| glutamine synthetase [Escherichia coli O157:H7] | 2.65E-11 | 51870.9 | 15834046 | 25 |
| hypothetical protein [Escherichia coli K12] | 1.61E-13 | 54655.0 | 16129572 | 22 |
| glycerol kinase [Escherichia coli O157:H7] | 3.05E-13 | 56195.4 | 15834105 | 21 |
| aminopeptidase A/I [Escherichia coli O157:H7 EDL933] | 1.11E-14 | 54845.1 | 15804852 | 20 |
| hypothetical protein [Escherichia coli O157:H7] | 2.32E-12 | 53629.2 | 15829953 | 20 |

Table 2. Spectra count for the HMGR band in the crude lysate.

| Sample crude HMGCR _v -1 | | | | |
|--|-----------------|----------------|---------------|---------------|
| Reference | P (pro) | MW | Accession | Spectra count |
| protein chain elongation factor EF-Tu [Escherichia coli O157:H7] | 2.44E-14 | 43286.4 | 15834157 | 244 |
| HMDH_HUMAN 3-hydroxy-3-methylglutaryl-coenzyme A reductase (P04035) | 5.25E-13 | 97412.7 | P04035 | 238 |
| isocitrate dehydrogenase [Escherichia coli K12] | 1.53E-12 | 45727.5 | 16129099 | 91 |
| transcription termination factor Rho [Escherichia coli O157:H7] | 3.33E-15 | 46974.6 | 15833970 | 45 |
| NADH dehydrogenase I chain F [Escherichia coli K12] | 7.44E-14 | 49261.0 | 16130219 | 30 |
| citrate synthase [Escherichia coli K12] | 2.22E-15 | 47983.9 | 16128695 | 28 |
| 3-oxoacyl-[acyl-carrier-protein] synthase I [Escherichia coli K12] | 1.11E-14 | 42586.1 | 16130258 | 21 |
| putative peptidase [Escherichia coli K12] | 3.33E-15 | 46151.4 | 33347672 | 16 |
| enolase [Escherichia coli O157:H7] | 2.82E-13 | 45626.5 | 15832893 | 14 |
| respiratory NADH dehydrogenase [Escherichia coli K12] | 4.98E-13 | 47328.7 | 16129072 | 12 |
| chloramphenicol acetyltransferase [Plasmid R100] | 2.38E-12 | 25646.3 | 9507572 | 12 |

Table 3. Spectra count for the HMGCR_v-1 band in the crude lysate.

Most of the time with mass spectrometric data; we are at the mercy of the sequence database. Efforts to isolate a viable HMGCR_v_1 have failed so far⁷³, and even eukaryotic expression systems have not been able to successfully express a catalytically active form of the enzyme. Work done by others did not find any success beyond the isolation of alternatively spliced HMGCR mRNA levels.⁶⁹ Since no sequence has been entered in the protein database for HMGCR_v_1, therefore we were not able to identify the crude HMGCR_v_1 band with an exact sequence that matches the variant. Exon 13 only encodes about 6 % of the catalytic domain, and in our liquid chromatography with tandem mass spectrometry (LC-MS/MS) the remaining 94 % of the fragmented peptide sequences correlated with the wild type HMGCR, therefore although the SDS-PAGE

shows two separate bands in the insoluble lysate fraction, the spectra counts for the two different bands correlated with the wild type enzyme. We therefore believe that the HMGCR ν _1 was expressed successfully in our plasmid vector, but instead of forming a complex in the tetrameric enzyme, the expressed variant protein went into the insoluble cell lysate, and did not participate in forming a catalytically active protein. Our previous work indicates that exclusive HMGCR ν _1 association expressed in *E. coli* alone also resulted in an insoluble enzyme.⁷³

HMG-CoA reductase activity is extensively regulated on transcriptional levels, post-transcriptional levels, and feedback mechanism and we believe that alternative splicing may be an additional regulatory mechanism for endogenous cholesterol homeostasis. Understanding the mechanism involving HMGCR alternative splicing may lead to a better understanding of its role in regulating cellular cholesterol levels.

Alternative splicing of HMGCR or other genetic variations in the enzyme may result in an insoluble or inactive form of the enzyme, but the direct consequences of these variations have been altered clinical significance of statins in the treatment of hypercholesterolemia and even adverse drug reactions. We believe that personalized medicine should be taken into account in screening compounds for improved selection of clinical trial patients, which will have a positive effect on pharmaceutical industry. The failure of alternative drug discovery methods in the development of breakthrough lead compounds can be attributed to a decrease in the use of natural products in drug discovery screening.⁸⁷ In any advanced technology high throughput screening (HTS)

technique, there can be hurdles for institutional laboratories in playing important role in the drug discovery process, some of these hurdles to mention are, the expenses and resources associated with each screen and screen consumables, the time and people resources required for each screen, and the difficulty of preparation and stability of the substrate or reagents involved in the screening assays.⁹⁵ The method we propose for screening ligands for our wild type HMGCR target is very simple and cost effective.

We measured the enzyme activity of our purified enzyme prior to utilizing the enzyme for our screening technique. The oxidation of NADPH to NADP⁺ is accompanied by a decrease in absorbance at 340nm (A₃₄₀), thus providing a spectrophotometric means of detection which is directly proportional to the HMGCR activity in the sample. The reaction is thus measured by the decrease in absorbance at 340 nm using the extinction coefficient $6220 \text{ M}^{-1} \text{ cm}^{-1}$ for NADPH. One unit of NADPH causes the oxidation of 1.0 μmol NADPH at 25°C at pH 7.0. The enzyme activity was calculated from the slope (rate) linear portion of the curve (red slope in fig 33) by selecting the highest and lowest points of the linear curve. The change in absorbance at 340 nm was determined during a selected time interval, and the enzyme activity was calculated using the equation described in the techniques and instrumentation section. The mean enzyme activity calculated for wild type HMGCR and HMGCR+ HMGCR_{v_1} was $2.17 \mu\text{M min}^{-1}$ and $1.62 \mu\text{M min}^{-1}$ respectively.

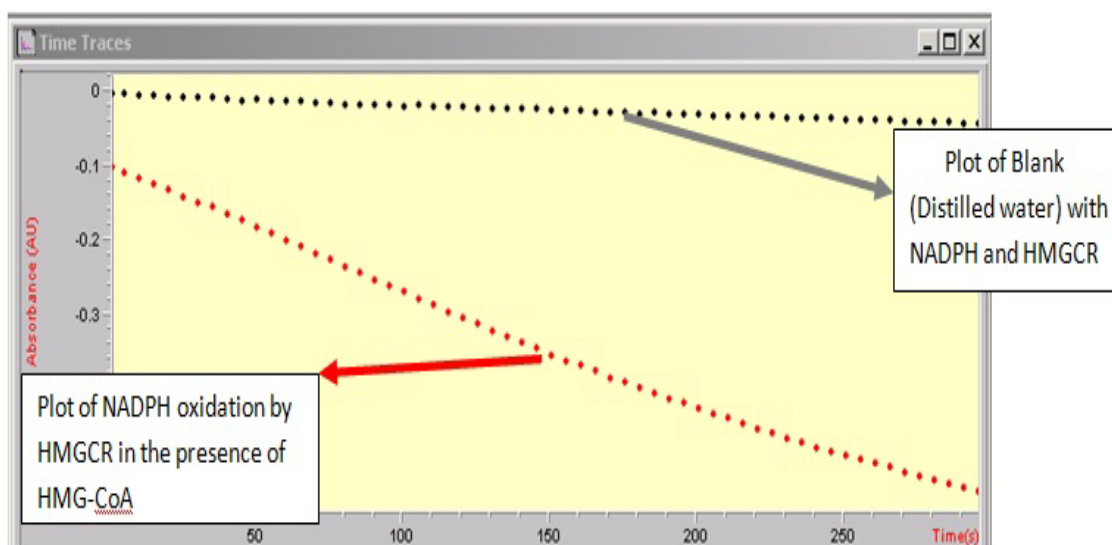


Figure 33. Figure of slope (rate) of the linear portion of the curve when the absorbance (A 340) values are plotted as a function of time (in seconds) for the wild type HMGR.

The initial enzyme concentration used for enzyme activity determination was 0.398 mg/ml (4.08 μ M) wild type HMGR and 0.367 mg/ml (3.77 μ M) HMGR+ v_1 . Slight variation between enzyme activities of the wild type HMGR versus the HMGR+ v_1 can be attributed to pipetting errors. To compensate for the slight variation in the concentration difference between the wild type HMGR and the HMGR+ v_1 , 1.21 μ L and 1.31 μ L respectively of each enzyme was pipetted into the reaction mixture. Upon verification of the enzyme activities, it was determined that they were appropriate for bioprospecting and subsequent identification of the analytes using LC/MS analysis. A comparable study of enzyme activity for a His-tag free HMGR has been carried out on

rat liver enzyme,⁹³ however no such comparable study has been published for human HMGCR.

After successful binding of the protein to the column the prepared library was run across the column for the detection of analyte with probable affinity for the protein. Bioprospecting was preceded by screening for lovastatin in a decreasing concentration as mentioned in the previous section. In order to determine the concentration and quality of lovastatin in the dry extract, the response was correlated against an initially measured LC/MS response for a pure lovastatin (M2147-25MG Mevalonin from Aspergillus, Sigma Aldrich) under similar conditions as those selected for the dry extract obtained from the bound enzyme.

A cocktail of buffers (listed in the materials and methods section) used in the extraction of lovastatin from HMGCR was prepared and run as a blank in the LC/MS instrument prior to our analytes to detect any possible peak interference. All such peaks were identified in figures (35-40) and were subtracted in further analysis of lovastatin extracts.

Pure mevalonin (lovastatin) when injected as a standard in the LC-MS showed two prominent peaks with approximate retention times of 8 and 11 minutes (Fig 41). The atmospheric pressure ionization electrospray (API-ES) technique both in the positive and negative mode was used to fragment ions to aid in structural elucidation. The API-ES positive mode revealed adduction of chloride ion to lovastatin (Fig 42). The adduct ion M^+Cl^- was seen at the 11 min retention time corresponding to mass spectral fragment at mass-to-charge ratio m/e 459.2. No other prominent m/e peaks corresponding to the 8 and

11 minutes retention times were detected that can be correlated clearly to any of the possible lovastatin fragmentation pattern shown in Fig 34 (a-h). The API-ES negative mode on the other hand showed significant correlation to several fragmentation patterns both at the 8 and 11 minutes retention times (Fig 43). The mass spectra fragments were correlated to the two compounds compactin and lovastatin. These two compounds differ by a single methyl group at the circled position as shown in figure 35. It is not clear whether in addition to lovastatin (mevalonin), compactin was already present in the purchased mevalonin from sigma aldrich, or that the ionization chamber gave rise to the formation of compactin. In our subsequent spectral analysis we only considered the AP-ES negative mode to avoid the complexity associated with the chloride adduction to our ion of interest.

At the 8 minute retention time in the AP-ES negative mode, the peaks noted in the mass spectral fragments Fig (45) for our standard were very prominent peaks at m/e 421.2, 422.2 and 423.2 which we correlated to the open form lovastatin Fig 34 (a). At the 11 minutes retention time Fig (46), there were three prominent peaks in the mass spectrum appearing at m/e 323.1, 337.1 and 407.2, each of which was correlated to compactin open form without side chain Fig 34 (f), lovastatin open form without side chain Fig 34 (d) and compactin open form Fig 34 (g) respectively. The majority of the open form is indicative of the lactone ring opening that results from the addition of NaOH to the analyte.

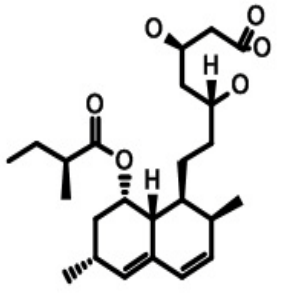
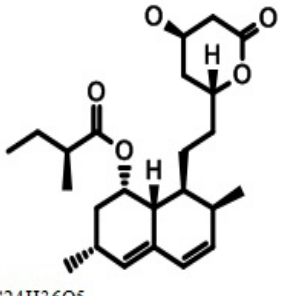
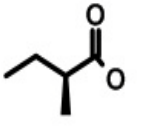
Once the prominent peaks were determined from our LC/MS by analyzing the pure standard (lovastatin), we then subsequently analyzed lovastatin by pulling it down the

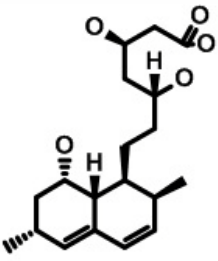
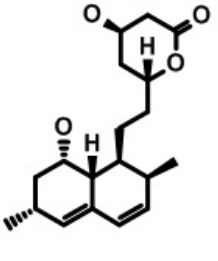
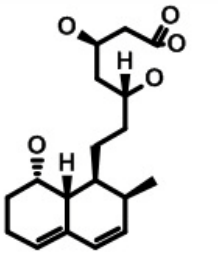
chromatography column with the bound HMGCR, as described in the materials and methods section. We began with 5mM lovastatin and in subsequent analysis reduced the concentration to half of the previous analysis. The various concentrations of lovastatin used were 5mM, 2.5 mM, 1.25 mM, 0.625 mM, 0.313 mM, 0.156 mM and 0.07 mM. Lovastatin in its open form was detected up until a concentration of 0.625 mM (Figures 49, 52, 54, 56). We believe that a fresh, never used, cobalt resin can go below the detection level seen in our analysis, since the same resin had been used and regenerated repeatedly a number of times before. Considerably smaller protein pellet was seen after elution for the last three concentrations. There is therefore, the possibility that the resin was exhausted, resulting in cobalt ion leakage.

Finally we screened for natural compound inhibitors bound to HMGCR, eluted from the chromatography column, as described in the experimental section. Lovastatin at 5 mM concentration was first added to the library and run across the chromatography column with bound HMGCR. The extract showed two bands that correlated to two forms of lovastatin, lovastatin open form at 5.07 min interval (Fig 61), and lovastatin open form without side chain at 7.01 min interval (Fig 60). Both bands were of a weaker intensity compared to the previous extracts where lovastatin alone was run through the column. This can be attributed to dilution of NaOH caused by 1 ml addition of the natural products library to the mixture. Dilution of NaOH probably resulted in the hinderance of lovastatin conversion from the closed to the open form, which is the form required for its binding to HMGCR. The presence of lovastatin in the extract indicated that no other inhibitor in the library had greater affinity for the binding sites occupied by lovastatin.

Finally pure library without lovastatin was run across the column with bound HMGCR. LC/MS analysis of the extract showed a prominent peak starting at 9.89 min interval (Fig 62). Drilling into the peak at 9.89 min in the ESI positive mode showed several overlapping *m/e* fragments. The peaks detected were deconvoluted using the Automated Mass Spectral Deconvolution and Identification System (AMDIS) software, a computer program developed at The National Institute of Standards and Technology (NIST) that extracts spectra for individual components. Several *m/e* fragments (not shown) when deconvoluted were identified as impurities that appeared to be present throughout the chromatogram, therefore these peaks were ignored. The fragments of interest were those with *m/e* of 239, 261, 477 and 499 (Fig 63). These four peaks when deconvoluted were overlapping and were visible around the 9.89 retention time (Fig 62). From the NIST library search we interpreted the peak to be resulting from (4-(2-hydroxyethyl)-1-piperazineethanesulfonic acid (HEPES) present in our equilibrium buffer rather than coming from our library. HEPES has a Molecular Weight of 238.3. In our chromatogram it shows up as the most abundant peak at *m/e* of 239 Daltons after being protonated by one H⁺. Some of the other peaks in this spectrum make sense. For instance, 261 is probably a sodium salt of the HEPES after gaining sodium adduct (+23). Another peak at 477 is probably a dimer of HEPES: $(2 \times 238) + H^+ = 477$. This is very common, especially at high concentration (here 50 mM HEPES), where compounds often form dimers during ionisation.. 499 is probably a sodium salt of the dimer. It is 23 amu above 477, indicating a 499-dimer that has sodium adduct (+23). The sodium adducts in all cases were expected to be very common, since our buffers had considerable amount of

NaCl. Further analysis is required to determine the nature of interaction between HEPES and HMGCR. HEPES as a ligand for other proteins has also been shown elsewhere.⁹⁶

| | | |
|--|---|--|
|  <p>C₂₄H₃₈O₆ Exact Mass: 422.27 Mol. Wt.: 422.55 m/e: 422.27 (100.0%), 423.27 (26.6%), 424.27 (4.5%)C, 68.22; H, 9.06; O, 22.72</p> <p>Fig 34 (a) <u>Lovastatin open form</u></p> |  <p>C₂₄H₃₆O₅ Exact Mass: 404.26 Mol. Wt.: 404.54m/e: 404.26 (100.0%), 405.26 (26.6%), 406.26 (4.3%) C, 71.26; H, 8.97; O, 19.7</p> <p>Fig 34 (b) <u>Lovastatin closed form</u></p> |  <p>C₅H₁₀O₂ Exact Mass: 102.07 Mol. Wt.: 102.13 m/e: 102.07 (100.0%), 103.07 (5.6%) C, 58.80; H, 9.87; O, 31.33</p> <p>Fig 34 (c) <u>Side chain fragment</u></p> |
|--|---|--|

| | | |
|---|---|---|
|  <p>C₁₉H₃₀O₅ Exact Mass: 338.21 Mol. Wt.: 338.44 m/e: 338.21 (100.0%), 339.21 (20.7%), 340.22 (2.1%), 340.21 (1.0%) C, 67.43; H, 8.93; O, 23.64</p> <p>Fig 34 (d) <u>Lovastatin</u> open form, without side chain.</p> |  <p>C₁₉H₂₈O₄ Exact Mass: 320.2 Mol. Wt.: 320.42 m/e: 320.20 (100.0%), 321.20 (20.7%), 322.21 (2.1%) C, 71.22; H, 8.81; O, 19.97</p> <p>Fig 34 (e) <u>Lovastatin</u> closed form, without side chain.</p> |  <p>C₁₈H₂₈O₅ Exact Mass: 324.19 Mol. Wt.: 324.41 m/e: 324.19 (100.0%), 325.20 (20.0%), 326.20 (2.9%) C, 66.64; H, 8.70; O, 24.66</p> <p>Fig 34 (f) <u>Compactin</u> open form, without side chain.</p> |
|---|---|---|

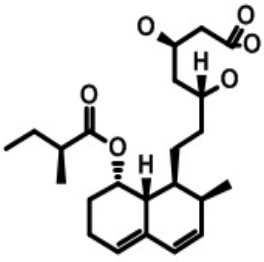
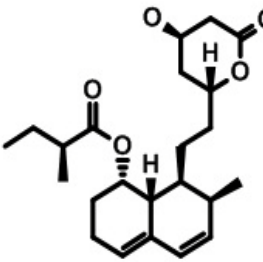
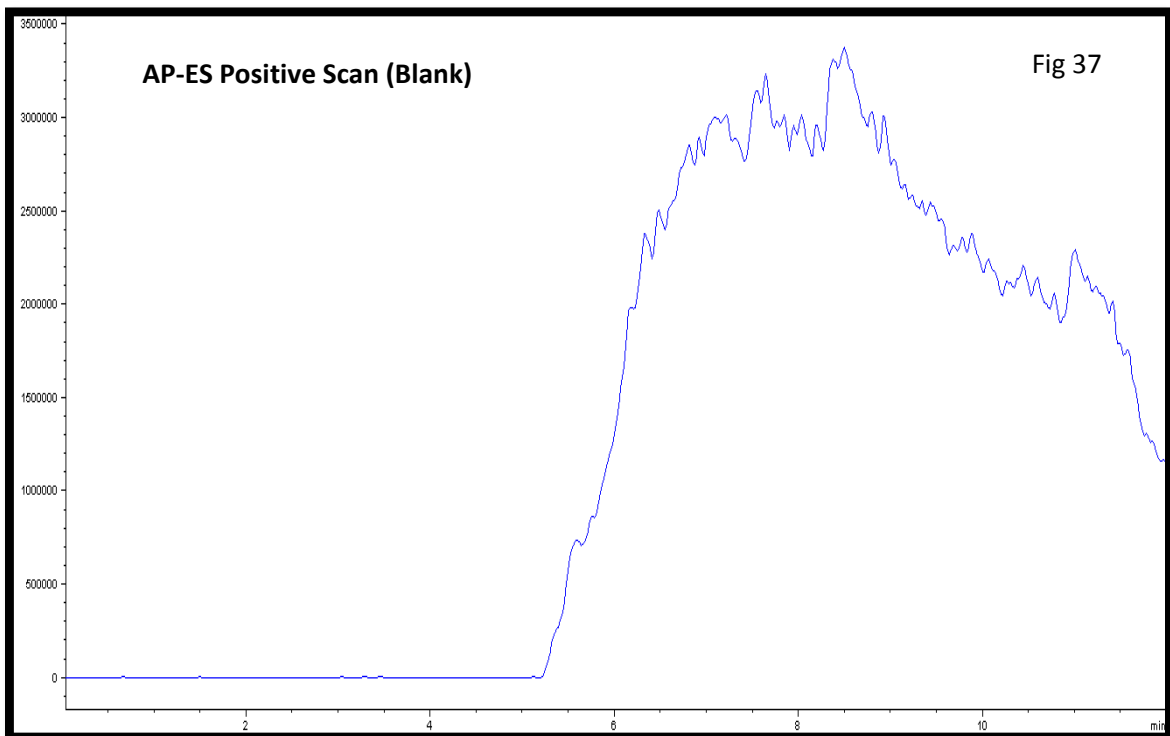
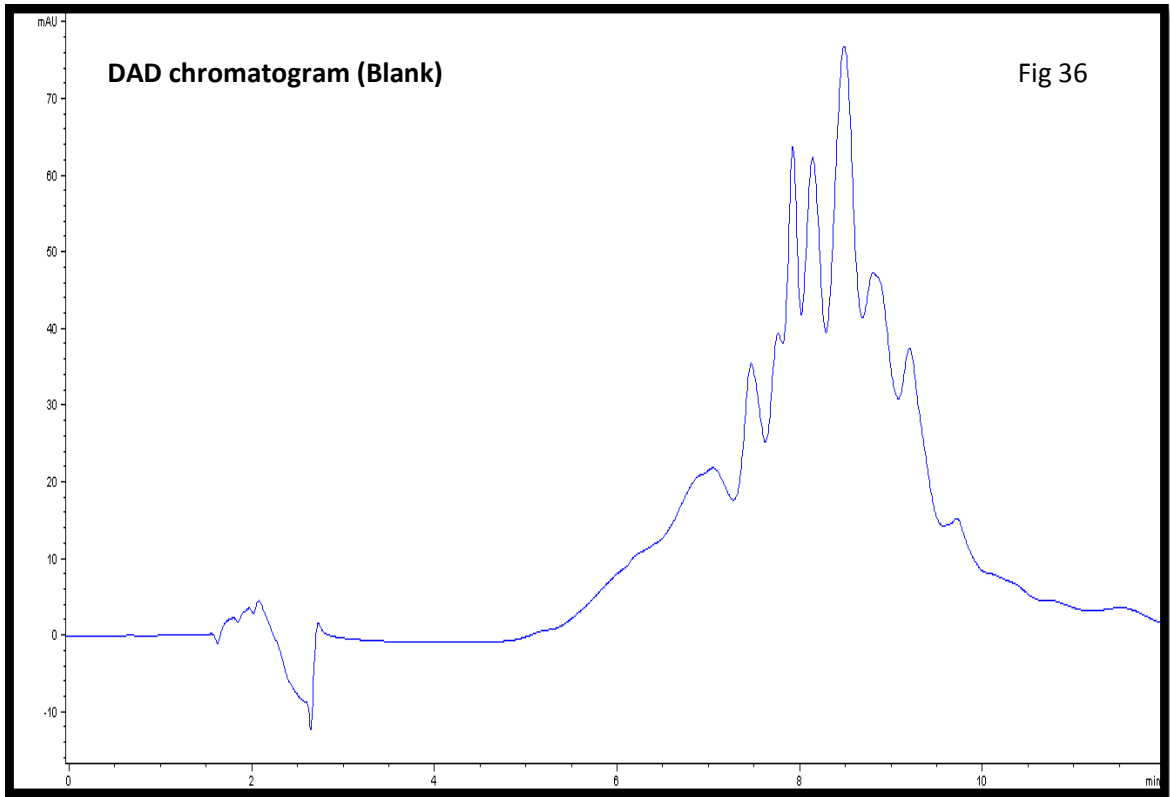
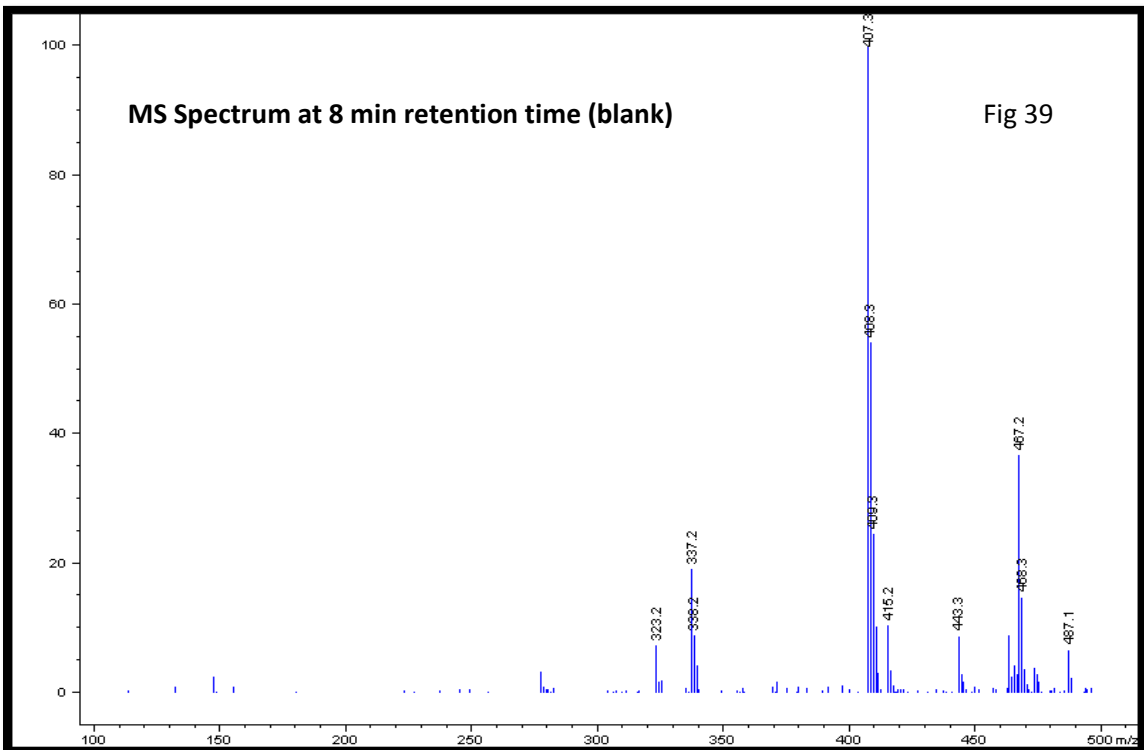
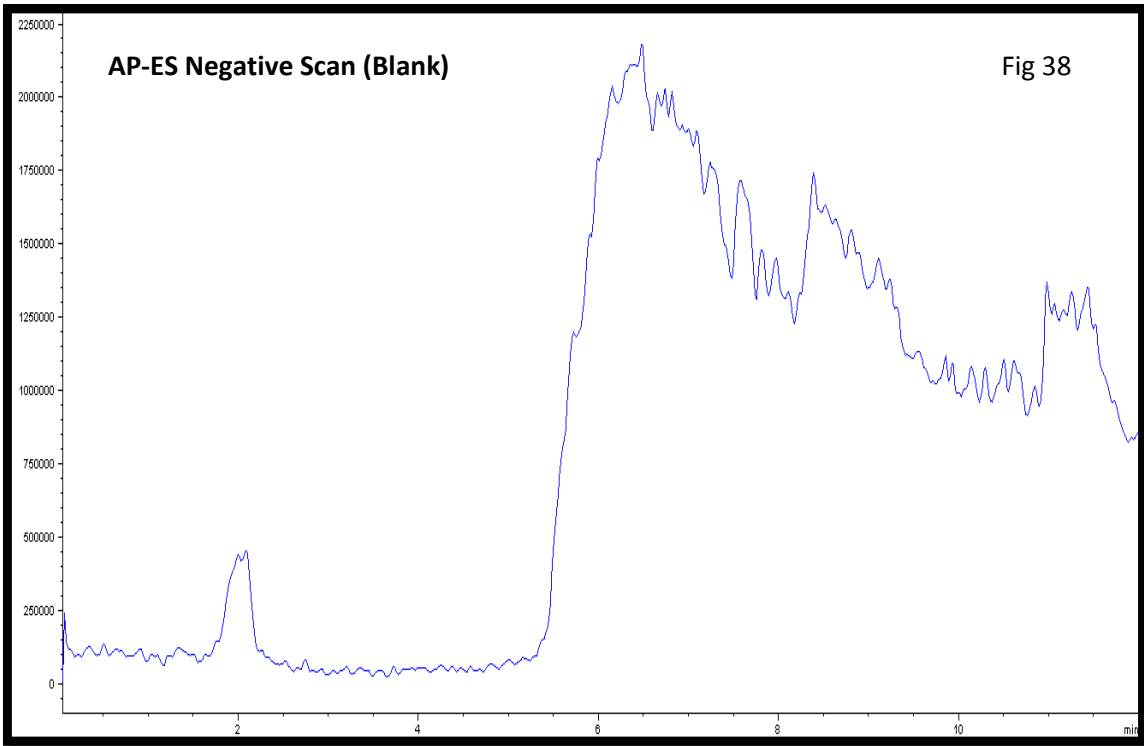
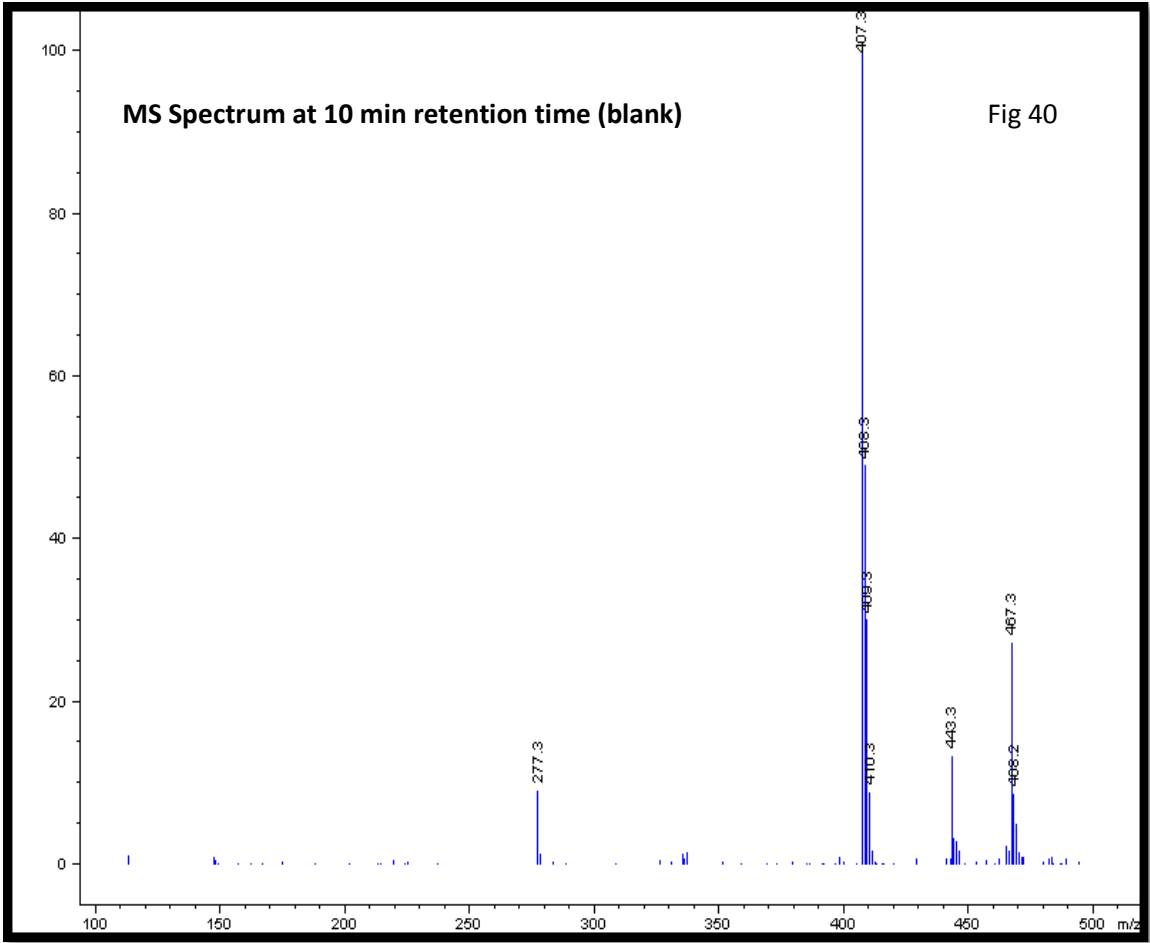
| | | |
|--|---|---|
|  <p>C₂₃H₃₆O₆ Exact Mass: 408.25 Mol. Wt.: 408.53 m/e: 408.25 (100.0%), 409.25 (24.9%), 410.26 (4.4%) C, 67.62; H, 8.88; O, 23.50</p> <p>Fig 34 (g) <u>Compactin</u>, open form.</p> |  <p>C₂₃H₃₄O₅ Exact Mass: 390.24 Mol. Wt.: 390.51 m/e: 390.24 (100.0%), 391.24 (25.1%), 392.25 (3.1%), 392.24 (1.0%) C, 70.74; H, 8.78; O, 20.49</p> <p>Fig 34 (h) <u>Compactin</u>, closed form.</p> |  <p>Fig 35 <u>Compactin</u> and <u>lovastatin</u> differ at the circled methyl/ hydrogen.</p> |
|--|---|---|

Fig (34, 35) Lovastatin and its fragmentation patterns.







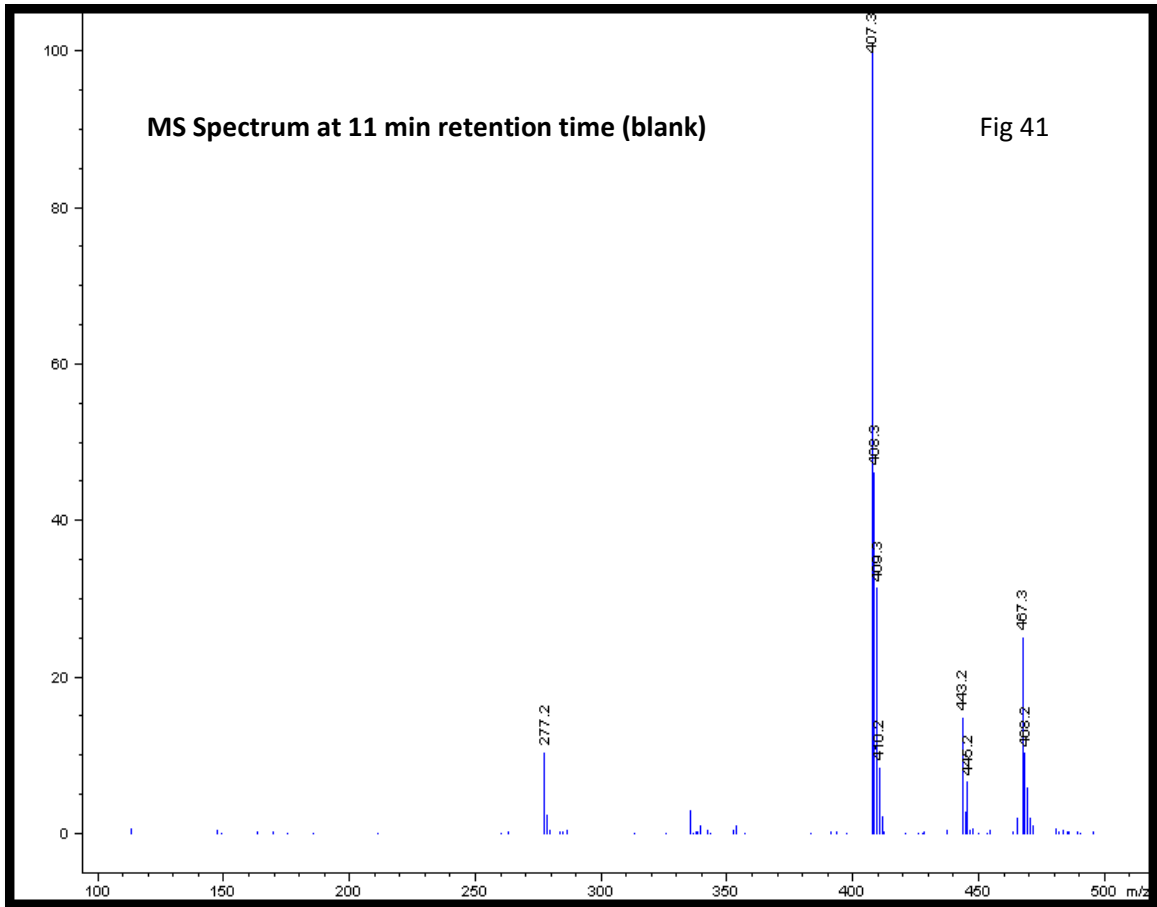
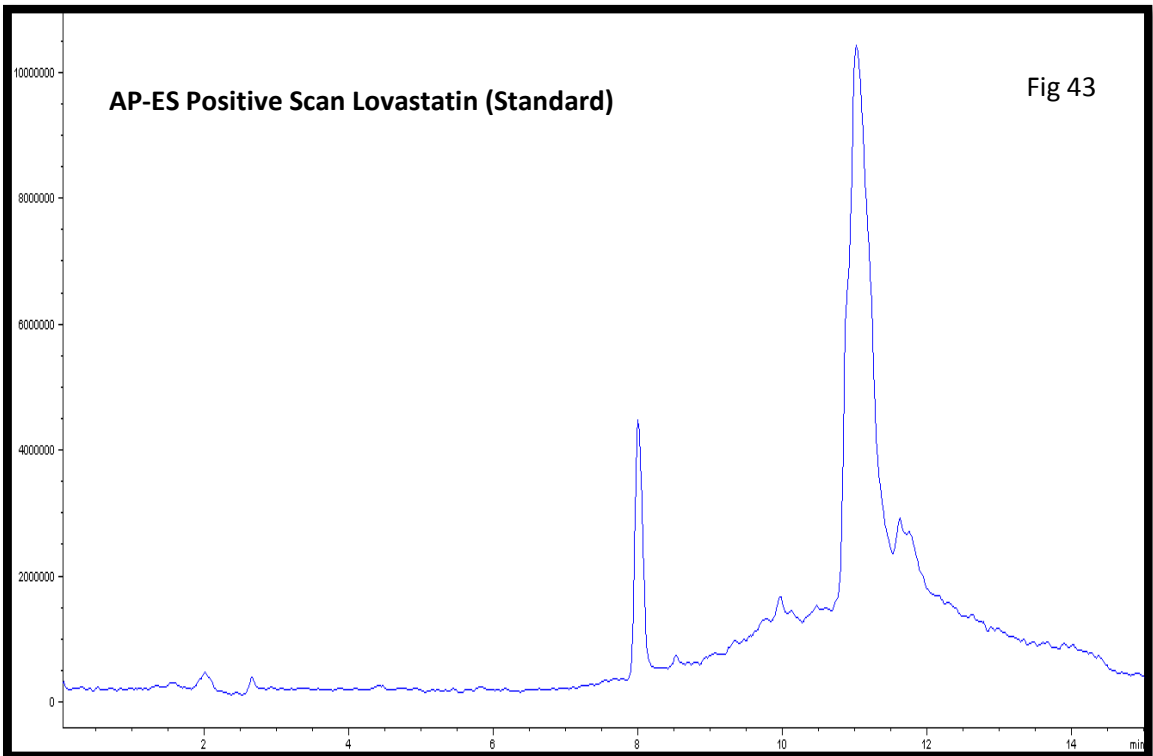
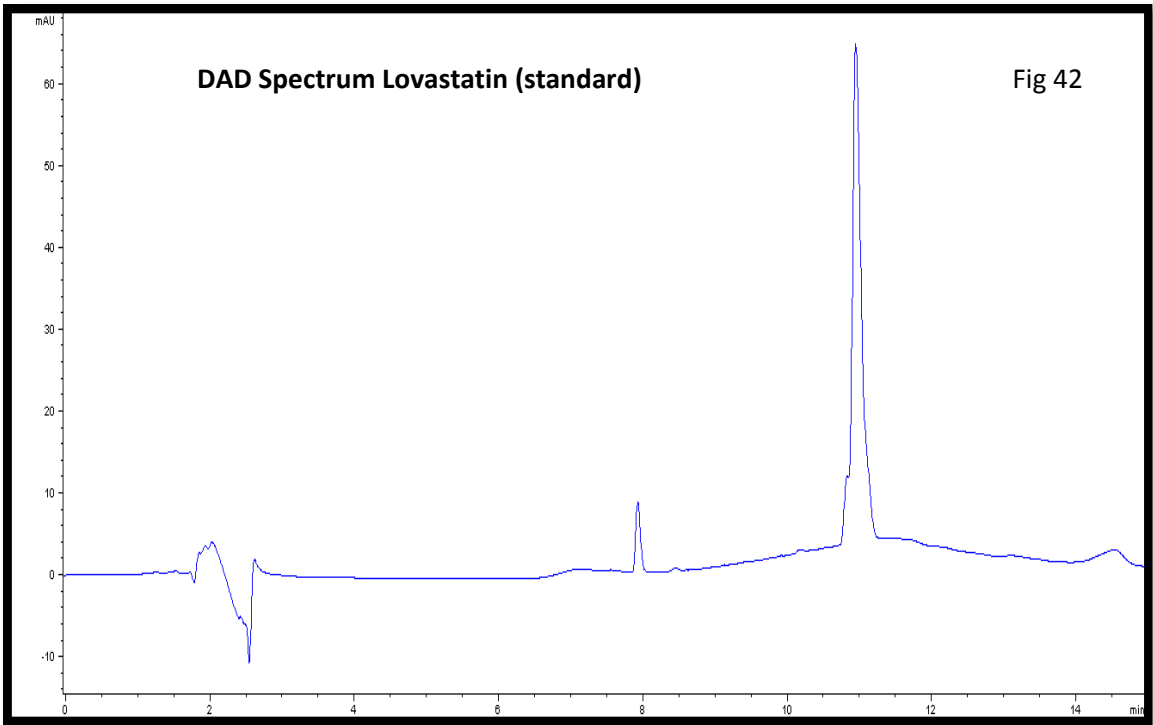
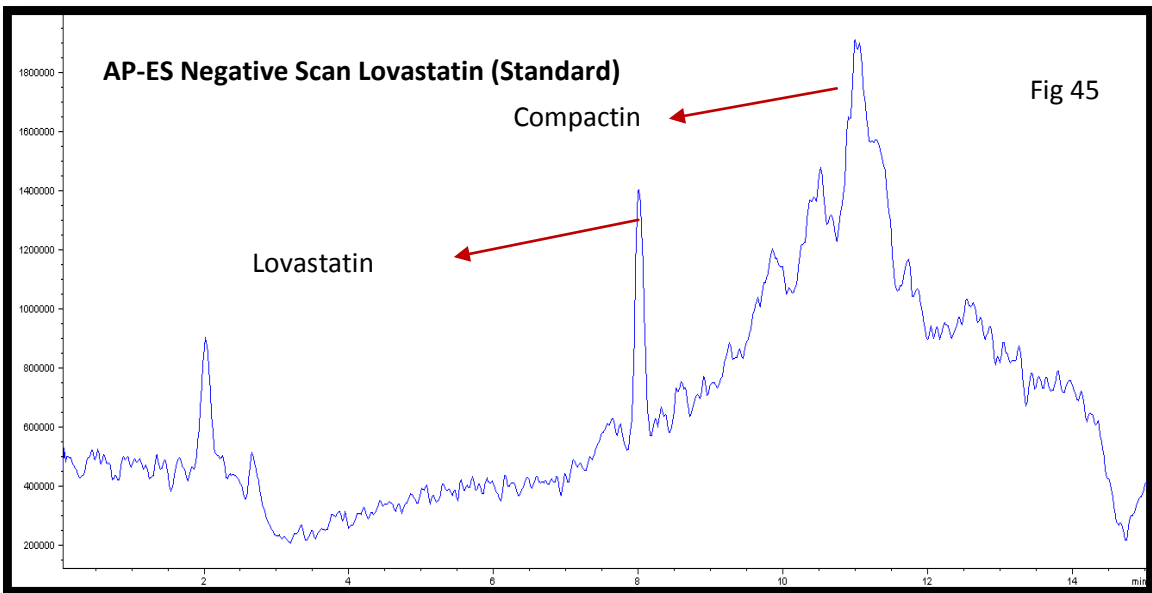
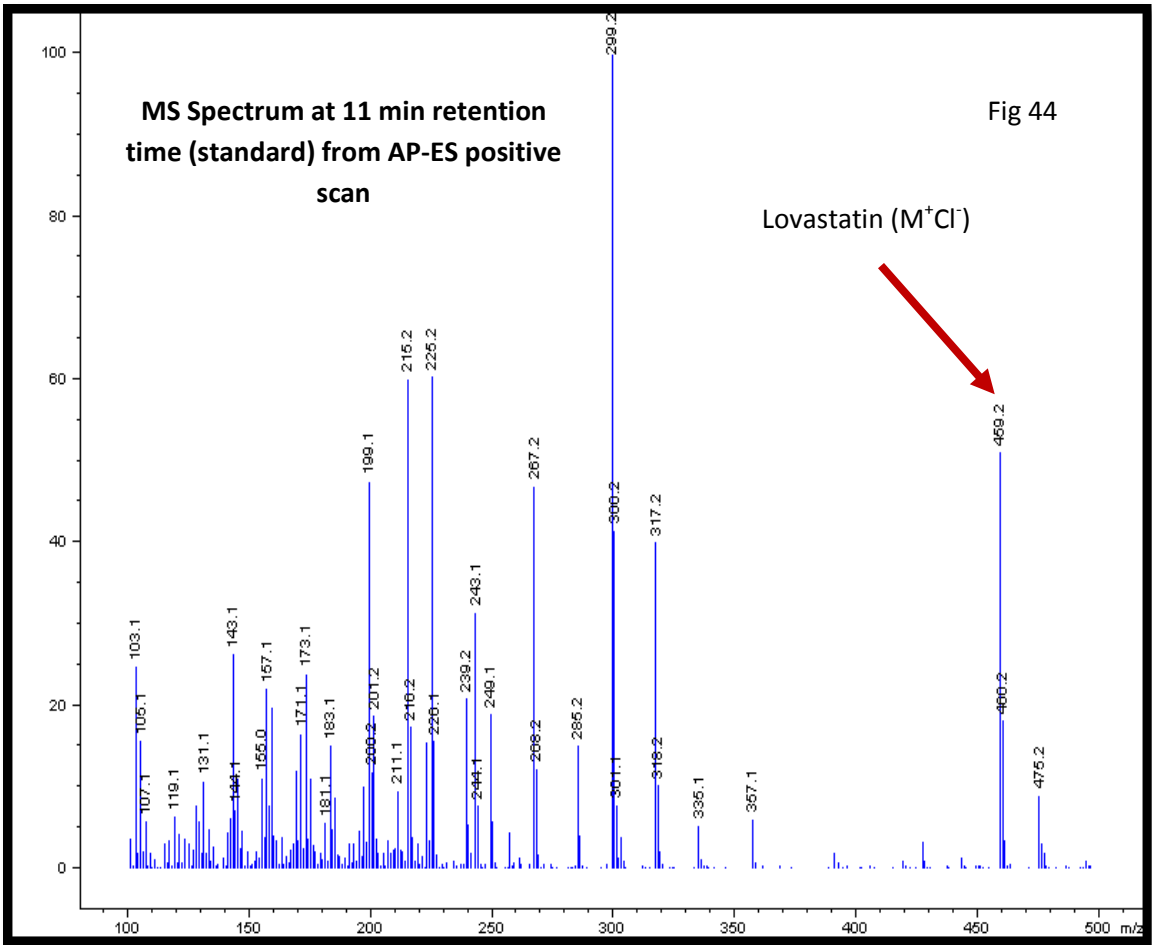
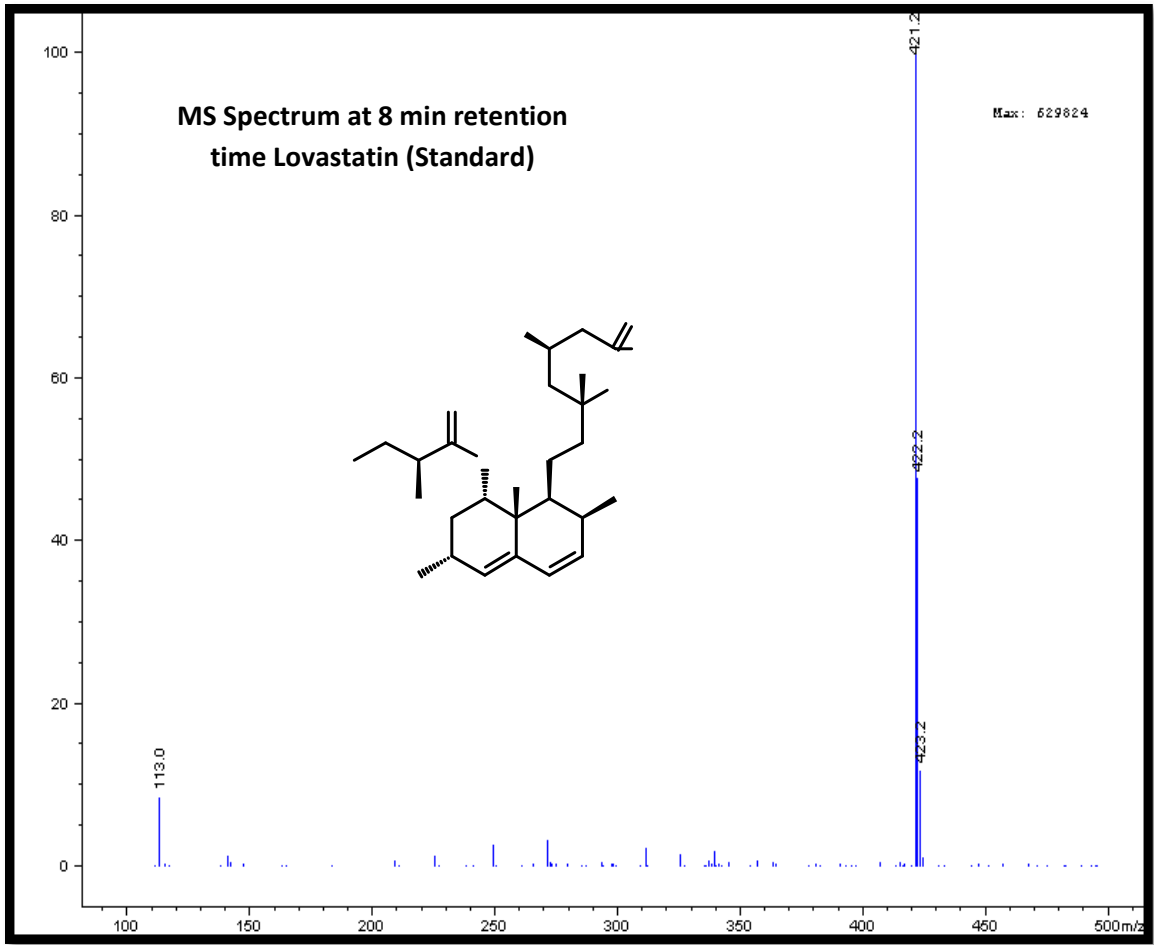


Fig (36-41) LC-MS results from blank buffers.







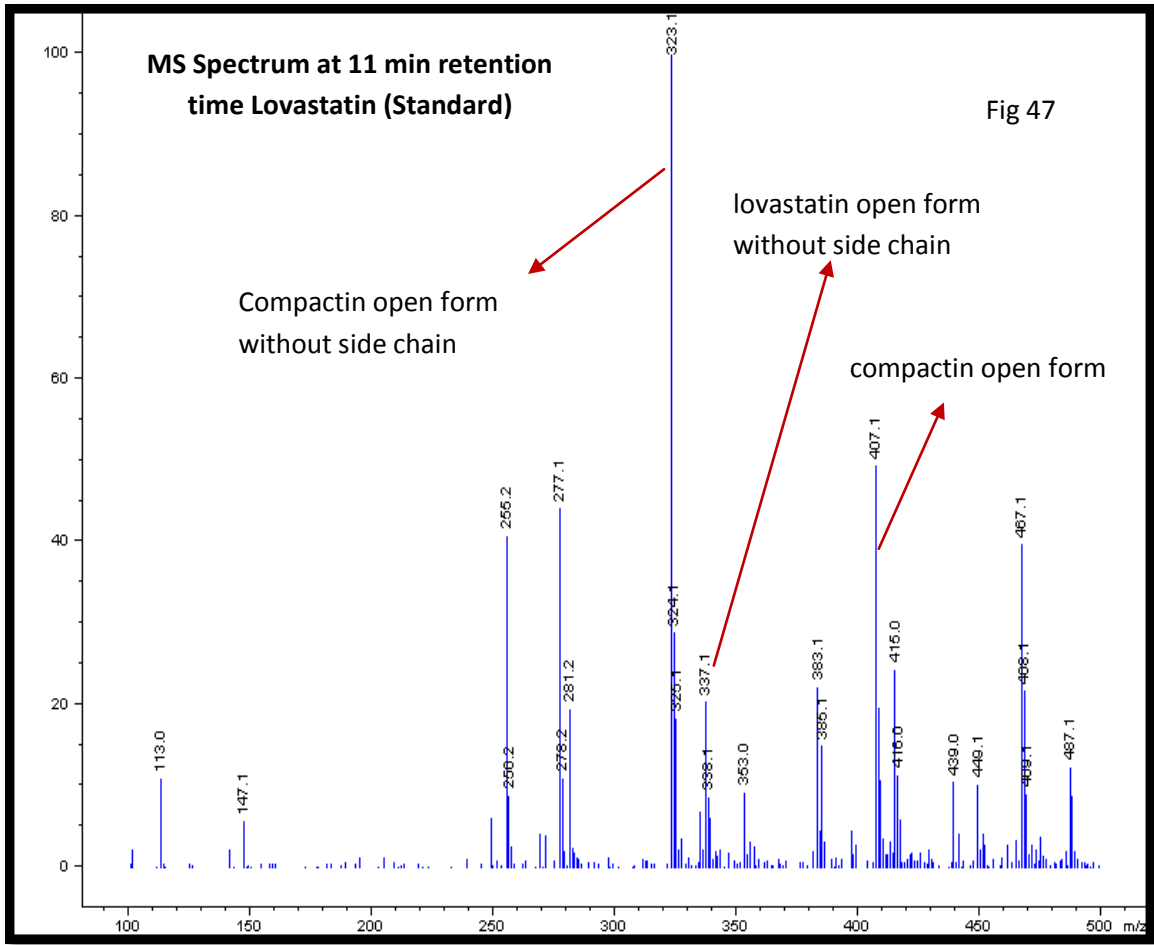
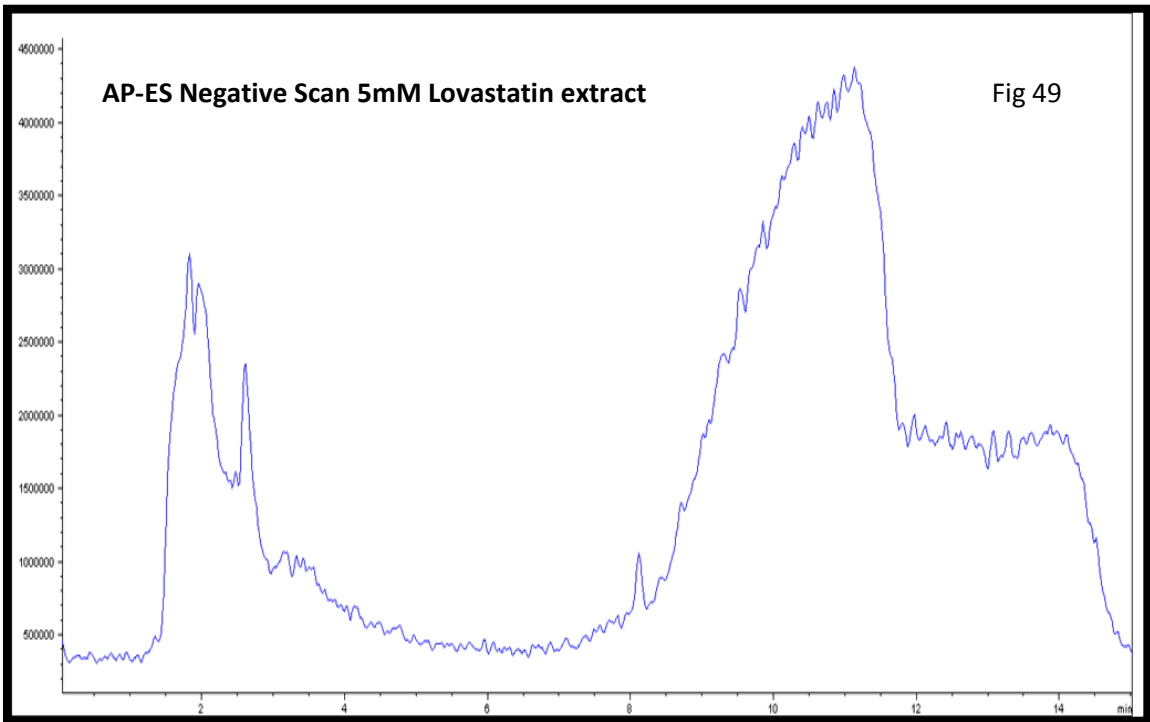
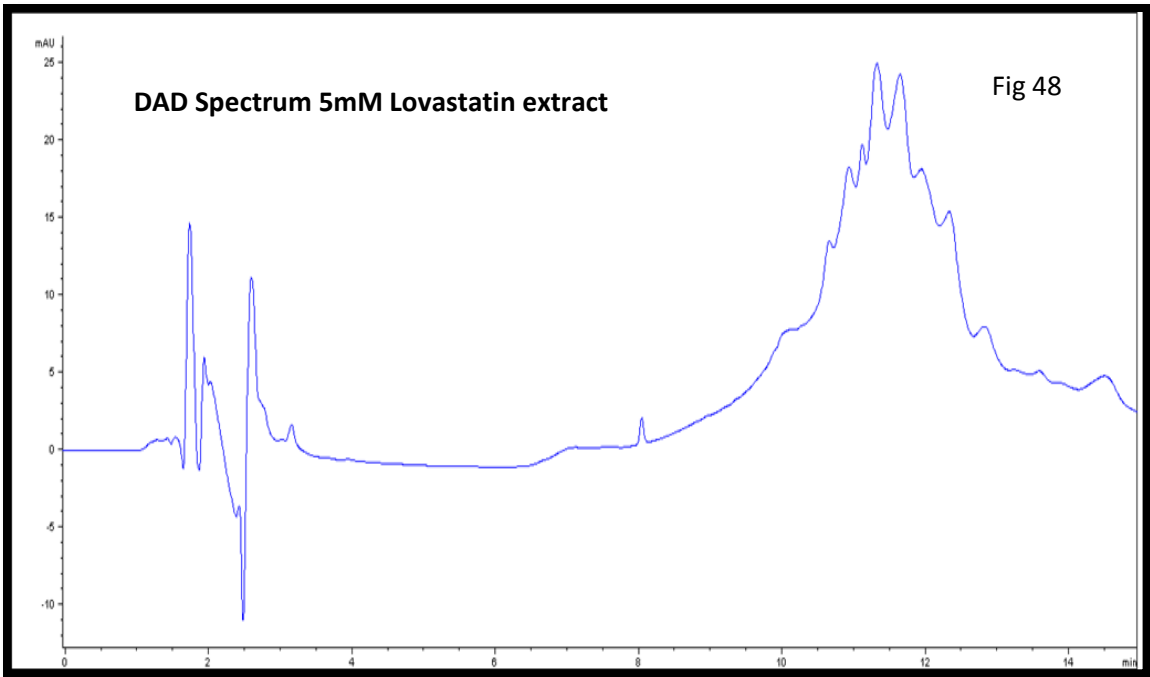
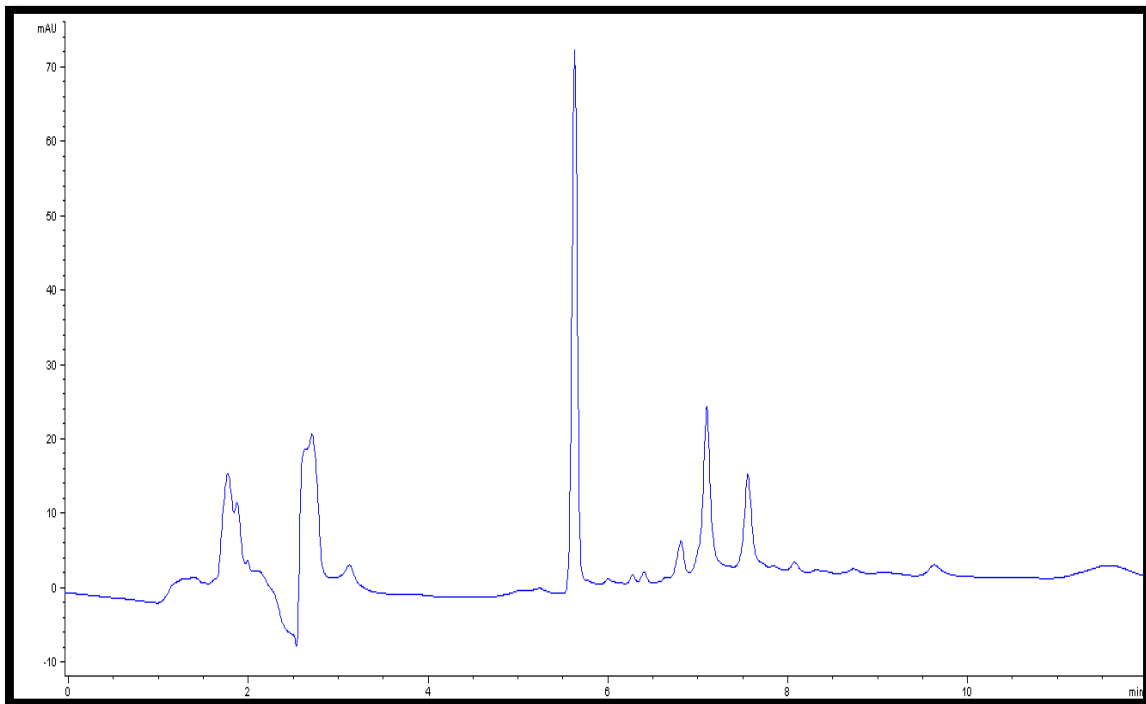
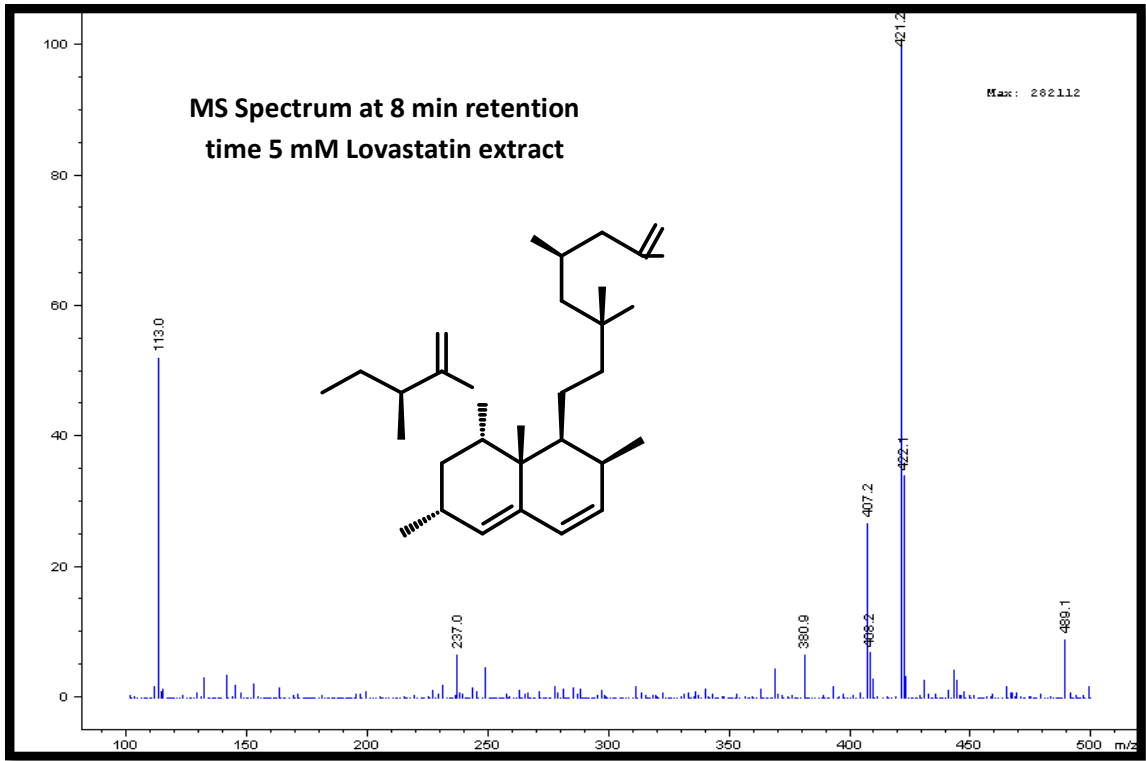
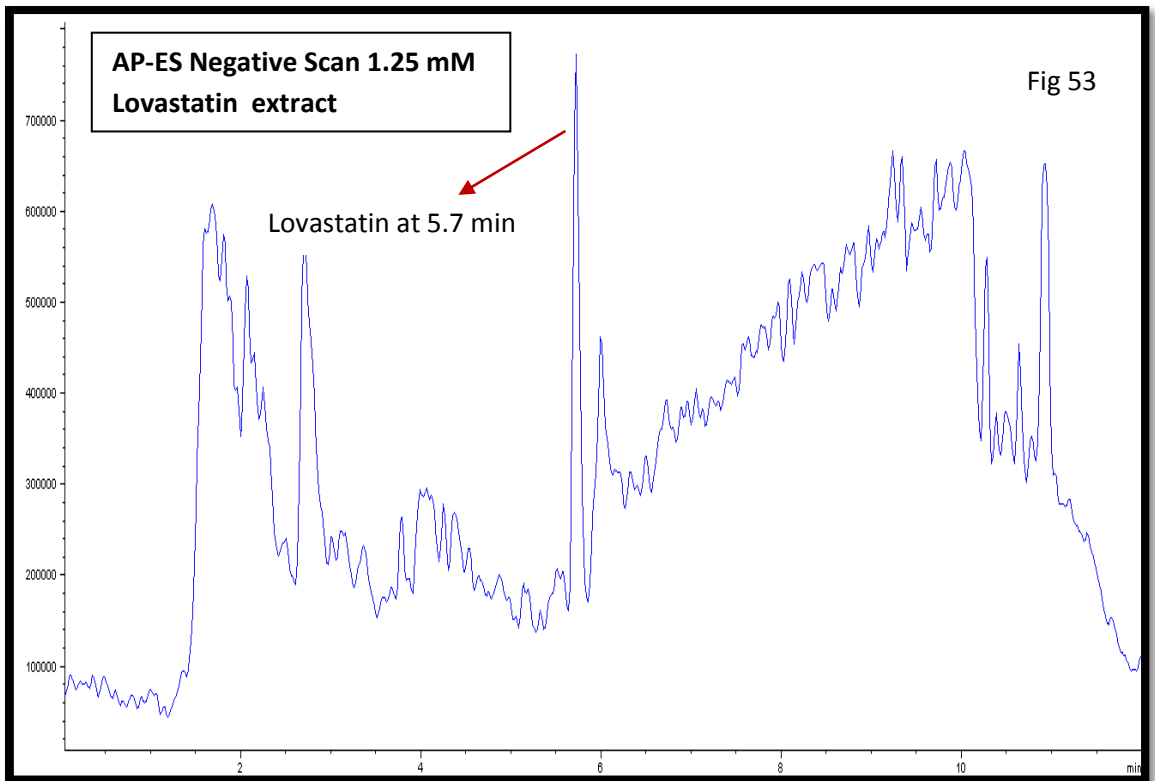
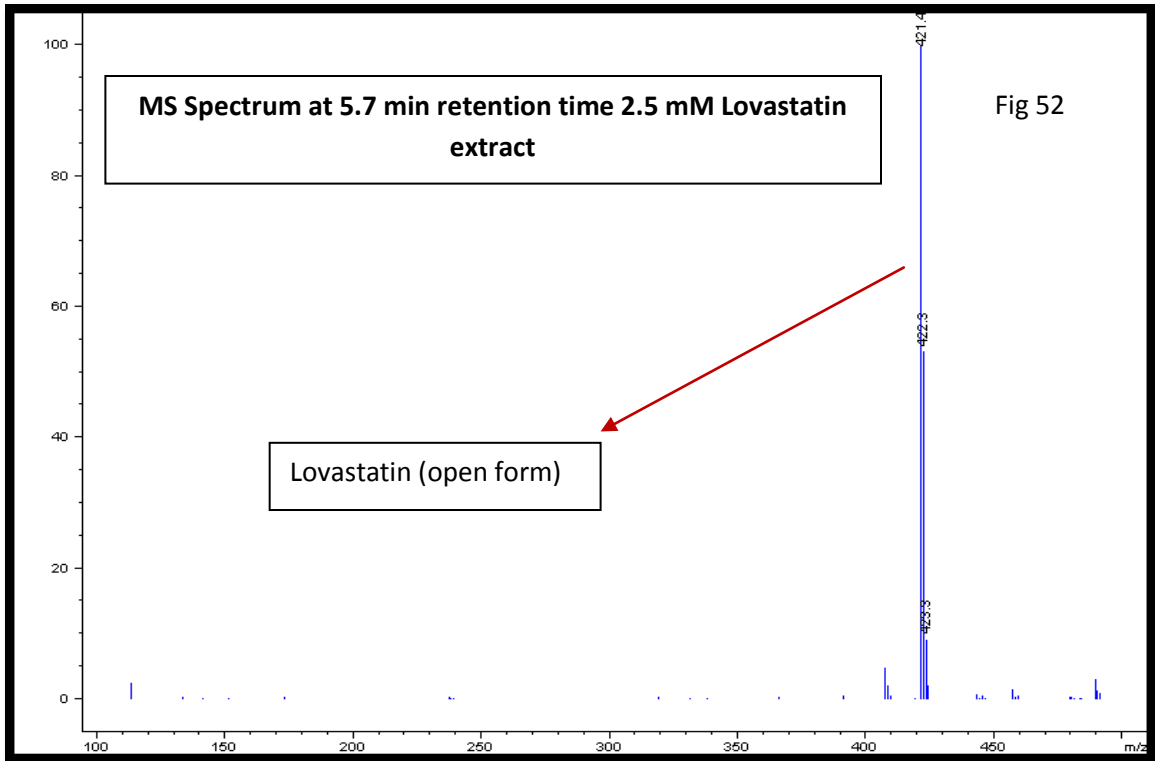
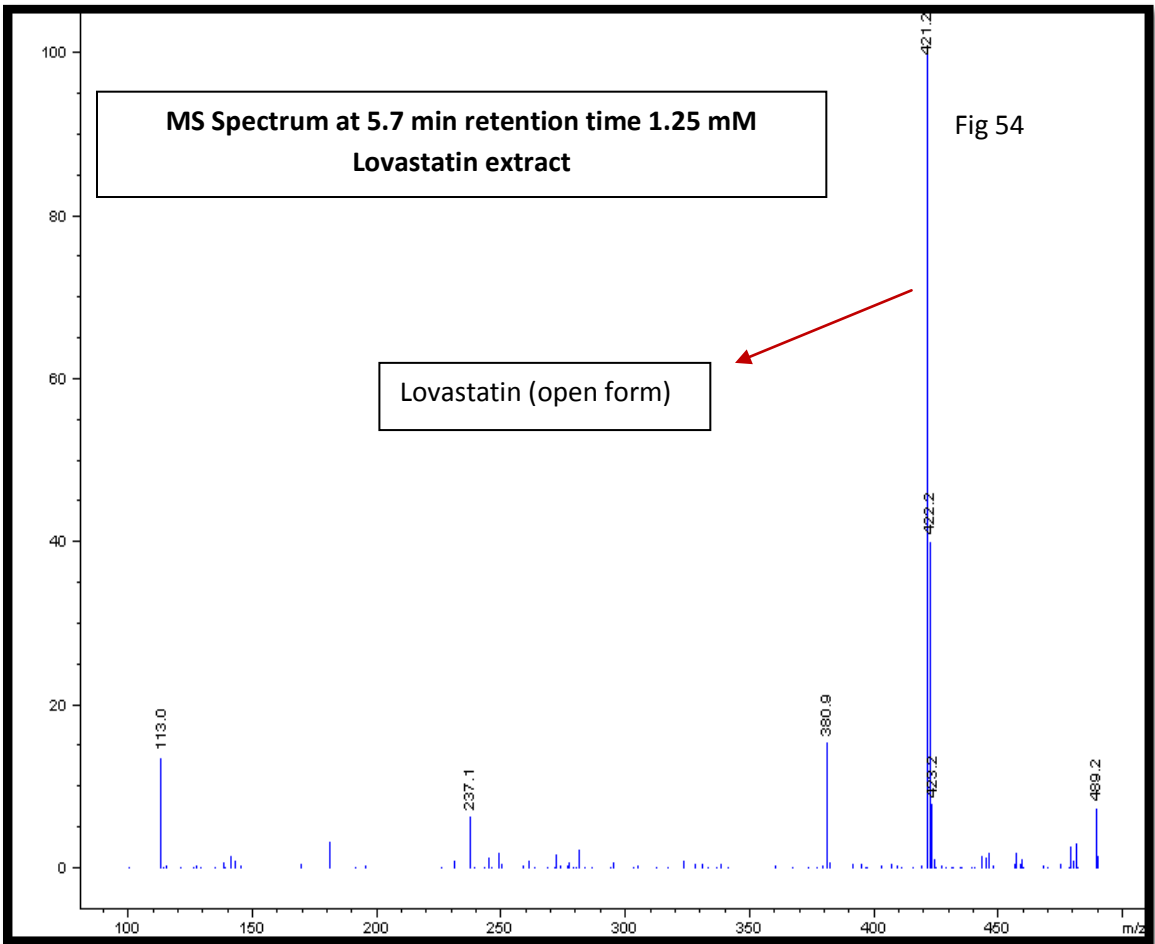


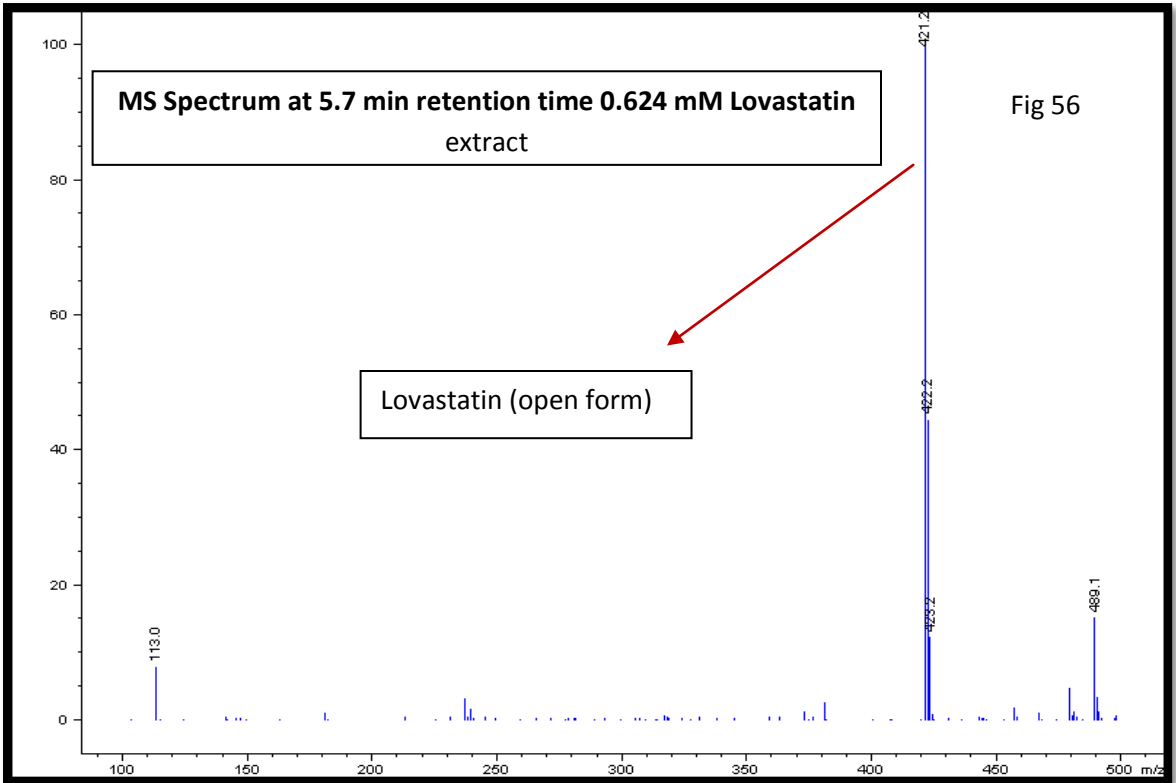
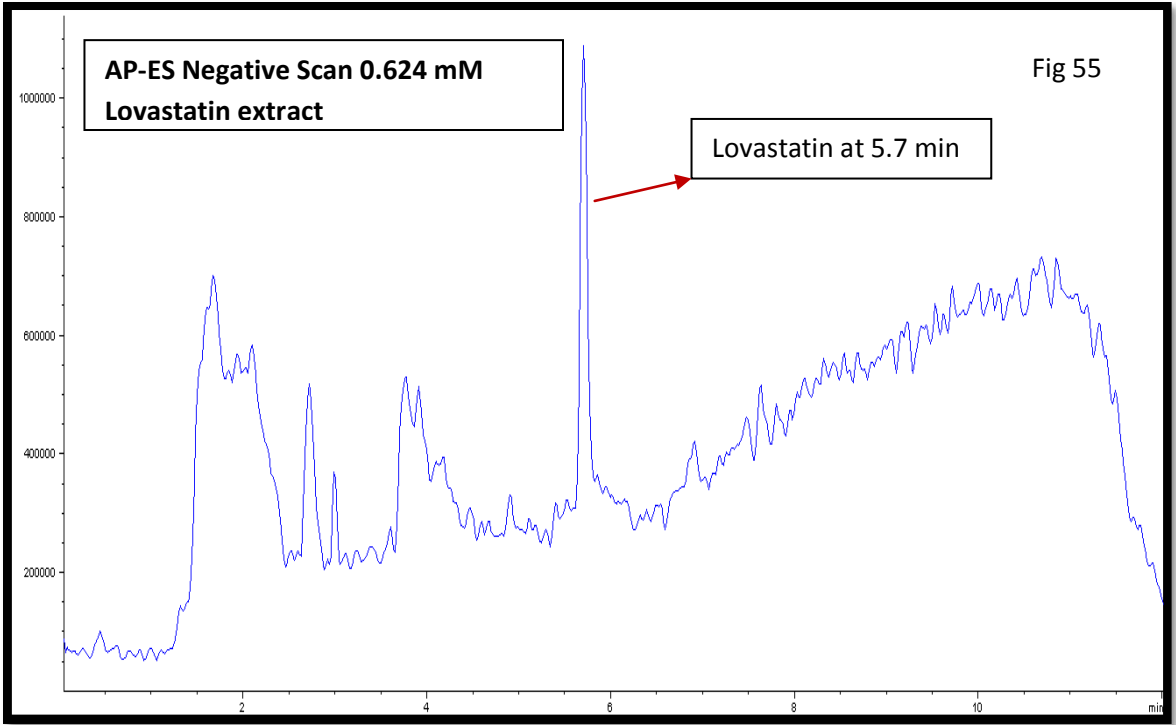
Fig (42-47) LC-MS results from pure lovastatin standard.

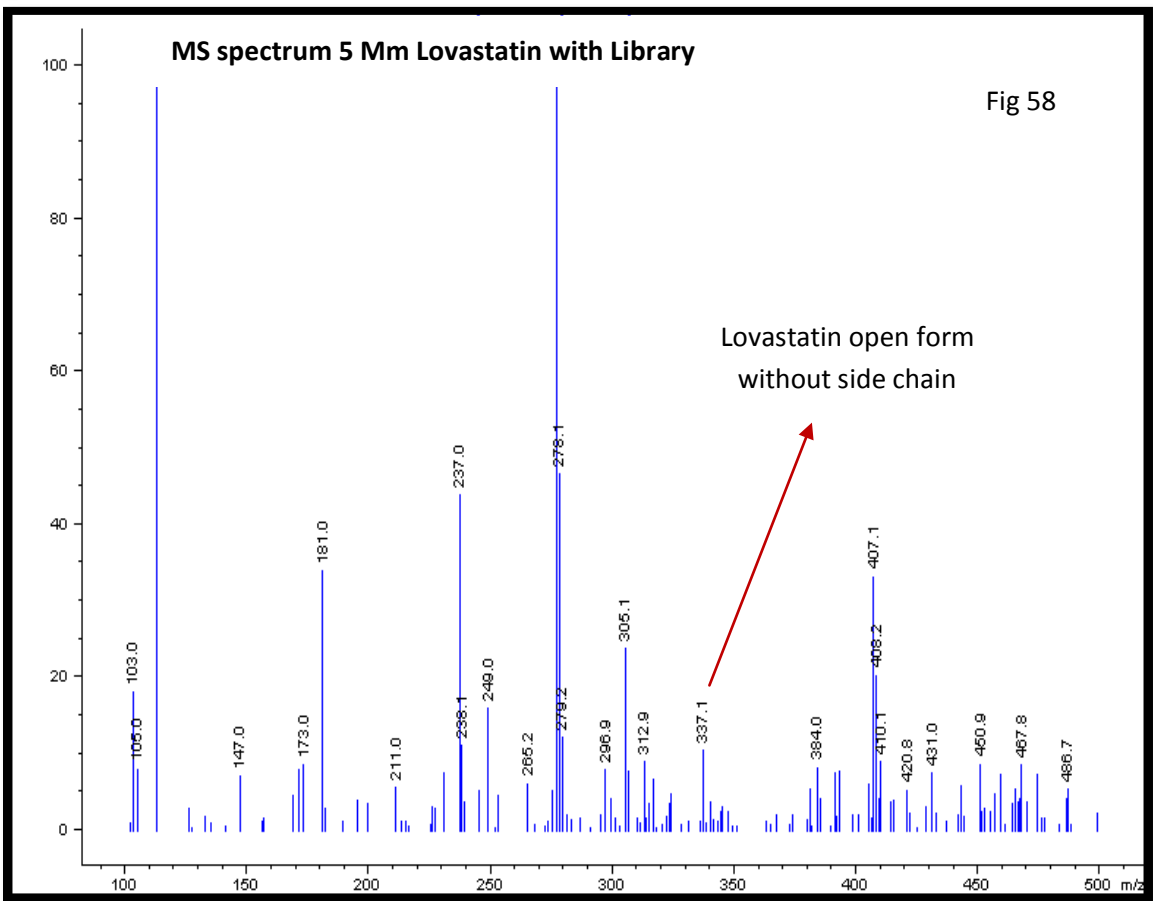
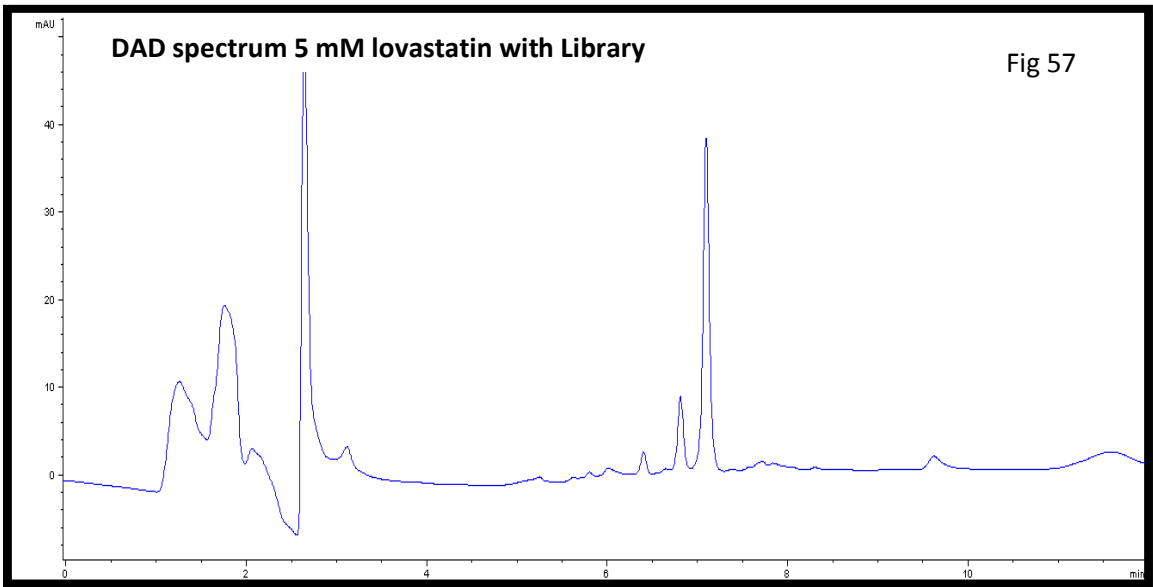












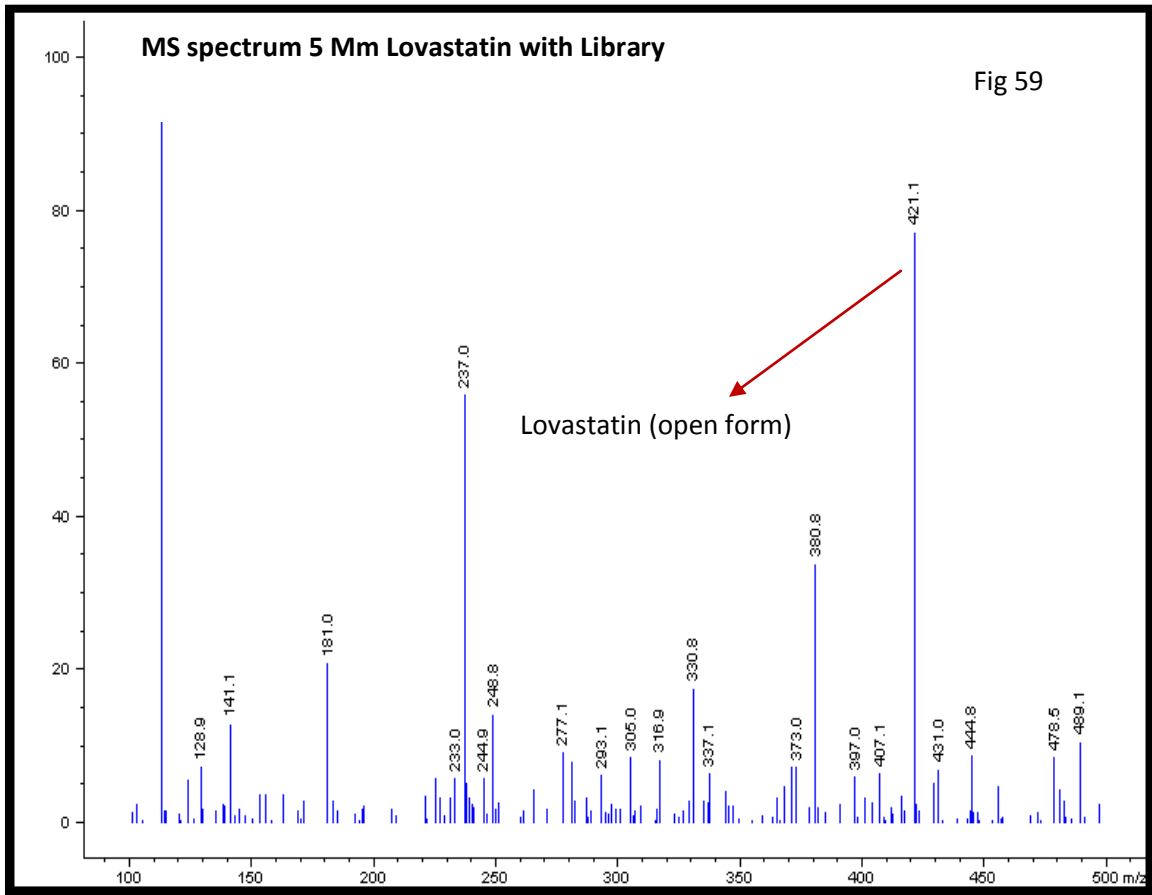
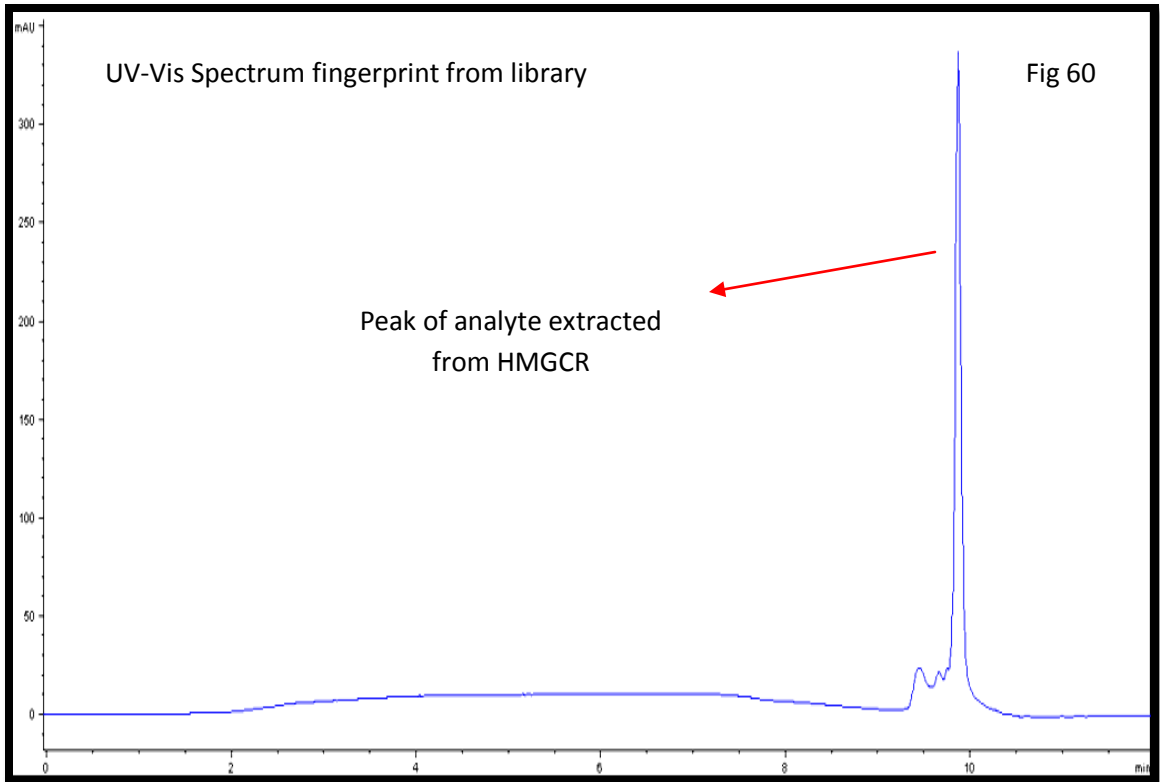


Fig (48-59) LC-MS results from lovastatin extracted after binding to HMGCR.



UV-Vis Spectrum showing a strong peak around 10 minute retention time.

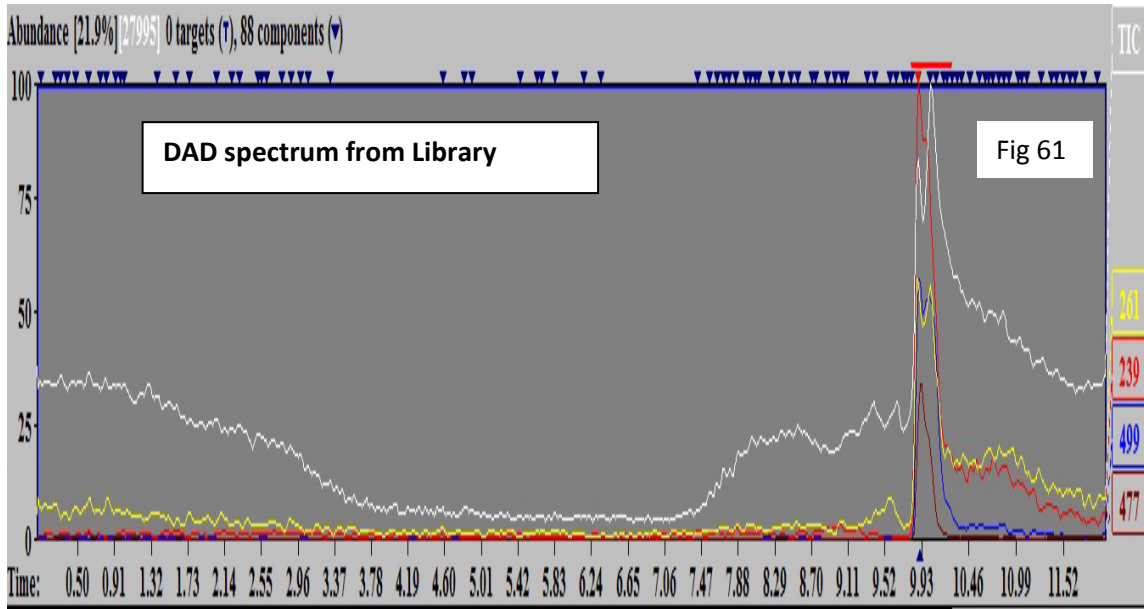


Fig (60) Deconvoluted chromatogram from eluted library extract bound to HMGR.

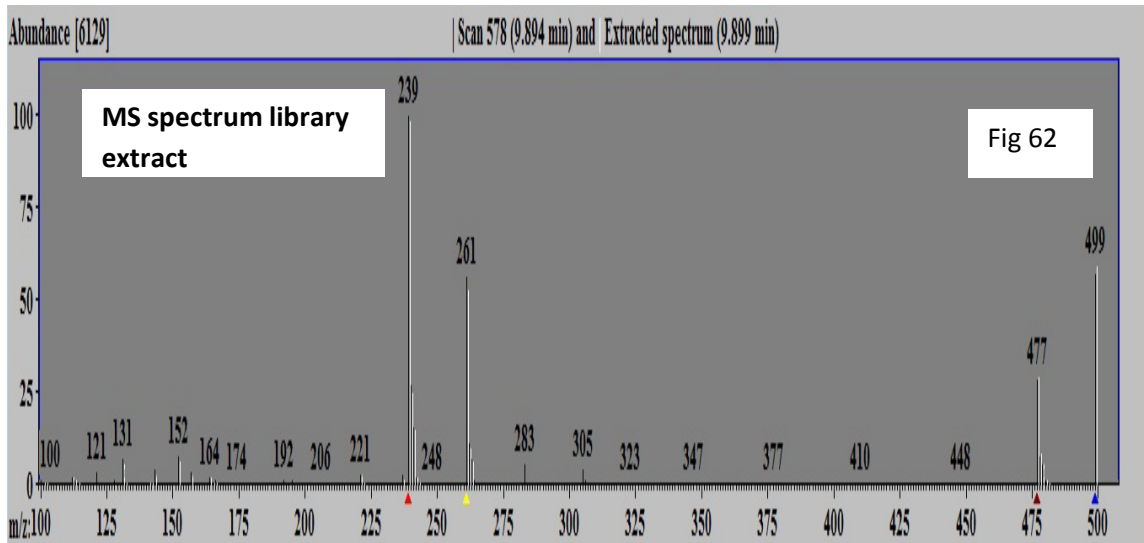


Fig (61) MS spectrum showing HEPES monomer and its dimer protonated and or with sodium adduct.

IV CONCLUSION

In this project we have obtained a basic study of the reasons behind the variation in interpersonal responses to statin drugs for the treatment of hypercholesterolemia. Our findings contradict some of the work previously published by other groups concerning this enzyme, particularly regarding the HMGCRv1 isoform. A lack of detailed structural evaluation of HMGCR and its isoforms complicates interpretation of the interpersonal responses to statin drugs. Previous studies based their conclusion on hypothetical grounds that came from the isolation of mRNA's of the HMGCR isoforms. In this study we were able to show that the HMGCRv1 is not a viable enzyme. This abridge form of the enzyme lacks important structural elements that renders the enzyme inactive and misfolded. We believe that the intake of diet with statin drugs can modify the clinical significance of these drugs. Natural products have been used throughout history for disease treatments. The reason many drugs fail to find their way to the market under tough regulation, can be attributed to the excessive use of combinatorial libraries and synthetic drugs. Only a limited number of high throughput screening (HTS) facilities are available, and institutions with limited resources can not avail of this technology. Furthermore brute force HTS and the use of combinatorial libraries fail to detect important natural product ligands that can have a promising therapeutic effect. In this study we utilized the use of a simple apparatus setup to perform bioprospecting. Mammalian HMGCR enzyme is bound to endoplasmic reticulum (ER). The binding of HMGCR to the chromatographic column was used to mimic the binding of

HMGCR to the ER. The method we proposed for bioprospecting is simple and cost effective. Lovastatin is a known inhibitor for HMGCR, and we have successfully isolated this ligand from the cobalt resin chromatography column after its binding to the substrate. Ultimately this work provides a solid foundation upon which further bioprospecting studies can build. We believe that this technique can be used for any biological substrate ligand binding procedures while keeping the buffer system close to the physiological condition.

REFERENCES

REFERENCES

1. Epstein, F. H. Relationship between low cholesterol and disease. Evidence from epidemiological studies and preventive trials. *Ann. N. Y. Acad. Sci.* **748**, 482–490 (1995).
2. Jacobs, D. *et al.* Report of the Conference on Low Blood Cholesterol: Mortality Associations. *Circulation* **86**, 1046–1060 (1992).
3. Maxfield, F. R. & Tabas, I. Role of cholesterol and lipid organization in disease. *Nature* **438**, 612–621 (2005).
4. Myant, N. B. Cholesterol metabolism. *J Clin Pathol Suppl (Assoc Clin Pathol)* **5**, 1–4 (1973).
5. Tabas, I. Cholesterol in health and disease. *J Clin Invest* **110**, 583–590 (2002).
6. Arthur A., S. Biochemistry of Lipids, Lipoproteins and Membranes: D.E. Vance and J. Vance (Eds.). *Chemistry and Physics of Lipids* **62**, 319–320 (1992).
7. Myant, N. B. *Cholesterol metabolism, LDL, and the LDL receptor.* (Academic Press: 1990).
8. Fahy, E. *et al.* A comprehensive classification system for lipids. *J. Lipid Res.* **46**, 839–861 (2005).
9. Bhagavan, N. V. & Ha, C.-E. *Essentials of Medical Biochemistry: With Clinical Cases.* (Academic Press: 2011).
10. Wang, K. C. & Ohnuma, S. Isoprenyl diphosphate synthases. *Biochimica et Biophysica Acta (BBA) - Molecular and Cell Biology of Lipids* **1529**, 33–48 (2000).
11. Istvan, E. S. Structural mechanism for statin inhibition of 3-hydroxy-3-methylglutaryl coenzyme A reductase. *Am. Heart J* **144**, S27–32 (2002).
12. Spector, A. A. Fatty acid binding to plasma albumin. *J. Lipid Res.* **16**, 165–179 (1975).
13. Biggerstaff, K. D. & Wooten, J. S. Understanding Lipoproteins as Transporters of Cholesterol and Other Lipids. *Advan in Physiol Edu* **28**, 105–106 (2004).
14. Vance, D. E. *Biochemistry of lipids, lipoproteins and membranes.* (Elsevier: 2008).

15. Yokoyama, S. Release of cellular cholesterol: molecular mechanism for cholesterol homeostasis in cells and in the body. *Biochimica et Biophysica Acta (BBA)/Molecular and Cell Biology of Lipids* **1529**, 231–244
16. Brown, M. S. & Goldstein, J. L. A receptor-mediated pathway for cholesterol homeostasis. *Science* **232**, 34–47 (1986).
17. Weber, C. & Noels, H. Atherosclerosis: current pathogenesis and therapeutic options. *Nat. Med.* **17**, 1410–1422 (2011).
18. Libby, P., Ridker, P. M. & Hansson, G. K. Progress and challenges in translating the biology of atherosclerosis. *Nature* **473**, 317–325 (2011).
19. Panda, T., Basak, T., Saraswathi, G. & Théodore, T. Kinetic Mechanisms of Cholesterol Synthesis: A Review. *Ind. Eng. Chem. Res.* **50**, 12847–12864 (2011).
20. Pilloff, D. *et al.* The kinetic mechanism of phosphomevalonate kinase. *J. Biol. Chem.* **278**, 4510–4515 (2003).
21. Swanson, K. M. & Hohl, R. J. Anti-cancer therapy: targeting the mevalonate pathway. *Curr Cancer Drug Targets* **6**, 15–37 (2006).
22. Endo, A., Tsujita, Y., Kuroda, M. & Tanzawa, K. Inhibition of cholesterol synthesis in vitro and in vivo by ML-236A and ML-236B, competitive inhibitors of 3-hydroxy-3-methylglutaryl-coenzyme A reductase. *Eur. J. Biochem.* **77**, 31–36 (1977).
23. Kita, T., Brown, M. S. & Goldstein, J. L. Feedback regulation of 3-hydroxy-3-methylglutaryl coenzyme A reductase in livers of mice treated with mevinolin, a competitive inhibitor of the reductase. *J. Clin. Invest.* **66**, 1094–1100 (1980).
24. Brown, M. S. & Goldstein, J. L. Multivalent feedback regulation of HMG CoA reductase, a control mechanism coordinating isoprenoid synthesis and cell growth. *J. Lipid Res.* **21**, 505–517 (1980).
25. Horton, J. D., Goldstein, J. L. & Brown, M. S. SREBPs: activators of the complete program of cholesterol and fatty acid synthesis in the liver. *J Clin Invest* **109**, 1125–1131 (2002).
26. Nakanishi, M., Goldstein, J. L. & Brown, M. S. Multivalent control of 3-hydroxy-3-methylglutaryl coenzyme A reductase. Mevalonate-derived product inhibits translation of mRNA and accelerates degradation of enzyme. *J. Biol. Chem.* **263**, 8929–8937 (1988).
27. McGee, T. P., Cheng, H. H., Kumagai, H., Omura, S. & Simoni, R. D. Degradation of 3-hydroxy-3-methylglutaryl-CoA reductase in endoplasmic reticulum membranes is

- accelerated as a result of increased susceptibility to proteolysis. *J. Biol. Chem.* **271**, 25630–25638 (1996).
28. Roitelman, J. & Simoni, R. D. Distinct sterol and nonsterol signals for the regulated degradation of 3-hydroxy-3-methylglutaryl-CoA reductase. *J. Biol. Chem.* **267**, 25264–25273 (1992).
 29. Ravid, T., Doolman, R., Avner, R., Harats, D. & Roitelman, J. The ubiquitin-proteasome pathway mediates the regulated degradation of mammalian 3-hydroxy-3-methylglutaryl-coenzyme A reductase. *J. Biol. Chem.* **275**, 35840–35847 (2000).
 30. Sato, R., Goldstein, J. L. & Brown, M. S. Replacement of serine-871 of hamster 3-hydroxy-3-methylglutaryl-CoA reductase prevents phosphorylation by AMP-activated kinase and blocks inhibition of sterol synthesis induced by ATP depletion. *Proc. Natl. Acad. Sci. U.S.A.* **90**, 9261–9265 (1993).
 31. Clarke, P. R. & Hardie, D. G. Regulation of HMG-CoA reductase: identification of the site phosphorylated by the AMP-activated protein kinase in vitro and in intact rat liver. *EMBO J.* **9**, 2439–2446 (1990).
 32. Hardie, D. G. Minireview: the AMP-activated protein kinase cascade: the key sensor of cellular energy status. *Endocrinology* **144**, 5179–5183 (2003).
 33. Smith, M. B. M. E. B., Lee, N. J. N. J., Haney, E. E. & Carson, S. S. *Drug Class Review: HMG-CoA Reductase Inhibitors (Statins) and Fixed-dose Combination Products Containing a Statin: Final Report Update 5*. (Oregon Health & Science University: Portland (OR), 2009).at <<http://www.ncbi.nlm.nih.gov/pubmed/21089253>>
 34. Rozman, D. & Monostory, K. Perspectives of the non-statin hypolipidemic agents. *Pharmacol. Ther.* **127**, 19–40 (2010).
 35. Stone, N. J. Lipid management: Current diet and drug treatment options. *The American Journal of Medicine* **101**, 40S–49S (1996).
 36. Raal, F. J. & Santos, R. D. Homozygous familial hypercholesterolemia: Current perspectives on diagnosis and treatment. *Atherosclerosis* (2012).doi:10.1016/j.atherosclerosis.2012.02.019
 37. Varady, K. A. & Jones, P. J. H. Combination diet and exercise interventions for the treatment of dyslipidemia: an effective preliminary strategy to lower cholesterol levels? *J. Nutr.* **135**, 1829–1835 (2005).
 38. Henneman, L., van Cruchten, A. G., Kulik, W. & Waterham, H. R. Inhibition of the isoprenoid biosynthesis pathway; detection of intermediates by UPLC-MS/MS. *Biochim. Biophys. Acta* **1811**, 227–233 (2011).

39. Knight, L. A. *et al.* Activity of mevalonate pathway inhibitors against breast and ovarian cancers in the ATP-based tumour chemosensitivity assay. *BMC Cancer* **9**, 38 (2009).
40. Zhang, F. L. *et al.* Characterization of Ha-ras, N-ras, Ki-Ras4A, and Ki-Ras4B as in vitro substrates for farnesyl protein transferase and geranylgeranyl protein transferase type I. *J. Biol. Chem.* **272**, 10232–10239 (1997).
41. James, G., Goldstein, J. L. & Brown, M. S. Resistance of K-RasBV12 proteins to farnesyltransferase inhibitors in Rat1 cells. *Proc. Natl. Acad. Sci. U.S.A.* **93**, 4454–4458 (1996).
42. Salam, W. H. & Bloxham, D. P. Hypolipidemic effect of polymethylenemethane thiosulfonates: inhibitors of acetoacetyl coenzyme A thiolase. *J. Pharmacol. Exp. Ther.* **241**, 1099–1105 (1987).
43. Scharnagl, H. *et al.* The effects of lifibrol (K12.148) on the cholesterol metabolism of cultured cells: evidence for sterol independent stimulation of the LDL receptor pathway. *Atherosclerosis* **153**, 69–80 (2000).
44. Schafer, B. L. *et al.* Molecular cloning of human mevalonate kinase and identification of a missense mutation in the genetic disease mevalonic aciduria. *J. Biol. Chem.* **267**, 13229–13238 (1992).
45. Qiu, Y. & Li, D. Bifunctional inhibitors of mevalonate kinase and mevalonate 5-diphosphate decarboxylase. *Org. Lett.* **8**, 1013–1016 (2006).
46. Tobert, J. A. Lovastatin and beyond: the history of the HMG-CoA reductase inhibitors. *Nature Reviews Drug Discovery* **2**, 517–526 (2003).
47. Endo, A. Compactin (ML-236B) and related compounds as potential cholesterol-lowering agents that inhibit HMG-CoA reductase. *J. Med. Chem.* **28**, 401–405 (1985).
48. Vaughan, C. J., Gotto, A. M., Jr & Basson, C. T. The evolving role of statins in the management of atherosclerosis. *J. Am. Coll. Cardiol.* **35**, 1–10 (2000).
49. Kapur, N. K. & Musunuru, K. Clinical efficacy and safety of statins in managing cardiovascular risk. *Vasc Health Risk Manag* **4**, 341–353 (2008).
50. Gerson, R. J. *et al.* Animal safety and toxicology of simvastatin and related hydroxy-methylglutaryl-coenzyme A reductase inhibitors. *Am. J. Med.* **87**, 28S–38S (1989).
51. Smith, P. F. *et al.* HMG-CoA reductase inhibitor-induced myopathy in the rat: cyclosporine A interaction and mechanism studies. *J. Pharmacol. Exp. Ther.* **257**, 1225–1235 (1991).

52. Downs, J. R. *et al.* Primary prevention of acute coronary events with lovastatin in men and women with average cholesterol levels: results of AFCAPS/TexCAPS. Air Force/Texas Coronary Atherosclerosis Prevention Study. *JAMA* **279**, 1615–1622 (1998).
53. Pedersen, T. R. *et al.* Randomised trial of cholesterol lowering in 4444 patients with coronary heart disease: the Scandinavian Simvastatin Survival Study (4S). 1994. *Atheroscler Suppl* **5**, 81–87 (2004).
54. Pedersen, T. R. *et al.* Safety and tolerability of cholesterol lowering with simvastatin during 5 years in the Scandinavian Simvastatin Survival Study. *Arch. Intern. Med.* **156**, 2085–2092 (1996).
55. MRC/BHF Heart Protection Study of cholesterol lowering with simvastatin in 20,536 high-risk individuals: a randomised placebo-controlled trial. *Lancet* **360**, 7–22 (2002).
56. Shepherd, J. *et al.* Prevention of coronary heart disease with pravastatin in men with hypercholesterolemia. 1995. *Atheroscler Suppl* **5**, 91–97 (2004).
57. Willerson, J. T. Effect of pravastatin on coronary events after myocardial infarction in patients with average cholesterol levels. *Circulation* **94**, 3054 (1996).
58. Prevention of cardiovascular events and death with pravastatin in patients with coronary heart disease and a broad range of initial cholesterol levels. The Long-Term Intervention with Pravastatin in Ischaemic Disease (LIPID) Study Group. *N. Engl. J. Med.* **339**, 1349–1357 (1998).
59. LaRosa, J. C., He, J. & Vupputuri, S. Effect of statins on risk of coronary disease: a meta-analysis of randomized controlled trials. *JAMA* **282**, 2340–2346 (1999).
60. Ahmad, S. *et al.* (3R,5S,E)-7-(4-(4-fluorophenyl)-6-isopropyl-2-(methyl(1-methyl-1h-1,2,4-triazol-5-yl)amino)pyrimidin-5-yl)-3,5-dihydroxyhept-6-enoic acid (BMS-644950): a rationally designed orally efficacious 3-hydroxy-3-methylglutaryl coenzyme-a reductase inhibitor with reduced myotoxicity potential. *J. Med. Chem.* **51**, 2722–2733 (2008).
61. Pfefferkorn, J. A. *et al.* Design and synthesis of novel, conformationally restricted HMG-CoA reductase inhibitors. *Bioorg. Med. Chem. Lett.* **17**, 4531–4537 (2007).
62. Thompson, J. F. *et al.* Comprehensive whole-genome and candidate gene analysis for response to statin therapy in the Treating to New Targets (TNT) cohort. *Circ Cardiovasc Genet* **2**, 173–181 (2009).
63. Donnelly, L. A. *et al.* A paucimorphic variant in the HMG-CoA reductase gene is associated with lipid-lowering response to statin treatment in diabetes: a GoDARTS study. *Pharmacogenet. Genomics* **18**, 1021–1026 (2008).

64. Krauss, R. M. *et al.* Variation in the 3-hydroxy-3-methylglutaryl coenzyme A reductase gene is associated with racial differences in low-density lipoprotein cholesterol response to simvastatin treatment. *Circulation* **117**, 1537–1544 (2008).
65. Chasman, D. I. *et al.* Pharmacogenetic study of statin therapy and cholesterol reduction. *JAMA* **291**, 2821–2827 (2004).
66. Medina, M. W., Gao, F., Ruan, W., Rotter, J. I. & Krauss, R. M. Alternative splicing of 3-hydroxy-3-methylglutaryl coenzyme A reductase is associated with plasma low-density lipoprotein cholesterol response to simvastatin. *Circulation* **118**, 355–362 (2008).
67. Medina, M. W. & Krauss, R. M. The role of HMGCR alternative splicing in statin efficacy. *Trends Cardiovasc. Med.* **19**, 173–177 (2009).
68. Medina, M. W. The relationship between HMGCR genetic variation, alternative splicing, and statin efficacy. *Discov Med* **9**, 495–499 (2010).
69. Burkhardt, R. *et al.* Common SNPs in HMGCR in micronesians and whites associated with LDL-cholesterol levels affect alternative splicing of exon13. *Arterioscler. Thromb. Vasc. Biol.* **28**, 2078–2084 (2008).
70. Birzele, F., Csaba, G. & Zimmer, R. Alternative splicing and protein structure evolution. *Nucleic Acids Res* **36**, 550–558 (2008).
71. Istvan, E. S., Palnitkar, M., Buchanan, S. K. & Deisenhofer, J. Crystal structure of the catalytic portion of human HMG-CoA reductase: insights into regulation of activity and catalysis. *EMBO J.* **19**, 819–830 (2000).
72. Breitling, R. & Krisans, S. K. A second gene for peroxisomal HMG-CoA reductase? A genomic reassessment. *J. Lipid Res.* **43**, 2031–2036 (2002).
73. Jawaid, S. *et al.* Human hydroxymethylglutaryl-coenzyme A reductase (HMGCR) and statin sensitivity. *Indian J. Biochem. Biophys* **47**, 331–339 (2010).
74. KNAPPE, J., RINGELMANN, E. & LYNEN, F. [On beta-hydroxy-beta-methylglutaryl reductase of yeast. On the biosynthesis of terpene. IX]. *Biochem Z* **332**, 195–213 (1959).
75. Durr, I. F. & Rudney, H. The Reduction of B-Hydroxy-B-Methylglutaryl Coenzyme A to Mevalonic Acid. *J. Biol. Chem.* **235**, 2572–2578 (1960).
76. Bensch, W. R. & Rodwell, V. W. Purification and Properties of 3-Hydroxy-3-Methylglutaryl Coenzyme A Reductase from *Pseudomonas*. *J. Biol. Chem.* **245**, 3755–3762 (1970).
77. Kleinsek, D. A., Ranganathan, S. & Porter, J. W. Purification of 3-hydroxy-3-methylglutaryl-coenzyme A reductase from rat liver. *Proc Natl Acad Sci U S A* **74**, 1431–1435 (1977).

78. Edwards, P. A., Lemongello, D. & Fogelman, A. M. Improved Methods for the Solubilization and Assay of Hepatic 3-Hydroxy-3-Methylglutaryl Coenzyme A Reductase. *J. Lipid Res.* **20**, 40–46 (1979).
79. Rétey, J., von Stetten, E., Coy, U. & Lynen, F. A probable intermediate in the enzymic reduction of 3-hydroxy-3-methylglutaryl coenzyme A. *Eur. J. Biochem.* **15**, 72–76 (1970).
80. Qureshi, N., Dugan, R. E., Nimmannit, S., Wu, W. H. & Porter, J. W. Purification of beta-hydroxy-beta-methylglutaryl-coenzyme A reductase from yeast. *Biochemistry* **15**, 4185–4190 (1976).
81. Frimpong, K. & Rodwell, V. W. Catalysis by Syrian hamster 3-hydroxy-3-methylglutaryl-coenzyme A reductase. Proposed roles of histidine 865, glutamate 558, and aspartate 766. *J. Biol. Chem.* **269**, 11478–11483 (1994).
82. Bochar, D. A., Stauffacher, C. V. & Rodwell, V. W. Investigation of the conserved lysines of Syrian hamster 3-hydroxy-3-methylglutaryl coenzyme A reductase. *Biochemistry* **38**, 15848–15852 (1999).
83. Lawrence, C. M., Chi, Y.-I., Rodwell, V. W. & Stauffacher, C. V. Crystallization of HMG-CoA reductase from *Pseudomonas mevalonii*. *Acta Crystallographica Section D Biological Crystallography* **51**, 386–389 (1995).
84. Taberner, L., Bochar, D. A., Rodwell, V. W. & Stauffacher, C. V. Substrate-induced closure of the flap domain in the ternary complex structures provides insights into the mechanism of catalysis by 3-hydroxy-3-methylglutaryl-CoA reductase. *Proc. Natl. Acad. Sci. U.S.A.* **96**, 7167–7171 (1999).
85. Istvan, E. S. Structural mechanism for statin inhibition of 3-hydroxy-3-methylglutaryl coenzyme A reductase. *Am. Heart J.* **144**, S27–32 (2002).
86. Mornar, A., Damic, M. & Nigovic, B. Pharmacokinetic Parameters of Statin Drugs Characterized by Reversed Phase High-Performance Liquid Chromatography. *Analytical Letters* **44**, 1009–1020 (2011).
87. Harvey, A. L. Natural products in drug discovery. *Drug Discov. Today* **13**, 894–901 (2008).
88. Jenkins, D. J. A. *et al.* Assessment of the longer-term effects of a dietary portfolio of cholesterol-lowering foods in hypercholesterolemia. *Am. J. Clin. Nutr.* **83**, 582–591 (2006).
89. Williams Drug Discovery Benefits from Venomous Clues. *Proteomics Insights* 67 (2010).doi:10.4137/PRI.S6097

90. Ginsburg, G. S. & McCarthy, J. J. Personalized medicine: revolutionizing drug discovery and patient care. *Trends Biotechnol.* **19**, 491–496 (2001).
91. Walsh, G. *Proteins: Biochemistry and Biotechnology*. (John Wiley & Sons: 2001).
92. Shevchenko, A. *et al.* Linking Genome and Proteome by Mass Spectrometry: Large-Scale Identification of Yeast Proteins from Two Dimensional Gels. *PNAS* **93**, 14440–14445 (1996).
93. Kleinsek, D. A., Dugan, R. E., Baker, T. A. & Porter, J. W. 3-hydroxy-3-methylglutaryl-CoA reductase from rat liver. *Meth. Enzymol.* **71 Pt C**, 462–479 (1981).
94. Breslow, J. L. *et al.* Identification and DNA sequence of a human apolipoprotein E cDNA clone. *J. Biol. Chem.* **257**, 14639–14641 (1982).
95. Butler, M. S. The role of natural product chemistry in drug discovery. *J. Nat. Prod.* **67**, 2141–2153 (2004).
96. Bujacz, G. *et al.* Binding of Different Divalent Cations to the Active Site of Avian Sarcoma Virus Integrase and Their Effects on Enzymatic Activity. *J. Biol. Chem.* **272**, 18161–18168 (1997).

CURRICULUM VITAE

Hameed A. Khan graduated from University of Peshawar (Pakistan) in 1996, with a two year Bachelors of Arts in English Literature and Political Science. He received his four years Bachelor of Science from George Mason University in Biochemistry, in 2007. In 2007 he got employed by Quest Diagnostics Nichols Institute, Chantilly Virginia, where he started his career in the Special Chemistry Department as a medical technologist trainee, and by 2012 got promoted to the position of medical technologist II. He has also been involved in research projects at George Mason University, Prince William campus, since 2010.